

EFFECTS OF ULTRAFINE PARTICULATE MATTER ON OFFSPRING GROWTH AND
DEVELOPMENT

A Dissertation

by

DREW DABNEY PENDLETON

Submitted to the Graduate and Professional School of
Texas A&M University
in fulfillment of the requirements for the degree of

DOCTOR OF PHILOSOPHY

Chair of Committee, Natalie M. Johnson
Committee Members, Stephen S. Safe
 David W. Threadgill
 Michael F. Criscitiello
Intercollegiate Faculty Chair, Ivan Rusyn

December 2021

Major Subject: Toxicology

Copyright 2021 Drew Pendleton

ABSTRACT

One of the most prevalent environmental health issues affecting the globe in the 21st century is that of air pollution and its resulting health effects. A major component of ambient air pollution is termed particulate matter (PM), which accounts for a considerable burden of adverse health outcomes including disease and death across the globe. Maternal exposure to PM during pregnancy has been recently understood to induce significant harm on the health and development of children. However, the smallest fraction of PM, known as ultrafine particulates (UFPs), have yet to be regulated as larger fractions have been and are still being studied and characterized. Additionally, the body of evidence for adverse effects of prenatal UFP exposure in regard to metabolic and developmental outcomes is still growing. In this research, I will discuss recent findings from our mouse model for prenatal ultrafine particle (UFP) exposure and impacts on metabolism and development. Our findings demonstrate *in utero* UFP exposure does impact growth and development in a sex and dose specific manner. Sustained trends of inhibited weight gain, differences in organ weights, and differences in fat content combined with measurements of oxidative stress and altered bone development implicate the development of adverse health conditions later in life following prenatal UFP exposure. Overall, this research highlights the growing need to develop effective environmental and public health policies to regulate and reduce exposure to ambient PM and UFPs.

ACKNOWLEDGEMENTS

Throughout the process of creating this dissertation and the data collected herein I have received a great deal of support, assistance, and inspiration from multiple significant sources. First and foremost, I must thank my Graduate Advisor and Committee Chair, Dr. Natalie Johnson, whose guidance and suggestions were invaluable to the completion of this document. Additionally, I would like to thank the Texas A&M Laboratory Animal Resources and Research (LARR) for providing the necessary background information and animal handling training for this project. I would also like to thank the Director of the Texas A&M Institute for Genomic Medicine, Ben Morpurgo, for his assistance in obtaining the necessary facilities and mouse colonies for this research.

This research could not have been completed successfully during the COVID-19 pandemic without the assistance and guidance of my colleagues; Carmen Lau, Jonathan Behlen, Nicholas Drury, Ross Shore, Toriq Mustapha, Dennis Rhodes, and Dylan McBee. Many thanks to my committee members, Drs. Johnson, Threadgill, Safe, and Criscitiello for asking probing questions that pushed me to investigate and to explore these concepts to the extent of my abilities. Finally, I would like to thank Dr. Natalie Johnson and the faculty of the Interdisciplinary Faculty of Toxicology for their support and endless encouragement.

CONTRIBUTORS AND FUNDING SOURCES

Support provided by National Institute of Environmental Health Sciences T32 ES026568 and R01 ES028866; Texas A&M University T3 award.

TABLE OF CONTENTS

	Page
ABSTRACT	ii
ACKNOWLEDGEMENTS	iii
CONTRIBUTORS AND FUNDING SOURCES	iv
TABLE OF CONTENTS	v
LIST OF FIGURES	vii
LIST OF TABLES	ix
NOMENCLATURE	x
CHAPTER I INTRODUCTION	1
Particulate Matter Air Pollution.....	1
Sources & Size	1
Chemical Composition & Variability	2
Health Effects	4
Cytotoxicity/Genotoxicity	5
Inflammation	6
Lung Cancer	8
Heart Disease	9
Relevant Regulations	10
Summary of Human Evidence – Epidemiologic Studies on Gestational Exposure	11
Pregnancy Outcomes	12
Fetal Growth Effects	17
Obesity	19
Diabetes	20
Bone Health	21
Summary of Nonhuman Evidence – Animal Models on Gestational Exposure	22
Developmental Effects	22
Cardiopulmonary Development	24
Metabolic Effects (Glucose Metabolism/Lipid Metabolism)	25
Mechanisms of Action	29
Oxidative stress	29
Basic definitions	29
Thiols	30
Redox Biology & Biochemistry	32
Oxidative stress & protein modification	33
Nrf2 Oxidative Stress & PM	35

Inflammation	37
Basics of inflammation	37
Biochemistry & cell biology of inflammation	38
Significance and Specific Aims.....	38
 CHAPTER II METABOLIC STUDY 1: GESTATIONAL EXPOSURE TO ULTRAFINE PARTICLES ALTERS POSTNATAL GROWT	40
Introduction.....	40
Methods.....	41
Results	44
Discussion & Conclusions	51
 CHAPTER III METABOLIC STUDY 2: GESTATIONAL EXPOSURE TO ULTRAFINE PARTICLES ALTERS BONE DENSITY AND HEPATIC LIPID CONTENT.....	55
Introduction	55
Methods	57
Results.....	61
Discussion	77
Conclusions.....	83
 CHAPTER IV GESTATIONAL EXPOSURE TO ULTRAFINE PARTICLES AND ANTIOXIDANT NRF2 PROTECTION FROM OXIDATIVE STRESS.....	84
Introduction.....	84
Methods.....	86
Results.....	90
Discussion.....	94
Restate Outcomes	95
Conclusions.....	96
 CHAPTER V SUMMARY OF KEY FINDINGS AND RECOMMENDATIONS FOR FUTURE STUDIES	97
Findings of Aim 1	97
Findings of Aim 2	97
Findings of Aim 3	98
Overall	99
Recommendations for Future Studies	99
 REFERENCES	100

LIST OF FIGURES

	Page
• Fig 1. Study design for assessing effects of gestational exposure to ultrafine particles (UFPs) on offspring growth.....	42
• Fig 2. Offspring body weight (BW) and relative organ weight on PND 5.....	45
• Fig 3. Offspring growth trends during nursing from PND 5-21	46
• Fig 4. Offspring growth trends post-weaning with introduction of a low fat (LF) or high fat (HF) diet from postnatal week 3-15.....	46
• Fig 5. Offspring feed intake analysis measured post diet assignment.....	47
• Fig. 6. Offspring glucose tolerance test trends.....	48
• Fig 7. Offspring body composition analysis measured by EchoMRI on PND 105.....	49
• Fig 8. Offspring relative organ weight on PND 105.....	50
• Fig 9. Study design for assessing effects of gestational exposure to ultrafine particles (UFPs) on offspring growth.....	58
• Fig 10. Dam weight gain data.....	61
• Fig 11. Offspring body weight (g) from postnatal week 1 to postnatal week 15.....	62
• Fig 12. Pup Crown to Rump measurements (cm) from postnatal week 1 to 15	63
• Fig 13. Whole body fat% determined via DEXA scanner	63
• Fig 14. Liver histology via oil red O for evaluating lipid accumulation	64
• Fig 15. Whole body bone mineral density (BMD) determined via DEXA scanner	65
• Fig 16. Whole body bone mineral content determined via DEXA scanner	66
• Fig 17. Right femur bone mineral density (BMD) determined via DEXA scanner	67
• Fig 18. Left femur bone mineral density (BMD) determined via DEXA scanner.....	67
• Fig 19. Right tibia bone mineral density (BMD) determined via DEXA scanner	68

- Fig 20. Left tibia bone mineral density (BMD) determined via DEXA scanner.....69
- Fig 21. Proximal femur bone mineral density (BMD) determined via DEXA scanner.....69
- Fig 22. Mid femur bone mineral density (BMD) determined via DEXA scanner.....70
- Fig 23. Distal femur bone mineral density (BMD) determined via DEXA scanner.....71
- Fig 24. Proximal tibia bone mineral density (BMD) determined via DEXA scanner.....72
- Fig 25. Mid tibia bone mineral density (BMD) determined via DEXA scanner.....72
- Fig 26. Distal tibia bone mineral density (BMD) determined via DEXA scanner.....73
- Fig 27. Thiol quantification for oxidative stress biomarkers.....75
- Fig 28. Thiol quantification for oxidative stress biomarkers.....76
- Fig 29. % change from reduced to oxidized thiols in offspring PND5 liver tissue following prenatal UFP.....77
- Fig. 30. Reduced glutathione (GSH) and oxidized glutathione (GSSG) measurements of PND5 liver samples via HPLC redox assay.....91
- Fig. 31. Reduced cysteine (CyS) and oxidized cysteine (CySS) measurements of PND5 liver samples via HPLC redox assay.....93

LIST OF TABLES

	Page
• Table 2.1. Histological evaluation of hepatic tissue for lipid accumulation for assessing oxidative stress.....	51
• Table 3.1. DEXA machine data summaries.....	74
• Table 3.2. Summaries of HPLC redox assay thiol analysis and % change.....	77

NOMENCLATURE

- Air Quality System (AQS)
- Antioxidant Response Element (ARE)
- Aryl Hydrocarbon Receptor (AhR)
- Association for Assessment & Accreditation of Lab Animal Care International (AAALAC)
- Benzo(a)pyrene Diolepoxide (BPDE)
- Bone Mineral Content (BMC)
- Bone Mineral Density (BMD)
- Boston Area Community Health/Bone Survey (BACH/Bone study)
- Brown Adipose Tissue (BAT)
- C-terminal telopeptide of type I collagen (CTx)
- Cardiopulmonary Disease (CPD)
- Cardiovascular Disease (CVD)
- Childhood Overweight or Obesity (COWO)
- Chronic Obstructive Pulmonary Disease (COPD)
- Clean Air Act (CAA)
- Comparative Risk Assessment (CRA)
- Cysteine/Cystine (CyS/CySS)
- Cytochrome P450, Family 1, Subfamily A, Polypeptide 1 (CYP1A1)
- Cytochrome P450, Family 1, Subfamily B, Polypeptide 1 (CYP1B1)
- Dansyl Chloride (DC)
- Developmental Origin of Health and Disease (DOHaD)
- Diabetes Mellitus (DM)
- Diesel Exhaust (DE)
- Diesel Exhaust Particles (DEP)
- Diesel Motor Emissions (DME)
- Diesel Particulate Matter (DPM)
- Dual-Energy X-ray Absorptiometry (DEXA)
- ENVIRONMENTAL Influence On early AGEing (ENVIRONAGE)
- Epididymal White Adipose Tissue (eWAT)
- GATA Binding Protein 4 (GATA4)
- Gestational Day (GD)
- Glucose Tolerance Test (GTT)
- Glucose Transporter 2 (GLUT2)
- Glucose-Induced Insulin Secretion (GIIS)
- Glutamate Cysteine Ligase (Gclm ^{+/-})
- Glutathione Peroxidase (GPx)

- Glutathione/Glutathione Disulfide (GSH/GSSG)
- H2A Histone Family Member X (H2AX)
- Hazard Ratio (HR)
- Heme Oxygenase-1 (HO-1)
- High-Performance Liquid Chromatography (HPLC)
- Immunoglobulin E (IgE)
- Ischemic Heart Disease (IHD)
- Kelch-like ECH-associated protein 1 (Keap1)
- Low-Fat Diet (LFD) & High-Fat Diet (HFD)
- Metallothionein-1 (MT-1)
- MicroRNA (miRNA)
- MicroRNA 21 (miR-21)
- mitochondrial DNA (mtDNA)
- Mitogen Activated Protein Kinase (MAPK)
- Nanoscale Particulate Matter (nPM)
- National Ambient Air Quality Standards (NAAQS)
- Non-Alcoholic Steatohepatitis (NASH)
- Nonalcoholic Fatty Liver Disease (NAFLD)
- Infant Low Birth Weight (LBW)
- Insulin Resistance (IR)
- Interleukins (IL-x)
- International Agency for Research on Cancer (IARC)
- Intrauterine Growth Retardation (IUGR)
- Iodoacetic Acid (IAA)
- North Carolina Detailed Birth Record (NCDBR)
- Nuclear factor erythroid 2-related factor 2 (Nrf2)
- Paraoxonase 2 (PON2)
- Particulate Matter (PM)
- Polycyclic Aromatic Hydrocarbons (PAHs)
- Postnatal Day (PND)
- Preterm Delivery (PTD)
- Protein Kinase B (Akt)
- Reactive Oxygen Species (ROS)
- Relative Risk (RR)
- Rhode Island Child Health Study (RICHHS)
- Southern California Air Quality Management District (SCAQMD)
- Superoxide Dismutase (SOD)

- Texas A&M Institute for Genomic Medicine (TIGM)
- Thyroid Hormone Receptor (TR)
- Tumor Necrosis Factor- α (TNF- α)
- Ultrafine Particles (UFPs)
- Uncoupling Protein 1 (UCP1)
- US Environmental Protection Agency (US EPA)
- White Adipose Tissue (BAT)
- World Health Organization (WHO)
- Years of Life Lost (YLL)

CHAPTER I INTRODUCTION

Particulate Matter & Air Pollution:

Sources & Size:

Air pollution has long been associated with various acute and chronic adverse health effects including pre-mature mortality, heart disease, lung cancer, chronic obstructive pulmonary disease (COPD), and asthma. A major component that drives health effects of exposure to air pollution is particulate matter (PM). As defined by the EPA and WHO, PM constitutes a complex mixture of solid particles and liquid droplets found in the air. It is vital to recognize that PM exhibits a spectrum of sizes including $>10\ \mu\text{m}$ (PM_{10}), $>2.5\ \mu\text{m}$ ($\text{PM}_{2.5}$), and $>0.1\ \mu\text{m}$ ($\text{PM}_{0.1}$) in diameter. These size fractions are classified as “coarse” (PM_{10}), “fine” ($\text{PM}_{2.5}$), and “ultrafine” ($\text{PM}_{0.1}$) (Kim et al., 2015). Overall, the fractions of PM found in ambient air pollution derived from combustion normally consist of 90-95% coarse particles, whereas smaller particles comprise 1%-8% of the total mass. Additionally, the larger fractions also contain each of the fractions smaller than itself, such as PM_{10} actually is $<\text{PM}_{10}$ and includes both $\text{PM}_{2.5}$ and $\text{PM}_{0.1}$, and the $\text{PM}_{2.5}$ size fraction includes particles of $2.5\ \mu\text{m}$ and $<100\ \text{nm}$ ($\text{PM}_{0.1}$). Importantly, fine and ultrafine PM exhibit a much higher surface area and particle numbers than coarse PM, enabling them to adsorb and interact with a variety of substances while airborne. This high surface area and high adsorption capacity makes ultrafine particles (UFPs) in particular a concern for enhanced toxicity (Kwon et al., 2020).

The small size of the fine and ultrafine particles enables them to be deposited and retained deeply within lung tissues and to cross into blood circulation. The fine and ultrafine fractions of PM have been shown to penetrate deeply into the respiratory airways and even alveoli in comparison to the coarse particulates, all of which ultimately results in various adverse

health effects (Valavanidis et al., 2008). As mentioned in Kelly et al., "...the behavior of particles in the atmosphere and within the human respiratory system is determined largely, but not wholly, by their physical properties which have a strong dependence on size, varying from a few nanometers to tens of micrometers." Particulate matter of the fine and ultrafine fractions penetrate deeply into the alveoli and terminal bronchioles, whereas the coarse particles become deposited in the primary bronchi, and even larger particles will deposit in the nasopharynx (Kelly et al., 2012). Additionally, these size fractions of PM have been well characterized and associated with a variety of toxic health effects. Generally, the smaller in size the fraction, the higher the toxicity (Kok et al., 2006).

Chemical Composition & Variability:

PM is generated from a wide variety of both natural and human processes, such as wildfires, industry, transport, waste management, dust, agriculture, soil, ocean spray, and more. PM exists in two phases following their generation, which are classified as primary and secondary particles. Primary particles are generated and released into the atmosphere directly from their sources. Secondary PM are formed within the atmosphere due to a variety of chemical reactions which subsequently produces new chemicals and compounds of low volatility. These new particles then condense into a solid or liquid phase that persists in the atmosphere for prolonged periods of time and travel by wind (Kelly et al., 2012).

One of the most widely noted and concerning sources of airborne PM is fossil fuel combustion and diesel motor emissions (DMEs) which produces diesel particulate matter (DPM), also referred to as diesel exhaust particles (DEPs). Like all PM, DME is a complex mixture of hundreds of different chemical constituents in addition to gaseous aerosols, liquid compounds, trace metals, semi volatile substances, and solid materials. These components can

include sulfur compounds, nitrogenous compounds, polycyclic aromatic hydrocarbons (PAHs), carbon monoxide, and more. As previously mentioned, combustion derived PM, i.e. DPM, consists of both fine and ultrafine particles which exhibit large surface areas and high porosity, permitting these particles to have high adsorption affinity for organics. These organics and other chemical constituents that are a part of the PM mass have been studied and have been found to exhibit carcinogenic, mutagenic, and oxidative stress inducing properties (Valavanidis et al., 2008, Wichmann et al., 2008).

Numerous studies and reviews of PM demonstrate atmospheric particles with chemical compositions containing PAHs, trace metals, acids, and other constituents such as sulfur dioxide and nitrogen oxides. However, despite the variability of PM characteristics, few if no studies have ascertained any single chemical species that determine the subsequent adverse health effects, but instead are driven by combinations of species and non-chemical factors (Davidson et al. 2007, Bell et al 2007). In particular, the surface characteristics of PM is a significant driver of toxic effects which may result from interactions with organic carbons, sulfates, nitrates, and/or transition metals (Schlesinger et al., 2008). This important chemical characteristic is further substantiated by Mostofsky et al., in which multiple models were analyzed in combination to evaluate the association between chemical constituents of PM and the likelihood of ischemic stroke. Investigators detected associations between multiple PM constituents and increased risk of stroke (Mostofsky et al., 2012). Nevertheless, emerging evidence from both human epidemiological studies and animal exposure models have consistently verified that PM is a major contributor to development of debilitating diseases and considerable years of life lost to disability.

In addition to the widely variable chemical composition of PM, ultrafine PM exhibits spatial and temporal variation between the source of generation and the end receptor, i.e. exposed human populations. Observed spatial and temporal variations, according to several published studies, are the result of a number of factors including emission source(s), weather conditions, geography, and many more that can induce a transformative effect on airborne PM. According to a recent review, the greatest source of variability in ultrafine particulate matter stems from the mixture of hot gases and particles from vehicular emissions. Furthermore, mechanical and atmospheric turbulence together with the processes of coagulation, nucleation, evaporation, and deposition continually drives the particle size distribution of diesel exhaust PM (Heal et al 2012). Additionally, season and region are also significant influences on PM chemical composition. Bell et al. noted that the degree of spatial and temporal variability in PM chemical constituents associated with season and region provided epidemiological implications in regards to hospital admissions (Bell et al 2007, Jalaludin et al, 2007). This evidence was verified in an experimental study in which PM_{2.5} and PM₁ were observed to reduce cell viability and induce DNA damage in A549 cells which varied significantly from season to season (Perrone et al 2013).

Health Effects:

Over the past several decades, studies have estimated that outdoor ambient PM exposure is responsible for a variety of different disease mortalities including adult cardiopulmonary disease, respiratory cancer, respiratory infections, etc. In a 2005 review by Cohen et al., a comparative risk assessment (CRA) conducted as part of the WHO's Global Burden of Disease project, PM_{2.5} air pollution contributes to approximately "0.8 million (1.2%) premature deaths and 6.4 million (0.5%) years of life lost (YLL)," (Cohen et al 2005). Overall, multiple

epidemiological studies of populations have produced ample amounts of evidence to confirm that PM is associated with increasing mortality and morbidity amongst exposed populations (Pope et al. 2006, Lu et al., 2015). Exposure to DE induces adverse health effects associated with both acute and chronic exposures. Noncancer effects following acute exposure to DE are observed in both human and animal studies, including irritation and inflammation of the respiratory system, as well as cardiopulmonary and neurophysiological symptoms (Ali et al., 2011).

According to an US EPA health assessment for diesel engine exhaust conducted in 2008, acute exposure to DE or DPM can aggravate immune response to common allergens, as well as trigger allergic responses to DE itself. This report took note of findings from previous studies in which human subjects given DPM intranasally demonstrated measurable increases in IgE antibodies and elevated proinflammatory cytokines. Chronic exposure to DE and DPM has also demonstrated an association with decreased pulmonary function and lung injury. Animal studies using various models investigating chronic exposure to DE and DPM have provided evidence of pulmonary injury and fibrosis (Ris et al 2008).

Cytotoxicity/Genotoxicity:

Driven by its highly variable assortment of chemical components and constituents, PM has been confirmed to have cytotoxic and genotoxic effects. Data gathered from numerous studies show that smaller size fractions of traffic related PM, i.e. PM_{2.5} and PM_{0.1} have mutagenic properties. This is more prevalent when chemical constituents, both organic and inorganic components, are factored into assessments for mutagenicity potential. This pattern is also observed in regards to assessing PM cytotoxicity (Kok et al., 2006).

Following this line of investigation, Borgie et al. exposed human bronchial epithelial cells (BEAS-2B) to PM_{2.5-0.3} collected from an urban and a rural site to evaluate genotoxic and

carcinogenic effects. Investigators observed increased phosphorylation of H2AX, telomerase activity, in addition to the upregulation of miR-21 in a dose-dependent manner along with significant expression in CYP1A1, CYP1B1, and AhR genes (Borgie et al., 2015). Evidence of carcinogenic properties and cytotoxic effects of PM was further collected by Landkocz in a 2016 study. The focus of this study was to characterize the mutagenicity and cytotoxicity of urban PM and its organic and inorganic constituents. To accomplish this goal, mutagenicity assays including the Ames test and a human bronchial cell (BEAS-2B) exposure model to assess for PM induced cell viability and proliferation via lactate dehydrogenase release and mitochondrial dehydrogenase activity following PM exposure. This study showed pronounced cytotoxic effects of PM_{2.5}, and the ultrafine fraction, including reduced membrane integrity and altered mitochondrial metabolism. Additionally, cell proliferation was observed to be significantly inhibited at low doses (Landkocz et al., 2017). Further evidence of PM_{2.5} cytotoxicity and genotoxicity were provided by Belcik et al. in a study of agglomerated PM_{2.5} and its chemical constituents. This study focused on assessing the mutagenicity properties via Ames assay, comet assay, and 4 parameter cytotoxicity test PAN-I assay. Notably, differences in genotoxic, cytotoxic, and mutagenic characteristics between seasons of collection and between volumes of dust pollution fractions (Belcik et al., 2018).

Inflammation:

In addition to having carcinogenic properties, PM_{2.5} and PM_{0.1} induce an inflammatory response in both humans and various animal models. This propensity to cause inflammation in living systems makes PM a significant contributor to lung-related diseases such as chronic obstructive pulmonary disease (COPD) and asthma. Traffic related PM and DEP have been documented and characterized to have a large range of chemical constituents which are

individually toxic, such as metals and PAHs, and even more so as mixtures adhering to the PM surface. Multiple studies demonstrate that PM can cause adverse health effects in the lungs, as the primary target of toxic effects by inducing oxidative stress and inflammation. Human lymphoblastoid cells (RPMI 1788) and human alveolar epithelial adenocarcinoma cells (A549) were analyzed for changes in inflammatory response gene expression, intracellular ROS generation, and oxidative DNA damage following PM exposure. Investigators concluded that DEP induces ROS generation and increased expression of inflammatory cytokines including IL-6 and IL-8. Findings from the human component of this investigation verified this and previous models in which there were increased levels of oxidative DNA damage and increased IL-8 expression in lymphocytes of exposed human subjects (Vattanasit et al., 2014).

Furthermore, studies have provided ample evidence of the association between PM or DEP exposure, ROS production, and inflammation in various tissues, in human studies and animal models. A recent review evaluated numerous articles to delineate the relationship between PM exposure, inflammation, and oxidative stress to determine if they are independent or linked together in the contexts of models and human population exposures. Multiple biomarkers of systemic inflammation were associated with PM dose. These studies, though varied in experimental models and effect sizes, strongly suggested that PM exposure induces both oxidative stress and inflammation simultaneously in a process in which one promotes the effects of the other, ultimately generating DNA damage (Moller et al., 2014). Another aspect of systemic inflammation induced by direct PM exposure is that of neurological effects that have been observed in various animal studies. One such study is that by Cole et al. where male and female C57Bl/6 mice were acutely exposed to DE and observed for changes in neuroinflammation. The investigators observed sex-specific differences in neurotoxicity through

lower expression of paraoxonase 2 (PON2). This study concluded that male mice were more susceptible to DE-induced neuroinflammation and oxidative stress leading to increased lipid peroxidation and microglia activation. These findings also revealed key genetic factors such as heterozygosity for glutamate cysteine ligase ($Gclm^{+/-}$) (Cole et al., 2016). The inflammatory properties of PM are further detailed in another recent literature review. In 2018, Losacco et al. summarized the evidence of PM exposure on lung function in humans and animals. As mentioned in previous sections, inhalation of ultrafine particles leads to a multitude of different health effects following dissemination into the alveoli and then proceeding to diffuse into systemic circulation. This systemic infiltration has been thoroughly studied and shown to increase inflammation and oxidative stress both locally (i.e., pulmonary) and systemically. These particles remain in the lung parenchyma for extended periods of time and thus reduce lung function, as well as induce acute and chronic pathologies. Deposition of PM and UFPs in deeper portions of the lungs introduces chemical agents which proceed to generate local and systemic tissue damage. Data and results from numerous studies have found pulmonary inflammation and injury following PM exposure is characterized as a local increase in neutrophils and macrophages. (Losacco et al., 2018). With respect to the respiratory system, PM exposure initiates the inflammatory response and modulates the alveolar macrophage function which ultimately reduces the hosts lung defense against infectious agents.

Lung cancer:

Particulate matter is classified as a human lung carcinogen according to the EPA and IARC. However, due to the complex and heterogenous nature of PM, there is a substantial collection of chemical constituents which constitute numerous driving factors of carcinogenic activity. A large number of studies have investigated the characteristics and chemical makeup of

PM and have identified key elements and chemicals that are commonly detected in PM fractions. One such study from 2016 conducted by Nielsen et al. using 14 cohort studies from multiple European countries to evaluate PM constituents and association with lung cancer. The members of these cohort studies provided over 3 million person-years at risk. The investigators assessed air pollution and PM for eight elements including; Zn, Ni, S, Si, Cu, Fe, V, and K. From the total cohort members, 1878 cases of lung cancer were diagnosed, and an accompanying meta-analysis revealed elevated hazard ratios (HR) for lung cancer were associated with all aforementioned elements, with the exception of V. Despite the trends of elevated HR's for these PM constituents, these were not significantly different for PM measured at residence. However, PM concentrations and elements from multiple sources produced stronger associations (Raaschou-Nielsen et al., 2016). Characterizing the chemical composition of PM and its associations in epidemiological studies has also revealed its ability to induce genetic instability. A 2017 review gathered literature from multiple database sources to evaluate how PM induces genetic instability in the form of DNA adducts, chromosomal aberrations, and more, as observed in mechanistic studies. From the studies featured in this review, PM was found to induce epigenetic alterations and changes in gene expression associated with lung carcinogenesis in both human and animal models. This includes altered post-transcriptional regulation of gene expression, more specifically of single stranded noncoding RNA sequences known as miRNA's which are associated with important signal pathways in normal processes and in diseases such as cancer (Santibanez-Andrade et al., 2017).

Heart Disease:

In addition to causing toxic injury to the lungs, PM_{2.5} and UFPs lead to adverse chronic health effects which increases global mortality (Heo et al., 2014). Many studies and reviews have

summarized evidence which associates PM exposure with increased mortality from cardiovascular disease (CVD), cardiopulmonary disease (CPD), and ischemic heart disease (IHD). A review by Kim et al. referenced several previous published articles that reported long-term exposure to PM_{2.5} results in increased risk of all-cause mortality (HR 1.26 [95% CI: 1.02, 1.54]) and coronary heart disease (CHD) mortality (HR 2.02, [95% CI: 1.07, 3.78]) (Kim et al., 2015).

Relevant Regulations:

As countries and communities have become more and more industrialized and urbanized, motorized vehicles and other sources of PM have directly led to a variety of environmental health-related disorders and constituted a major public health concern. To protect our public health and the well-being of communities, air quality standards were established in many countries. These air quality standards have become an integral part of national risk management and environmental policies. However, there has never been any success in establishing a safe or minimal threshold level of exposure below which no adverse health effects are observable. Guidelines are set for different PM fractions, namely PM₁₀ and PM_{2.5}, have been set to reduce harmful effects on public health and our environment. In the US, the US Environmental Protection Agency holds the mantle of producing, researching, and enforcing standards for air quality to best protect public health. The first significant regulatory effort in the US to address air pollution was the Clean Air Act (CAA) of 1970 which provided requirements to both study air pollution and to set limits emissions. This set of regulations lead to the establishment of the and definition of the National Ambient Air Quality Standards (NAAQS). These standards established limits on six primary pollutants (Anderson et al., 2012, Heal et al., 2012). PM is classified as one of the six criteria pollutants alongside ozone, carbon monoxide, lead, sulfur oxides, and nitrogen

oxides. Currently, the annual primary standard for PM_{2.5} is 12 µg m⁻³, whereas the daily (24-hour) standard is set to 35 and 150 µg m⁻³ (Kim et al., 2015).

Summary of Human Evidence – Epidemiologic Studies on Gestational Exposure:

A major area of public health concern and a growing scientific priority is the effects of PM_{2.5} and UFP exposure during the critical window of susceptibility, like pregnancy and fetal development. Only in recent years have researchers begun to systematically study how PM exposure during the prenatal period impacts the health and development of children. One of the earliest articles into this topic was written by Selevan et al. in 2000 as the product of a workshop that combined multiple disciplines and enabled discussion to identify areas of concern and future research directions. This article identified multiple critical knowledge gaps that would in time be investigated, including identification of windows of sensitivity, cross-species comparisons of exposure-dose outcomes, perinatal and adolescent exposure and consequences in adulthood, as well as agent-target interactions (Selevan et al., 2000).

Over more recent years, scientists have begun to understand the mechanisms by which exposure to PM and UFPs during critical windows of development impact perinatal outcomes and progeny long-term health. Several documented adverse health outcomes following gestational exposure to PM include preterm delivery (PTD), infant low birth weight (LBW), and intrauterine growth retardation (IUGR). With consideration for nutrition, each of these outcomes is associated with infant mortality and a range of morbidities such as neurological and cardiopulmonary diseases. One of the studied mechanisms of disease that drives known morbidities following PM exposure is oxidative stress, inflammation, and DNA damage (Kannan et al., 2006). Furthermore, studies have demonstrated that oxidative stress induced by fetal PM exposure contributes to placental disruption as well as endothelial dysfunction. Disruptions of

this nature to the proper function and state of *in utero* development has potential to negatively impact fetal growth and organogenesis. Generally, PM-induced placental disruption is associated with higher prevalence of IUGR, infant mortality, stillbirths, and preterm births in animal studies and human epidemiological cases. Additionally, animal studies have provided evidence on multiple pathologies that are difficult to measure in humans. A review by Backes et al. stated that “Studies exploring the health effects of air pollution, specifically PM, are difficult to summarize since measurement techniques and definitions have changed over time.... Additional difficulty in examining the effects of air pollution arises with the large number of confounding factors that can influence the type and amount of air pollution exposure...”. Finally, despite the large body of epidemiological evidence and observations which associates prenatal PM exposure to adverse health outcomes in children, the intricate mechanisms by which these disease states occur is still being clarified (Backes et al., 2013). In reference to previous discussion of the genotoxic properties of PM, there is evidence of carcinogenic effects in the context of *in utero* exposure and transplacental carcinogenesis. In a 2018 study by Neven et al., exposure to PM was found to be linked to a higher risk of mutations in Alu, a marker for overall DNA methylation in key tumor suppressor genes including p53, DAPK1, PARP1, APEX1, and more. This cohort study, which collected data from the ENVironmental Influence On early AGEing (ENVIRONAGE) birth cohort study of mothers and neonates in Belgium, found evidence of PM-induced epigenetic changes in key DNA repair pathways and tumor suppressor genes in fetal DNA repair systems (Neven et al., 2018). Additional outcomes related to pregnancy and offspring development are detailed in subsequent sections.

Pregnancy outcomes:

Preterm birth:

As mentioned previously, there is an established and well-studied relationship between PM exposure during pregnancy and preterm birth. One such study (Huynh et al. 2006) examined the effects of PM_{2.5} on preterm birth in a matched case-control study using monitoring data from the California Air Resources Board linked to California birth certificates. Following adjustment for maternal factors, Huynh's analysis found that exposure to high levels of PM_{2.5} was associated with a small effect on preterm birth, adjusted OR=1.15, [95% CI 1.07, 1.24]). The relationship is further substantiated by a multitude of studies. For instance, an epidemiological investigation by Wu et al. in 2009 examined the effects of residential exposure to local traffic-generated air pollution on preeclampsia and preterm delivery. Utilizing 81,186 birth records from hospitals in California's Los Angeles and Orange Counties to estimate individual exposure to local traffic-generated PM_{2.5} and UFPs throughout pregnancy, the investigators saw a 42% increase in risk for preeclampsia OR=1.42 [95% CI 1.26-1.59] and 81% increase risk for very preterm delivery (gestational age<30 weeks) OR=1.81 [95% CI, 1.71-1.92] for women in the highest PM_{2.5} exposure quartile (Wu et al., 2009). Additionally, in a statewide analysis, Chang et al. took data North Carolina's Air Quality System (AQS) monitoring network between 2001-2005 to examine the risks of preterm birth following PM_{2.5} during pregnancy. Using these measurements, the investigators found an interquartile range (IQR) (1.73 µg/m³) increase in cumulative PM_{2.5} was associated with a 6.8% increase in the risk of preterm birth. Additionally, with the use of Fused Air and Deposition Surfaces (FSD) database, this investigation found a significant adverse association between trimester 1, trimester 2, cumulative PM_{2.5} exposure and preterm birth (Chang et al., 2011). Another study based on data from women in Los Angeles, utilized multiple data sources to examine the risks of preterm birth outcomes following extended periods of exposure to high levels of traffic-related air pollution. Records of birth between 2004 and 2006

of women living within 5 miles of Southern California Air Quality Management District (SCAQMD) Multiple Air Toxics Exposure Study (MATES III) monitoring station. Results of this study, with adjustments for maternal age, race & ethnicity, education, parity, etc., there was a 21% and 11% increase in odds for preterm birth per IQR increase in ammonium nitrate PM_{2.5} and diesel PM_{2.5} (Wilhelm et al., 2011). An additional study conducted using data from pregnant women in Harris County, Texas. This study evaluated 177,816 births between 2005-2007 and categorized the exposures to PM_{2.5} into 3 categories; mildly (33-36 completed weeks of gestation), moderately (29-32 weeks of gestation), and severely (20-28 weeks of gestation) PTB. The results from this analysis showed that a 10 µg/m³ increase in PM_{2.5} exposure within the first 4 weeks of pregnancy significantly increased the odds of all categories of PTB by 16%, 71%, and 73%. The associations between PTB and PM_{2.5} exposure were strongest for moderately PTB and severely PTB (Symanski et al., 2014). A 2015 meta-analysis by Sun et al. that sought to quantitatively summarize the association between PM_{2.5} exposure and preterm birth further concluded an increase in risk. Results of this meta-analysis displayed increased risk of preterm birth in all relevant parameters including trimesters 1-3, at the individual level, regional level, retrospective or prospective studies. However, the studies evaluated displayed a significant amount of heterogeneity between methods, study designs, and study settings (Sun et al. 2015).

Small gestational age:

In 2004, a study by Parker et al. examined the associations between birth weight and air pollution in California, specifically that of PM_{2.5}, and found that an increased risk for small gestational age (SGA) and a difference in mean birth weight between infants with the highest and lowest exposures to PM_{2.5} (Parker et al., 2004). Further evidence was provided by Hyder et al. in 2014 who utilized US EPA air monitoring data and satellite data, combined with birth

certificate data. This study observed associations between PM_{2.5} exposure and infant low birth weight (LBW) and SGA, which added to the growing body of evidence on air pollution exposure and infant health (Hyder et al., 2014). In regards to SGA, a systematic review of 41 studies performed by Shah et al. in 2011, found that PM_{2.5} was indeed associated with SGA births despite heterogeneity of evaluation methods. This review indicated strong associations between high PM_{2.5} exposure with LBW and SGA (Shah et al., 2011).

Low birth weight:

An important birth outcome of significant concern to public health is low birth weight (LBW) observed in children following maternal exposure to PM_{2.5}. There is also an increased risk for long-term effects on children's health stemming from LBW. According to a 2009 review, "high rates of adverse outcomes meant 454,583 infants were born preterm and that 267, 218 infants were born low birth weight, creating a sizable population starting life with an increased risk of short-term and long-term health and developmental complications..." (Miranda et al., 2009). Thus, based on how prevalent maternal PM exposure is and the potential health complications which arise afterwards, many studies have been conducted to expand on the association between prenatal PM exposure and LBW. A study in 2009 evaluated birth data from the North Carolina Detailed Birth Record (NCDBR) between the years 2000-2002. The data from this study linked maternal residence to the closest air monitors throughout the duration of their pregnancy and estimated the county-level averages of air pollution concentrations. Ultimately, the study found that increased ambient concentrations of PM_{2.5} led to a reduction in birth weight by 4.6 g (95% CI: 2.3-6.8) throughout the entire pregnancy and a 10.4 g (95% CI: 6.4-14.4) reduction based on exposure in the 3rd trimester (Gray et al., 2010). In relation to the actual constituents of PM, Bell et al. examined whether the sources, constituents, or mass of

PM_{2.5} was associated with lower birth weight and found constituents including zinc, vanadium, nickel, silicon, and aluminum were driving this relationship (Bell et al., 2010). Additionally, Darrow et al. observed reduced birth weight in infants associated with higher concentrations of PM_{2.5} during late pregnancy (Darrow et al., 2011). Furthermore, these results are reflected in a later study by Liu et al. which evaluated the burdens of PTB and LBW attributed to ambient PM_{2.5} in Shanghai, China. The study authors calculated the population-weighted annual average concentration of ambient PM_{2.5} in 2013 was 56.19 µg/m³. This measurement exceeded China's Ambient Air Quality Standard of 15 µg/m³. The investigators estimated that 32.61% of PTBs and 23.36% of LBW that occurred in Shanghai in 2013 may have been attributable to this excess PM_{2.5} exposure (Liu et al., 2017). Placenta/birth weight ratio has also been found to be an important measure of significance in evaluating health impacts of traffic-related air pollution to measure impacts on placental transport of nutrients. This measure was studied extensively in a 2012 article by Yorifuji et al. and was found to be higher in association with traffic-related air pollution and residential proximity to major roads (Yorifuji et al 2012). Additional evidence of LBW associated with prenatal PM_{2.5} exposure includes evidence relative to the specific constituents of PM_{2.5}. Several studies have demonstrated significant reductions in birth weight are associated with elemental carbon, sulfate, zinc, copper, iron, bromine, vanadium, sulfur, ammonium and many more traffic related particles (Basu et al., 2014, Laurent et al., 2014). Evidence from numerous studies compiled in a systematic review by Lamichhane et al. published in 2015, reflects the overall evidence and outcomes of LBW associated with maternal PM_{2.5} exposure throughout pregnancy. From a review of 44 studies focused on maternal PM_{2.5} exposure, birth weight was found to decrease by as much as 10 to 22 g in association with trimester, source of PM, and concentration of exposure (Lamichhane et al., 2015).

Fetal growth effects:

The body of literature on the effects of maternal PM exposure has grown considerably. Within this expanding field includes the direct *in utero* effects of PM on the fetus itself and how the insult impacts fetal growth. There are a plethora of studies and ample evidence that prenatal PM exposure negatively impacts fetal growth and subsequent development. Fleisch et al. provided assessments of infant weight and length at birth from data derived from the US Project Viva cohort following prolonged exposure to traffic related PM. Authors found that the infants exposed to the highest quartile of neighborhood traffic density displayed lower fetal growth, in addition more rapid birth to 6-month weight for length gain and higher odds of weight for length at 6 months. In regards to PM_{2.5}, specifically exposure in the 3rd trimester, the results of this study indicated a possible association between higher traffic-related pollution and PM_{2.5} in the early life window lead to reduced fetal weight followed by rapid weight gain post birth (Fleisch et al., 2015). A review from that same year further substantiated this phenomenon, but with the added perspectives of diet and nutrition, psychological stress, and smoking which yielded relevant information in regards to negative developmental health. Ultimately, the evidence indicated that a multitude of environmental exposures including PM_{2.5} may induce similar insults and pathological outcomes such as deficient deep placentation. This condition, referred to as either defective or deficient deep placentation, can result in a cascade of maladaptive changes that contribute to a spectrum of pregnancy outcomes and developmental complications. Of great interest in this review, evidence suggested that the molecular insults from *in utero* exposures, in combination with a multitude of factors likely produce excessive oxidative stress and inflammation which may lead to a number of disease phenotypes. PM_{2.5} exposure can elicit oxidative stress in the form of excessive generation of reactive oxygen species (ROS) as a result

of disturbances to antioxidant defense systems such as cytochrome P450 (CYP450). This imbalance leaning towards a more oxidative environment can further exacerbate disease states as a prolonged or atypical inflammatory response which ultimately contributes to downstream disease phenotypes like fetal growth restriction (Erickson et al., 2014).

This information was further expanded by Kingsley et al. in which maternal air pollution exposure was measured along with the expression of placental imprinted genes in the Rhode Island Child Health Study (RICHS). PM_{2.5} was associated with altered gene expression of 41 genes including VTRNA2.1, CHD7, ZDBF2, and many more that are key in fetal development (Kingsley et al., 2017). Following this line evidence, microRNAs (miRNA) have also been investigated during recent years. Multiple placental miRNAs have been observed to display altered expression patterns resulting from PM exposure. Tsamou et al. investigated multiple placental miRNAs as part of the ENVIRONAGE birth cohort. This study concluded PM exposure was associated with significant changes in the expression of several miRNAs including miR-21, miR-146a, miR-222, miR-20a, and tumor suppressor phosphatase and tensin homolog (*PTEN*). Placental expression of miR-21, miR-146a, and miR-222 were inversely associated with PM_{2.5} exposure during the 2nd trimester, whereas PM exposure in the 1st trimester showed increased expression of miR-20a and miR-21. However, placental *PTEN*, while not being a miRNA is itself a downstream target of placental miRNAs, displayed a strong association and increased expression following PM exposure during the 3rd trimester (Tsamou et al., 2018). Furthermore, more recent studies are beginning to delineate the molecular pathways and transcriptomic changes in the placenta in relation to health effects. A recent study into this topic by Deyssenroth et al. identified a sensitive window that spans 12 weeks prior to and 13 weeks into gestation during which maternal PM_{2.5} exposure is significantly associated with reduced

infant birthweight. The key gene networks include genes which contribute to mitochondrial processes, cellular respiration, cell motility, autophagy, amino acid transport, and many more (Deysenroth et al., 2021).

Delving into another aspect of mounting molecular evidence of *in utero* PM exposure, multiple studies have used cord blood collected at delivery for analysis of DNA from cord leukocytes and mitochondrial DNA (mtDNA). Rosa et al. performed qPCR to determine mtDNA content. Analysis models that incorporated weekly PM estimates revealed the significant associations between PM-induced oxidative stress and lower mtDNA content in cord blood following exposure during late pregnancy, notably between 35-40 weeks. This data suggested that the third trimester is a period of increased sensitivity to PM and oxidative stress, which likely contributes to adverse fetal health outcomes (Rosa et al., 2017). This evidence was further expanded by Hu et al. in a similar study where the authors saw alterations in newborn cord blood mtDNA copy numbers, presenting even more evidence on the concept of increased sensitivity of the fetus to environmental exposures and potential for health effects later in life (Hu et al., 2020).

Obesity:

In addition to the growing evidence of *in utero* PM exposure contributing to fetal growth effects, there is mounting evidence that PM exposure in early life may also predispose individuals to childhood obesity. A variable rarely considered, maternal obesity before pregnancy, may pose an important modifying factor in the health and development of infants following chronic *in utero* PM exposure. In 2016, Mao et al. observed that the risk of childhood overweight or obesity (COWO) was significantly increased in children of overweight and obese mothers [RR=1.3 (95% CI: 1.2, 1.6)] and [RR=1.6 (95% CI: 1.3, 1.8)]. These results raised the important question of how adiposity and PM exposure interact to potentially influence the health

outcomes of children. Furthermore, these findings provided insight into the complex implications of *in utero* PM exposure and the development of disease later in life (Mao et al., 2016). Mao's findings connect to another study conducted by Lavigne et al. in 2016. In Lavigne's 2016 investigation, umbilical cord blood from over 1200 mother-infant pairs were studied to evaluate leptin and adiponectin levels in relation to PM_{2.5} exposure during pregnancy. Data from this study demonstrated an interquartile-range increase in average exposure to PM_{2.5} (3.2 µg/m³) during pregnancy was associated with an 11% increase in adiponectin levels. Additionally, the investigators also observed a 11% higher leptin levels. Both of these markers, adiponectin and leptin, are hormones classified as adipokines, secreted by adipocytes, and are important in maintaining energy, lipids, and glucose homeostasis. Authors observed a significant association between biomarkers of air pollution and cord blood leptin levels. This study contributed more to the growing field of interest in how air pollution and airborne PM influences metabolic processes and its role in the development of obesity (Lavigne et al., 2016).

Diabetes:

As noted by a number of studies over previous years, there is a rising prevalence of childhood diabetes mellitus (DM) in the US. These trends are of serious concern to public health not because of the health complications and burdens associated with diabetes. According to Puett et al., the relationship between ambient PM_{2.5} and diagnosed diabetes have drawn attention to the growingly significant concern for air pollution and human health effects. The data from this study showed a positive association with diabetes prevalence and increasing concentrations of PM_{2.5}. This study found that a 10 µg/m³ increase in PM_{2.5} exposure was accompanied by a 1% increase in diabetes prevalence (Puett et al., 2010). This relationship was consistently observed in 2004 and 2005 datasets from the CDC and EPA, and the results remained significant even

with different estimates of PM_{2.5} and models. Interestingly, even counties that were compliant with US EPA PM_{2.5} exposure limits showed an increase in diabetes prevalence, whereas counties with the highest exposure displayed a >20% increase in diabetes compared to those with the lowest levels of PM_{2.5} (Pearson et al., 2010). There is a current lack of data on the relationship between prenatal exposure to PM and diabetes risk in childhood.

Bone Health:

An additional endpoint of increasing interest is the growing body of evidence on the association between PM exposure and bone health. Childhood is a crucial period for the proper development of bones as this is time when the majority of bone mass accumulation takes place. However, the relationship between air pollution, namely fine and ultrafine PM, on bone development is not fully understood and still yet to be studied effectively. Of the few studies measuring bone health in relation to exposure, whether prenatal or post-natal, study methods often include the evaluation of bone density in addition to biomarkers related to bone turnover or bone loss. One such study utilizing these markers was conducted and published by Liu et al. in 2015. Investigators reported a positive association between PM_{2.5-10} exposure and bone turnover markers. The specific bone markers analyzed in this study were osteocalcin and C-terminal telopeptide of type I collagen, referred to as CTx. Liu et al. observed a positive and significant association between PM_{2.5-10} exposure and both markers, 32.3 (95% CI: 6.1, 58.5) ng/L for CTx and 3.0 (95% CI: 0.1, 5.8) ng/ml for osteocalcin. Overall, the author concluded that exposure to ambient air pollution and road traffic led to enhanced bone turnover or bone loss in children (Liu et al 2015). These findings were further expanded in a 2017 publication by Prada et al. in which two independent studies were conducted. The main objective of Prada's first study was to examine the relationship between long term concentrations of PM_{2.5} and the development of

osteoporosis-related fracture hospitalizations among 9.2 million Medicare enrollees. The population of this study consisted of individuals aged ≥ 65 years and took place between January of 2003 and December 2010. This study analysis revealed that the risk of bone fracture admissions at osteoporosis related sites was greater in areas with higher PM_{2.5} levels (RR=1.041, 95% CI:1.030,1.051). The second study examined the association of long term PM_{2.5} with serum calcium homeostasis biomarkers parathyroid hormone, calcium, and 25-hydroxyvitamin (25(OH)D) and annualized bone mineral density over the course of 8 years in men from the Boston Area Community Health/Bone Survey (BACH/Bone study) cohort. This investigation demonstrated that baseline PM_{2.5} concentrations were associated with lower parathyroid hormone. These findings lend additional weight to the growing body of evidence that air pollution may constitute a risk factor for bone fractures and osteoporosis (Prada et al 2017). In summary, despite the lack of studies linking *in utero* PM exposure with adverse bone health outcomes, current studies linking PM and osteoporosis/bone loss provides the rationale to investigate early life exposure effects on bone. Additionally, this suggests a need for further exploration of a potential window for susceptibility and impacts to bone development (Chang et al., 2015).

Summary of Nonhuman Evidence – Animal Models:

Developmental Effects:

Numerous animal studies have provided an extensive amount of evidence on the health impacts of PM_{2.5}. However, the mechanisms which connect exposure to adverse health outcomes are still being explored and understood. As referenced in earlier sections, one of the major sources of PM_{2.5} and UFPs is automobile exhaust in the form of diesel exhaust (DE). Like any form of particulate matter, DE is both a complex and heterogenous mixture of chemical

constituents such as soot, aerosols, gases, and ultimately diesel exhaust particles with toxic adherents. Numerous animal studies have provided evidence of DE and DEP induced health effects such as inhibited growth and weight, altered organ development, impacted sexual development, and many more. Additional data from animal studies following pre or postnatal DE, DEP, PM_{2.5}, and UFPs have evaluated developmental genes and neurological development. In 2013, a review by Ema et al. compiled evidence from multiple studies of neurological impacts in the offspring of mice whom were exposed to DE *in utero*. For instance, ICR mice were sacrificed and their brain tissues evaluated for pathological changes. Investigators observed numerous brain cells positive for caspase-3, a common enzymatic biomarker of apoptosis, which are suggestive of apoptotic processes, as well as signs of apoptosis in granular perithelial (GP) cells, and swelling of astrocyte endfoot in the cerebral cortex and hippocampus of offspring of dams exposed to DE. Another study mentioned in this same review featuring Slc:ICR dams, following exposure to DE, investigators observed lower levels of the dopamine metabolite known as homovanillic acid along with decreased locomotor activity. Additional studies observed increased expression mRNA for cytochrome P450 1A1 (CYP1A1), heme oxygenase-1 (HO-1), metallothionein-1 (MT-1), aromatase, and thyroid hormone receptor (TR). Such changes in gene expression within brain tissues of offspring mice indicates that the DE reaches past the placenta and into the developing fetus and the brain of the pups, resulting in disruptions of the brain's endocrine system. Other studies of similar design demonstrated other DE- and DEP-induced effects on the central nervous system and behavior of the progeny such as changes to the dopaminergic system, impacted steroid and thyroid hormone related gene expression (Ema et al., 2013). Further evidence for neurological health outcomes comes from Bolton et al. as part of a series of publications focused on *in utero* DEP exposure, diet, and brain health. As part of this

series, C57Bl/6 dams were exposed to DEP during pregnancy in order to investigate the hypothesis that prenatal exposure to DEP would prime the microglia and cause an exacerbated metabolic consequence following consumption of a high fat diet. The model examined the pups of either clean air or concentrated DEP air and followed by a low-fat diet (LFD) or high fat diet (HFD) in adulthood for 9 weeks. The male DEP exposed and HFD offspring in this study exhibited exaggerated weight gain, insulin resistance, and anxiety-like behavior in comparison to control. Additionally, these same mice were found to exhibit macrophage infiltration within the adipose and brain tissues. More importantly, DEP and HFD treated males expressed significantly higher levels of microglial and macrophage activation markers within the hippocampus. Ultimately, the evidence from studies suggests that prenatal exposure to air pollution predisposes or “programs” offspring to increased susceptibility to diet-induced metabolic, behavioral, and neuroinflammatory changes in adulthood in a sexually dimorphic manner (Bolton et al., 2014).

Cardiopulmonary Development:

As mentioned in previous sections, PM is well characterized and documented to induce a variety of adverse cardiopulmonary health effects. Traffic related PM and PM_{2.5} has been a global public health concern due to the significant association with cardiovascular related mortality and morbidity. Of the many animal studies that have been conducted and published to examine cardiovascular and cardiopulmonary outcomes of PM_{2.5} exposure, there are few that examine prenatal exposure in particular. For example, Weldy et al. conducted multiple studies into this growing area of interest and found *in utero* exposure to DE results in significantly increased susceptibility to various adverse cardiac outcomes. The outcomes observed include cardiac hypertrophy, myocardial fibrosis, pulmonary congestion, and systolic failure. It is important to note, Weldy’s study model included exposures to the dams both before and during

pregnancy, followed by the offspring being exposed to either filtered air or DE until 12 weeks of age. Additionally, this model applied transverse aortic constriction surgery to induce pressure overload. Furthermore, this investigation found that *in utero* and early life DE exposure modified the inflammatory cytokine response within the lungs of adults. These results provided preliminary evidence for the “fetal origins” hypothesis of adult disease pathways stemming from air pollution (Weldy et al., 2013). Additional findings by Gorr et al. demonstrated that not only did gestational PM_{2.5} exposure reduce the birth weight of FVB mice, but exposure also altered cardiovascular tissues. Namely, FVB mice who were perinatally exposed to PM_{2.5} exhibited reduced left ventricular fractional shortening, reduced ejection fraction, increased end-systolic volume, and reduced dP/dt maximum and minimum. Also, cardiomyocytes from the PM_{2.5} exposed mice exhibited reduced peak shortening, slower calcium reuptake, increased collagen deposition, and reduced response to β -adrenergic stimulation compared to filtered air exposed mice (Gorr et al., 2014). In another study from 2016, Chen et al. investigated the relationship between maternal exposure to PM_{2.5} during pregnancy and lactation period and the development of cardiovascular disease induced by administration of homocysteine in a rat model. The offspring of the PM_{2.5} exposed dams displayed myocardial apoptosis among other pathological changes including significantly decreased Nkx2-5 protein and mRNA expression along with reduced GATA4. These molecular changes progress into structural abnormalities in the filial cardiac tissue (Chen et al., 2016).

Metabolic Effects (Glucose Metabolism/Lipid Metabolism):

Various animal studies have been conducted over recent years to explore the connection and mechanisms between prenatal PM_{2.5} exposure and impacts on metabolic processes. One such investigation into this increasingly important health concern was published by Xu et al. in 2011.

Although this study was not a prenatal exposure model, it did demonstrate a number of relevant health effects of PM_{2.5} exposure on adult C57Bl/6 mice following a prolonged period of exposure, approximately 10 months. Investigators demonstrated that PM_{2.5} induced insulin resistance (IR) accompanied by decreased glucose tolerance. Additionally, this study demonstrated significantly decreased adiponectin and leptin levels, as well as oxidative stress via increased expression of Nrf2 regulated genes. Chronic PM_{2.5} exposure appears to have also decreased mitochondrial counts within visceral adipose tissues and mitochondrial size in interscapular adipose depots. These observations were associated with reduced expression of uncoupling protein 1 (UCP1) and the downregulation of genes specific to brown adipose tissue. Ultimately, these findings, although not prenatal exposure, suggest that prolonged PM_{2.5} exposure may impair glucose tolerance, IR, inflammation, and mitochondrial alterations, all of which collectively are conducive to higher risk of type 2 diabetes (Xu et al., 2011). According to Sun et al., PM_{2.5} exposure exaggerates insulin resistance in addition to inflammation and adiposity. By utilizing a C57Bl/6 mouse model in which male mice were fed a high fat diet for a period of 10 weeks and then exposed to either concentrated PM_{2.5} or filtered air. The mice exposed to PM_{2.5} exhibited systemic inflammation, visceral adiposity, and insulin resistance. Additional abnormalities resulting from PM_{2.5} exposure included decreased Akt and endothelial nitric oxide synthase phosphorylation in the endothelium along with increased protein kinase. Also, these mice displayed increased levels of macrophages in adipose tissue and upregulation of tumor necrosis factor- α (TNF- α) and interleukin-6 (IL-6) and lower interleukin-10/N-acetylgalactosamine specific lectin1. The data produced from this study revealed a potentially significant mechanism that links direct PM_{2.5} exposure with type 2 diabetes mellitus (Sun et al., 2008).

In regards to prenatal PM_{2.5} exposure and metabolic effects, increasing evidence are providing insight into the metabolic impacts and subsequent health effects. According to Bolton et al., prenatal DE exposure followed by a high fat vs. low fat diet resulted in sex-specific effects including differing degrees of weight gain, insulin resistance, and even behavioral changes. Investigators observed male mice had greater weight gain, lower activity, and higher insulin levels in HFD and DE exposed in comparison to filtered air exposed males. Also, both sexes of DE exposed and HFD fed mice were found to display microglial activation within the brain. These data indicate that prenatal air pollution exposure predisposes offspring to increased likelihood for diet induced weight gain and neuroinflammation in adulthood (Bolton et al., 2012). Additional evidence of metabolic impacts of prenatal PM_{2.5} or DEP comes from Bolton et al. in a 2014 study in which, following an earlier model, continued to observe male mice that were DEP & HFD exposed expressed significantly higher levels of microglial and macrophage activation within the hippocampus. On the contrary however, the female mice who were DEP & HFD exposed displayed suppression of these same activation markers (Bolton et al., 2014). These trends are further substantiated by a study (Chen et al. in a 2017) where investigators utilized a prenatal exposure model with C57Bl/6 mice. The data demonstrated that offspring of DEP exposed dams had significantly decreased body weight from postnatal week 2 onward. The observed weight loss was also associated with reduced food consumption and decreased expression of peptide NPY in the hypothalamus. These observations provide evidence of *in utero* exposure to DEP “programming” food intake and affecting offspring energy processes. However, the reduction in body weight was also accompanied by increased epididymal adipose tissue mass. Also, postnatal mothering by DEP exposed dams increased the bodyweight of offspring during lactation and subsequent adulthood accompanied by increased accumulation of

adipose and decreased UCP1 expression in brown adipose tissue. Additional evidence provided by Chen et al. further expanded the pool of evidence that DEP exposure throughout pregnancy programs offspring glucose metabolism and homeostasis. Using a prenatal C57Bl/6 mouse model, investigators observed exposed offspring displayed impaired glucose tolerance but not insulin sensitivity. Moreover, these same mice exhibited significantly decreased glucose-induced insulin secretion (GIIS) and decreased pancreatic islet and Beta cell size and altered functionality that could contribute to the development of diabetes. Notably, this study demonstrated significant decrease in the expression of pancreatic GLUT2 mRNA in DEP exposed offspring. The downregulation of pancreatic GLUT2 and the association of β - cell dysfunction suggests *in utero* DEP exposure may impact glucose sensing in offspring (Minjie Chen et al., 2018).

These findings are in line with those of Woodward et al. in which pregnant C57BL/6J dams were exposed to nanoscale particulate matter (nPM) with aerodynamic diameter of ≤ 200 nm. This investigation yielded observations, in male offspring, that included increased food consumption, increased fat mass, increased adiposity, glucose intolerance, and body weight gain. Furthermore, this study explored several molecular endpoints including altered gene expression in the in the hypothalamus including *Agrp*, *Npy*, and *Leprb*, all of which were significantly decreased and involved in appetite regulation. Additionally, genes involved in receptor mediated insulin signaling, such as *Inrs*, *Inrs1*, and *Irs2* were each significantly inhibited within adipose tissues of nPM exposed mice. These findings provide further evidence of maternal PM-induced metabolic effects (Woodward et al., 2018). Last, in a 2019 study, Xie et al. employed a model of PM_{2.5} intratracheal instillation in C57BL/6 dams. Investigators observed reduced body weight in adult offspring, as opposed to most other studies, accompanied by reduced adipocyte size within epididymal white adipose tissue (eWAT). In addition to reduced body weight, this study revealed

decreased gene expression profiles related to fatty acid synthesis (ACC1 & ACSL1), fatty acid oxidation (PPAR α), and pro-inflammatory cytokines (TNF α , IL-1 β , IL-6) in eWAT of PM_{2.5} exposed male offspring (Xie et al., 2019). Another study conducted by Wu et al. showed decreased glucose and free fatty acids in plasma, as well as enhanced accumulation of lipids in liver tissues (Wu et al., 2019).

Mechanisms of Action:

PM & Oxidative Stress:

Basic Definitions:

Oxidative stress is generally defined as a disruption of redox signaling and redox control mediated through pro-oxidants and antioxidants, also referred to as thiols. Both oxidative stress and normal redox signaling are quantified as the redox state of glutathione/glutathione disulfide (GSH/GSSG). In humans and other biological organisms, plasma and tissue GSH redox becomes oxidized (GSSG) for a variety of reasons. These reasons may include age, disease, and chemical stress/oxidative stress from chemical agents. In addition to GSH/GSSG, another set of thiols called cysteine (CyS) and cystine (CySS) are present in tissues and plasma as a protective system of sensitive antioxidants. These redox sensitive thiol systems are vital for a variety of functions including the maintenance of proper cell signal transduction, transcription factor binding to DNA, receptor activation, and maintaining the integrity of various proteins and macromolecules (Ghezzi et al., 2005, Jones et al., 2006, Jones et al., 2008). The antioxidant thiols involved in biological redox are nucleophilic and reductive in nature, making them reactive to oxidants, including reactive oxygen species (ROS) and other free radicals that are produced from numerous sources. Left unabated, these free radicals and ROS constitute a deleterious risk of cellular and tissue dysfunction ranging from protein misfolding to DNA damage. However, low

or moderate concentrations of ROS are necessary for physiological signaling, growth and development, as well as defense against microbial and infectious agents by inducing antioxidant responses (Espinosa-Diez et al., 2015).

In regards to air pollution, there is a pool of growing evidence which documents how PM impacts health on a molecular level by inducing oxidative stress and inflammation. Through these mechanisms, we now understand that PM yields direct and indirect effects on intracellular sources of ROS and pro-inflammatory mediators including macrophages in the lungs and other organ systems (Flecha et al., 2004). Through years of study and investigations, the molecular mechanisms by which PM causes oxidative stress have been characterized and better understood. In summary, PM of the various size fractions, especially PM_{2.5} and below, following inhalation are deposited into deep portions of the lungs where they can translocate across the alveolar barrier and pass into the circulatory system (Rocha et al., 2010). Once these particles cross into systemic circulation, they proceed to interact with a host of molecular targets and tissues in numerous ways depending on their chemical makeup and constituents. The smaller fractions of PM have been studied and identified as having the ability to interact with the neurological system, cardiac tissues, and many organs which contributes to a wide variety of diseases both acute and chronic. Now we understand that PM interactions with biological systems and cells leads to cell death via triggering necrosis, apoptosis, and autophagy (Peixoto et al., 2017).

Thiols:

A major component of all living organisms and biological system have evolved some degree of molecules, enzymes, and proteins that contain functional groups which feature expansive chemical reactivity to undergo a plethora of modifications. The molecules referred to as thiols, which are central to redox biology and combatting oxidative stress. The versatile

structure and properties of thiols, including the ability to form intra- and intermolecular disulfide bonds, and the reversible oxidation of these thiol reactions to function in important metabolites and proteins. Additionally, these thiols serve many cellular functions including DNA and protein synthesis, tissue modeling, signaling, cell differentiation, development, and more (Comini et al., 2016). As previously stated, thiols are important for the protection of important macromolecules and organelles from errant ROS and free radicals generated from normal and adverse processes throughout biological systems such as humans. The unique properties of these antioxidant molecules are physiologically significant in a wide array of processes due in part to their structure and flexibility. Thiols are characterized to exhibit unique features including a sulfur “hinge” which endows these low molecular weight (LMW) proteins such as GSH and CyS with a wide array of specialized and versatile functions. For instance, the sulfhydryl group of GSH and CyS makes it a frequently present amino acid in proteins that have an affinity for nucleophilic reactions which are significant in binding and interacting with metals and chemicals. These thiols also undergo both reversible and irreversible oxidation reactions which is vital to protecting cells and tissues against oxidizing agents and oxidative stress. Deprotonation of protein thiols results in the formation of highly reactive thiolate anions which proceed to undergo a number of oxidative modifications. From here, two-electron oxidation results in the formation of sulfenic acid intermediates which react with other protein thiols in turn to form disulfide bonds with LMW thiols such as GSH and CyS. Further oxidation of this sulfenic acid to sulfonic acid has been found to oftentimes be irreversible in the redox antioxidant thiol system. However, one electron oxidation of the thiolate anion creates a thiyl radical, which then persulfides or an S-nitrosothiol. Alternatively, thiolate anions can directly react with protein

disulfides as well as oxidized LMW thiols such as GSSG via thiol disulfide exchange reactions (Ulrich et al., 2019).

Thiols, both reduced and oxidized molecules, are quantifiable for evaluating redox status of plasma and tissues relative to healthy or diseased contexts. Given the low concentration of GSH and GSSG (1-10mM and 0.01-0.05mM, respectively) thiols present through different biological compartments including plasma, cells, and tissues, the use of high-performance liquid chromatography (HPLC) is an optimal method with which to measure LMW thiols (Tipple et al., 2012). Alternative biochemical methods for monitor oxidative stress and biological redox systems are well documented and practiced include tagging proteins and lipids, monitoring protein modifications, evaluating changes in redox states of live cellular compartments such as mitochondria and nuclei with probes, and many more (Rudyk et al., 2014).

Redox Biology & Biochemistry:

As mentioned in previous sections, oxidative stress induced by pro-oxidizing agents or uncontrolled release of ROS from disease or injury can result in damage to important cellular structures. Damage from unchecked oxidative stress or severe insult can lead to cellular apoptosis or necrotic cell death (Chandra et al., 2000, Circu et al., 2010, Parvez et al., 2018). Prolonged insults from various sources, can lead to oxidative stress and induce alterations in redox dependent signal transduction pathways that regulate important biological processes such as cell growth and division resulting in disease (Birben et al., 2012). These redox based signal transduction circuits have specific functions and roles in different cell cycle phases and different cell types. Disruptions and insults to these signal pathways can impact critical checkpoints that may alter cell fate. For instance, impacts to S phase via ROS induces S-phase arrest by means of PP2A-dependent dephosphorylation of pRB. Another example includes oxidative stress inducing

Nrf2 and Foxo3a promotion of antioxidant production for cell survival. Numerous signal pathways are known to trigger senescence to save the cell, and others that promote tumorigenesis via loss of P53 (Burhans et al., 2009). An example of a major environmental exposure that has been documented to induce carcinogenic effects via oxidative stress would be that of polycyclic aromatic hydrocarbons (PAHs) that are associated with ambient PM (Hanzalova et al., 2010). As mentioned before, cell proliferation is highly regulated via multiple transduction signal pathways, including redox dependent pathways that control cell cycle progression. Oxidative stress is both a significant marker and a mechanism of disease including cancer (Chiu et al., 2012).

Collectively, the complex system of antioxidant thiols and their functions in relation to one another and the metabolites and proteins with which they interact have been termed the redox proteome. As described by Jones et al in a 2013 publication, “the redox proteome serves as a complex and wide spread interface between genome-directed biologic structure and functions and the environmental determinants of those structures and functions.” Of particular importance are the CyS proteome due to its versatile sulfur switch structures that connects redox chemistry with structure, function, and disease. Overall, the interactions of the redox proteome with redox-active chemicals and pro-oxidizing agents is central to macromolecular structures, metabolism, regulation, development, and signaling which are all critical in maintaining homeostasis in the face of environmental changes and adverse conditions (Jones et al., 2013).

Oxidative stress & Protein modification:

With the understanding that PM_{2.5} exposure induces oxidative stress and plays a significant role in the development of disease. One such disorder of interest that is growing in evidence is that of nonalcoholic fatty liver disease (NAFLD). A recent study from 2019 was

conducted by Xu et al. The primary hypothesis of this study was to determine if PM_{2.5} increased hepatic inflammation and oxidative stress in exposed C57Bl/6 mice, which in turn would promote lipid accumulation within hepatic tissues as per characteristic of NAFLD. The investigators did observe increased insulin resistance coupled with glucose tolerance, along with abnormal hepatic function (Xu et al., 2019). Furthermore, Xu et al. demonstrated PM_{2.5} induced an increase in ROS in brown adipose tissue (BAT) in addition to decreased mitochondrial counts in both white adipose tissues (WAT) and BAT. Additionally, male ApoE knockout mice exposed to PM_{2.5} showed significantly different expression profiles of adipocyte specific genes in WAT and BAT. This study ultimately demonstrated PM_{2.5} induced oxidative stress and significant alterations in mitochondrial gene expression which suggests an imbalance between WAT and BAT functionality. These sort of physiological changes in adipose tissue development and function may predispose exposed subjects to metabolic dysfunction in adulthood (Xu et al., 2011). Similar results were seen in a 2016 human study by Grevendonk et al. in which mother-newborn pairs were evaluated from the ENVIRONAGE birth cohort to assess mitochondrial 8-OHdG levels as a marker for PM_{2.5} exposure. This study found a significant association between prenatal PM_{2.5} exposure and mitochondrial 8-OHdG levels in maternal blood. These findings indicated that PM exposure during pregnancy can induce mitochondrial oxidative stress and DNA damage in both mothers and their offspring, thus playing an important role in increasing systemic oxidative stress (Grevendonk et al., 2016).

Ambient PM_{2.5} has been characterized and confirmed to alter cell processes and cell fate, namely that of autophagy. PM_{2.5} of particular concern is that of traffic related DEP which frequently has combustion derived chemical constituents including benzo(a)pyrene diolepoxide (BPDE). Lai et al. conducted an *in vitro* study using human epithelial A549 cells to evaluate the

mechanisms of PM_{2.5} induced protein oxidation and degradation. Using this model, investigators demonstrated BPDE induced protein adducts caused by DEPs and further discovered methionine oxidation stemming from DEPs, urban dust, and carbon black particles. Additionally, proteasome and autophagy activation was detected from DEPs without ubiquitin accumulation in cells (Lai et al., 2016).

Nrf2 Oxidative Stress & PM:

A major molecular target of interest in PM_{2.5} induced oxidative stress is the Nrf2-Keap1 signaling pathway. This complex and physiologically significant molecular pathway is a critical component in protecting cells and tissues from oxidative stress and oxidative damage. Upon activation under conditions of oxidative stress, the Nrf2-Keap1 complex upregulates the expression of a number of antioxidant genes (Jaramillo et al., 2013). It is relevant to clarify that under normal conditions, the Nrf2 transcription factor remains in a basal state and present in the cytosol. However, when the cell is exposed to chemical agents or undergoes oxidative stress, Nrf2 is translocated from the cytosol into the nucleus where it proceeds to induce the expression of antioxidant genes (Bryan et al., 2013). Nrf2 and oxidative stress are of critical significance during embryonic development, not only for reasons of development but also recovery from insults. Utilizing a zebrafish model in which selected embryos were knockouts of key antioxidant redox genes including Nrf1 and Nrf2, investigators found that embryonic sensitivity to oxidative insults changed as the embryos progressed in growth. Additionally, knockdown of Nrf2 and its paralogs altered the GSH redox state but did not significantly affect the response of GSH to pro-oxidants. Ultimately, the results of this study suggested that embryos become more sensitive to oxidative stress later in development, and that neither Nrf1 or Nrf2 alone are necessarily essential for the recovery and response of GSH to oxidative stress, but rather there are additional

redox components (Sant et al., 2017). Another important aspect of the Nrf2-Keap1 pathway is that it plays a key role in inflammation response. According to Ahmed et al, Nrf2-Keap1 contributes to anti-inflammatory response by stimulating the recruitment of inflammatory cells and regulation of gene expression through the antioxidant response element (ARE) (Ahmed et al., 2017). Additionally, recent research suggests that Nrf2 provides a protective effect against PM_{2.5} induced toxicity. Pardo et al. conducted an *in vitro* study of human lung cells and found differing toxic effects in the form of mitochondrial ROS induced by PM_{2.5} extracts. The investigators in this study noted higher levels of ROS generated by lung cells following exposure to PM_{2.5} extracts containing dissolved metals while PAHs increased toxicity in Nrf2 silenced cells. Additionally, Nrf2 silenced cells exhibited lower mitochondrial membrane potential and lower mitochondrial DNA copy numbers following exposure to organic extracts from PM_{2.5}. These observations and data provide more evidence that Nrf2 provides a significant protective function of mitochondria against oxidative agents within lung cells and potentially other tissues (Pardo et al., 2019). Also, as evidence mounts and mechanisms surrounding Nrf2 continue to accumulate, we now understand that Nrf2 exhibits a master regulator and protective role in liver tissues. The Nrf2-Keap1 signal pathway has been characterized to demonstrate significant influences on the outcome of liver disease and injury. Recent studies have examined the mechanisms and processes of liver diseases including non-alcoholic fatty liver disease (NAFLD), non-alcoholic steatohepatitis (NASH), alcoholic liver disease (ALD), and even hepatocellular carcinoma (HCC) in relation to Nrf2 expression. These studies have surprisingly shown that Nrf2 is not always protective and is sometimes associated with the progression of disease such as cancer depending on conditions of chronic or acute oxidative stress or prolonged inflammation. Continued advancement in understanding the mechanisms of certain disease in relation to the

Nrf2 pathway is vital to developing improved methods of therapeutic interventions and treatment of disease (Xu et al., 2019).

Inflammation:

Basics of inflammation:

In addition to inducing oxidative stress in living organisms, PM_{2.5} generates an array of free radicals and subsequently inflammation in organ systems which may lead to further injury. Under disease conditions, cells of various types may release ROS and in an uncontrolled manner that induces the expression of proinflammatory mediators such as Ca²⁺. Cell derived ROS can result in significant increases of intracellular calcium, leading to the activation and phosphorylation of mitogen activated protein kinase (MAPK) family and initiate a cascade event and ultimately upregulation of various genes (Mazzoli-Rocha et al., 2010).

Biochemistry & cell biology of inflammation:

One of the major cell contributors to inflammation and oxidative stress are the macrophages that reside in many tissues and organ systems beyond the lungs. Following exposure to PM_{2.5} or other foreign substances, macrophages release ROS as part of a phagocytosis response to remove or degrade pathogens and foreign objects. However, these macrophages, alveolar macrophages in particular in regards to air pollution exposure, produce ROS in relatively large concentrations due in part to their expression of NAPDH oxidase. Following stimulation of macrophages, the “respiratory burst” of ROS can and often does lead to tissue damage and induces oxidative damage that alters cellular signals and functions. Oxidation of low-density lipoproteins has been found to lead to interfere with multiple signal pathways in macrophages and tissues (Forman et al., 2001). The generation of ROS and subsequent oxidative stress and inflammation induced by actual PM from real world sites have been observed. Many

studies have confirmed that PM and all size fractions of PM generate inflammation and oxidative stress, and further substantiates that the constituents adhering to that PM are important in evaluation and of health outcomes. PM-mediated ROS production is involved in the generation of inflammation and the activation of inflammatory cells in lung tissues and beyond. The activation of these inflammatory cells then proceeds to further increase the oxidative damage from ROS production and causes an assortment of damage including lipids, DNA, proteins and overall cellular damage (Moller et al., 2014).

Significance and Specific Aims

PM is associated with developmental effects in children exposed during gestation. Emerging evidence shows PM exposure leads to adverse metabolic syndromes. Despite accumulating evidence regarding the impact of PM on offspring metabolic health, the underlying mechanisms and particular role of ultrafine particles (UFPs), which compose a substantial portion of PM and possess enhanced oxidative capacity, are relatively unknown. Thus, there is a critical need to characterize the relationship between gestational UFP exposure and altered redox state in relation to offspring metabolic disease risk. Our central hypothesis is that *in utero* exposure to UFPs enhances offspring oxidative stress, thereby disrupting redox signaling, increasing risk of health endpoints related to development. We tested our hypothesis through the following specific aims:

Aim 1. Characterize offspring metabolic disease phenotypes following in utero UFP exposure with subsequent diet challenge. To examine prenatal UFP exposure and the risk of metabolic disease, we exposed time-mated C57Bl/6n mice throughout gestation to filtered air or UFPs. At weaning, offspring were placed on a high-fat or low-fat diet and tracked until 15 weeks of age for growth, feed intake, glucose homeostasis, and hepatic lipid accumulation.

Aim 2. Characterize offspring metabolic disease phenotypes following in utero UFP exposure (dose-response) without subsequent diet challenge. Here, we exposed time-mated C57Bl/6n mice throughout gestation to filtered air or UFPs at varying doses. Offspring were tracked until 15 weeks of age, again for growth (including bone density analysis) and hepatic lipid accumulation.

Aim 3. Elucidate offspring oxidative stress response to UFP exposure. To determine the consequences of UFPs and Nrf2 status on oxidative stress response, we exposed *Nrf2* deficient (*Nrf2*^{-/-}) and wild-type (*Nrf2*^{+/+}) mice to UFPs of filtered air throughout gestation. Offspring livers were collected at 5 days of age and analyzed for markers of oxidative stress (GSH/GSSG and Cys/CySS).

CHAPTER II METABOLIC STUDY 1: GESTATIONAL EXPOSURE TO ULTRAFINE PARTICLES ALTERS POSTNATAL GROWTH

Introduction:

Particulate matter (PM) is a major component of air pollution. PM is a mixture of solid particles such as dust, soot, smoke, and liquid droplets. Sources of PM emissions include a variety of natural and anthropomorphic sources like wildfires, industry, automobile traffic, and many more. PM also displays a wide variety of different physicochemical characteristics associated with its size and chemical makeup. PM can range in size from 10 micrometers in diameter (PM_{10}), 2.5 micrometers in diameter ($PM_{2.5}$), down to less than 0.1 micrometers ($PM_{0.1}$), also known as ultrafine particles (UFPs). In addition to the complex and heterogenous nature of PM, a wide variety of different chemical components such as PAHs, nitrates, sulfates, and metals, adhere to PM surfaces (Kelly et al., 2012). Human epidemiological studies overwhelmingly support PM exposure negatively influences human health. Multiple studies correlate PM exposure, either acute or chronic, to numerous adverse health outcomes related to cardiovascular, respiratory, and neurological systems (Kim et al., 2015).

Another major health issue is that of the increasing prevalence of obesity and metabolic disease. Recent studies conducted within the past decade have uncovered evidence that connects PM exposure and metabolic disease (Pearson et al., 2010). Studies in animal models have investigated possible linkages between PM and type 2 diabetes. Sun et al. observed insulin resistance, systemic inflammation, and increased adiposity in male C57Bl/6n mice following PM exposure coupled with a high-fat diet. Investigators concluded that $PM_{2.5}$ exposure enhances diabetic phenotypes and inflammation in mice (Sun et al., 2009).

PM exposure during important windows of development may also alter development and propensity for metabolic disease later in life. This phenomenon is commonly referred to as the

developmental programming of health and disease (DOHaD) paradigm. The central idea of this paradigm proposes that many metabolic disorders are linked to disturbances or stressors experienced during early life (Hales et al., 2001). A study published in 2015 found that infants exposed to high levels of traffic related air pollution during gestation had initial fetal growth suppression, followed by rapid weight gain (Fleisch et al., 2015). Differing outcomes in experiments models have supported, as well as refuted these findings. We hypothesized that the UFP component may play an important role in modulating risk. Currently, there is a scarcity of literature that focuses specifically on prenatal exposure to UFPs. Building off of research by Wu et al. (Wu et al., 2019), our model aimed to investigate the role of gestational UFP exposure in offspring metabolic outcomes after progeny were challenged with a high-fat or low-fat diet.

Methods:

Animals and Particulate Matter Exposure:

Male and female C57Bl/6n 8- to 10-week-old mice (Jackson Laboratory, Bar Harbor, ME) were maintained were maintained in a 12-hour light dark cycle and time-mated in an AAALAC approved facility at Texas A&M Institute for Genomic Medicine (TIGM). Mice had access to standard chow, 19% protein extruded rodent diet (Teklad Global Diets), and water *ad libitum*. All procedures were approved by the Institutional Animal Care and Use Committee (IACUC) of Texas A&M University, protocol #2019-0025. Following a one-week acclimation period and upon identification of a vaginal plug or sperm present on vaginal cytology (GD 0.5), females were randomly assigned to one of two exposure groups: filtered air (FA) or ultrafine particulate matter (PM, 500 $\mu\text{g}/\text{m}^3$). Exposure occurred in our custom-built whole-body exposure chambers for 6 hours per day from GD 0.5 to 17.5 (Fig. 1). Exposures occurred between 0800 and 1400 hours. PM

was composed of diesel soot (SRM 2975), ammonium sulfate, ammonium nitrate, and potassium chloride, as established by our previous model (Rychlik et al. 2019). Throughout exposure duration, PM mass concentration was continuously monitored and adjusted to maintain a stable exposure level. At the end of the exposure period on GD18.5, dams were transferred to individual housing and allowed to deliver spontaneously. Following birth, pups were allowed to nurse with dam until post-natal day 5 (PND5), wherein litters were culled to 2 males and 2 females. These remaining pups continued to nurse until weaning on PND21, at which point they were randomly assigned to either a low-fat (LF, 10%) or high-fat (HF, 45%) diet from PND21 to PND105 (Fig. 1). The composition of the low-fat and high-fat diets is previously reported in detail (Wu et al., 2019). During this time, mice were individually housed to obtain feed intake.

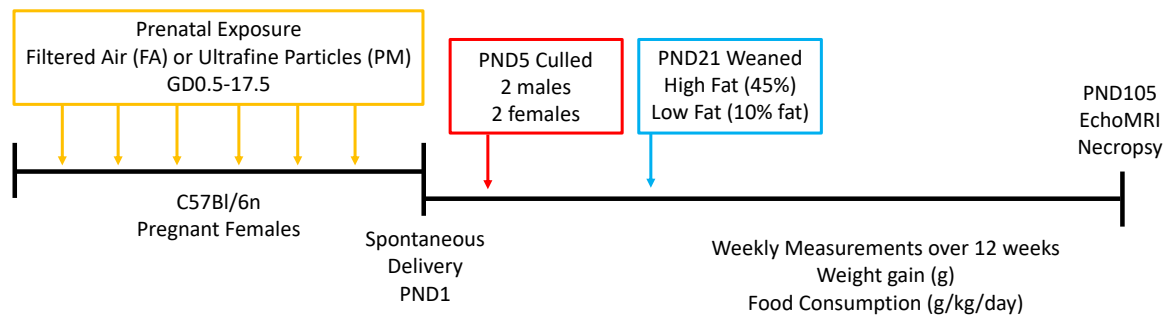


Fig 1. Study design for assessing effects of gestational exposure to ultrafine particles (UFPs) on offspring growth. C57Bl/6n mice were time-mated; confirmation of plug defined as GD0.5. Accordingly, pregnant dams were exposed to filtered air (FA) or to 500 $\mu\text{g}/\text{m}^3$ UFPs (PM) for 6 hours daily until GD17.5. Following delivery, litters were culled to 2 males and 2 females on postnatal day (PND) 5. Remaining offspring were weaned on PND21, wherein they were assigned to receive either a low fat (LF) diet or high fat (HF) diet providing 10% or 45% kcal% fat, respectively. Offspring were assessed for weight gain and food consumption on a weekly basis for 12 weeks and evaluated on PND105 (15 weeks of age) using EchoMRI body composition analysis.

Body Weight, Feed Intake, Glucose Tolerance Testing, and Body Composition Analysis:

Offspring body weights were measured at specific days following birth (PND5, 10, 15, 21) and then on a weekly basis from PND21 to PND105. Feed Intake, absolute and relative organ weights were recorded in culled offspring on PND5 and all remaining offspring undergoing dietary challenge on PND105.

Offspring were also subjected to the glucose tolerance test (GTT) on a monthly basis beginning on PND21 and repeated on PND49, and PND77. To measure blood glucose levels, Contour blood glucose meter and the product specific blood testing strips were utilized. Blood glucose meter was calibrated based on product recommendations utilizing glucose solution before each new box of test strips. To begin GTT, mice were fasted for 6 hours, starting in the morning, before initial blood glucose measurements (marked as 00 time). Following 6 hour fasting period, GTT assessments took place within the same facility in which mice were housed and around the same time as previous GTT assessments to reduce stress. GTT assessments were performed on a litter basis, meaning that the day of which an assessment was performed was based on the date in which that litter was born. At mark time 00 for GTT, the first mouse would be placed into a plastic tube to inhibit movement while retrieving a drop of blood from the tail via “tail bleed” technique. To successfully draw blood, a pair of clean surgical scissors were used to cut a very minor amount of tissue from the very tip of the mouse tail. Once the tip was cut and removed, the tail was gently squeezed to get blood and then placed onto the primed and activated blood glucose meter and test strip. Once first reading (00 minute) was obtained and logged, each mouse was then given a dose of glucose (2g/kg) by i.p. injection. Each time point of the GTT was staggered to provide enough time to log blood glucose data and ensure the safety and comfort of mice subjects.

Body composition, including whole body fat, water content, and lean tissue mass was determined with an Echo MRI (Echo Medical Systems, Houston, Texas) on PND105. After sacrifice, liver tissue was portioned into lobes for histopathology, via preservation in optimal cutting temperature compound (OCT) for oil red O staining.

Statistical Analysis:

Data are expressed as mean \pm SEM. All sample numbers are displayed within figures. Statistical analysis was performed using GraphPad Prism (V 9.0.2). Differences between groups were compared by one-way analysis of variance (ANOVA), prior to dietary challenge, or by two-way ANOVA after diet challenge to test the effect of two independent variables (preconception treatment vs. postnatal treatment). $p < 0.05$ was considered statistically significant.

Results:

To determine if gestational exposure to UFPs predisposes offspring to metabolic disease or developmental perturbations, we conducted a long-term observational study of prenatally-exposed pups. In addition to maternal exposure, these pups were assigned to receive a diet consisting of either low fat (10% daily fat intake) or high fat (45% daily fat intake) mouse chow. We performed multiple methods of measurements for phenotyping developmental disturbances.

First, we evaluated neonate body weights and organ weights for culled offspring (Fig. 2). Female offspring exposed to PM had significantly reduced body weights in comparison to FA-exposed offspring ($p=0.0030$). Most organ weights did not significantly differ in culled offspring. However, spleen tissue from neonates display a possible trend of increased relative weight in PM exposed pups. This trend is observed in both male and female pups, confirmation requires further investigation and larger sample size to determine true effect.

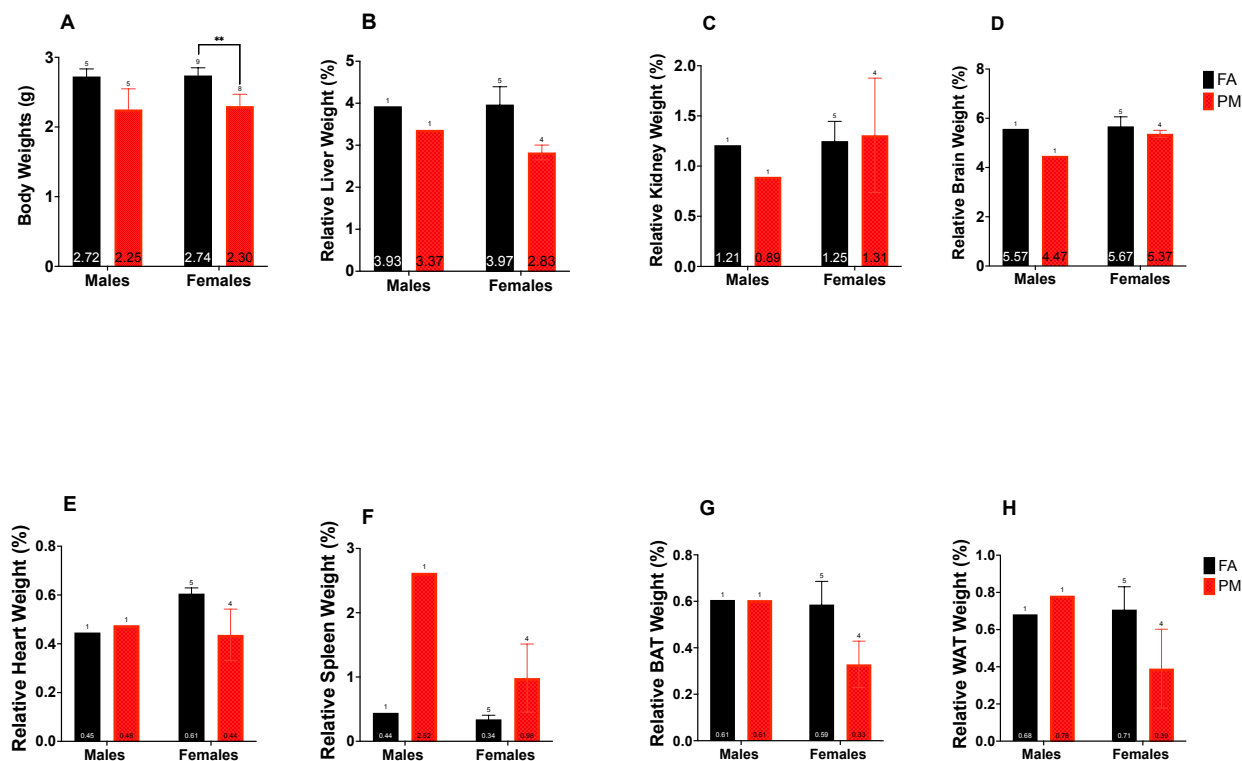


Fig 2. Offspring body weight (BW) and relative organ weight on PND5. Relative organ weights correspond to the percentages of the BW. (A) BW (g), (B) relative liver weight, (C) relative kidney weight, (D) relative brain weight. (E) relative heart weight, (F) relative spleen weight, (G) relative brown adipose tissue (BAT) weight, (H) relative white adipose tissue (WAT) weight. Values are mean ± SEM. ** $p < 0.01$. FA (filtered air), PM (ultrafine particles). Significant differences detected by Two-Way ANOVA, ONE-WAY ANOVA was not available for analysis.

The average weight gain of offspring was also tracked between PND 5 and PND 21 (Fig. 3). Significant differences detected by Two-Way ANOVA on PND 21 for male offspring ($p = 0.0137$), as well as on PND 10 ($p = 0.0095$), 15 ($p = 0.0458$), and 21 ($p = 0.0007$) for female offspring.

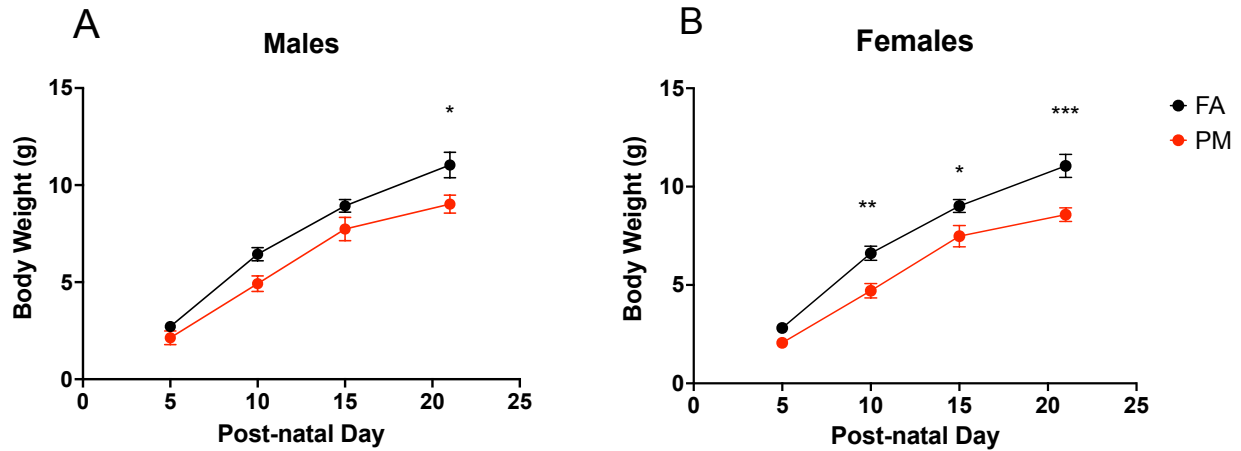


Fig 3. Offspring growth trends during nursing from PND5-21. (A) males, (B) females. Values are reported in mean \pm SEM. * $p < 0.05$. FA (filtered air), PM (ultrafine particles). Statistical significance detected by Two-Way ANOVA.

Adult growth trends were also assessed between post-natal week (PNW) 3 and 15 following low fat (LF) and high fat (HF) diet chow assignment (Fig. 4.). No significant differences were detected in body weights between diet or exposure groups in male offspring. Beginning at week 9, female offspring groups showed significant differences. Pups in the FA-HF group remained significantly heavier than other groups.

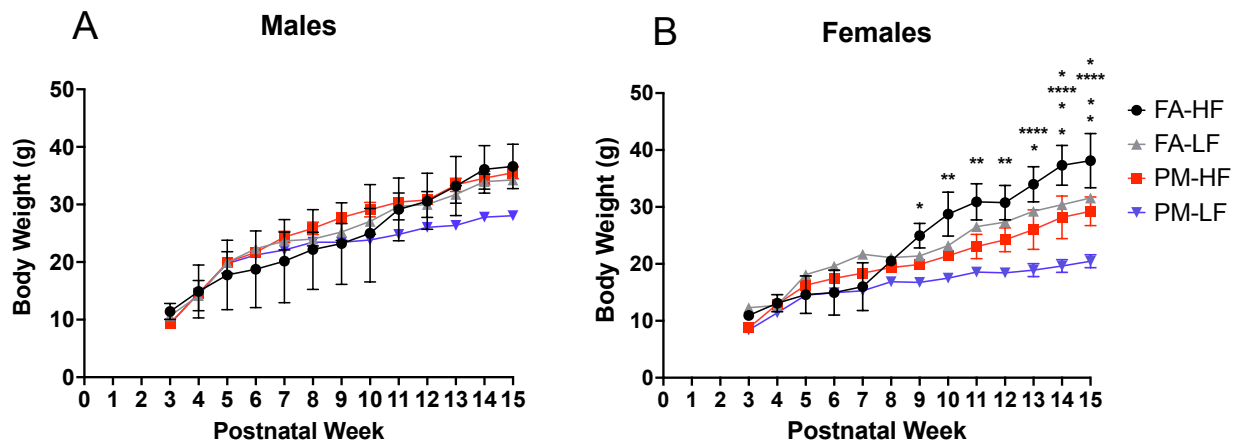


Fig 4. Offspring growth trends post-weaning with introduction of a low fat (LF) or high fat (HF) diet from postnatal week 3-15. (A) males, (B) females. Values are mean \pm SEM. * $p < 0.05$, ** $p < 0.01$, **** $p < 0.0001$. FA (filtered air), PM (ultrafine particles). Statistical significances detected by Two-Way ANOVA.

In addition to monitoring increasing body weight trends in C57Bl/6n pups, food consumption and intake was monitored on a weekly basis (Fig. 5). Monitoring of feed intake from PNW 4 until PNW 15 did not reveal significant differences in feeding behavior between exposure groups or sexes in males but were detected by Two-Way ANOVA in females.

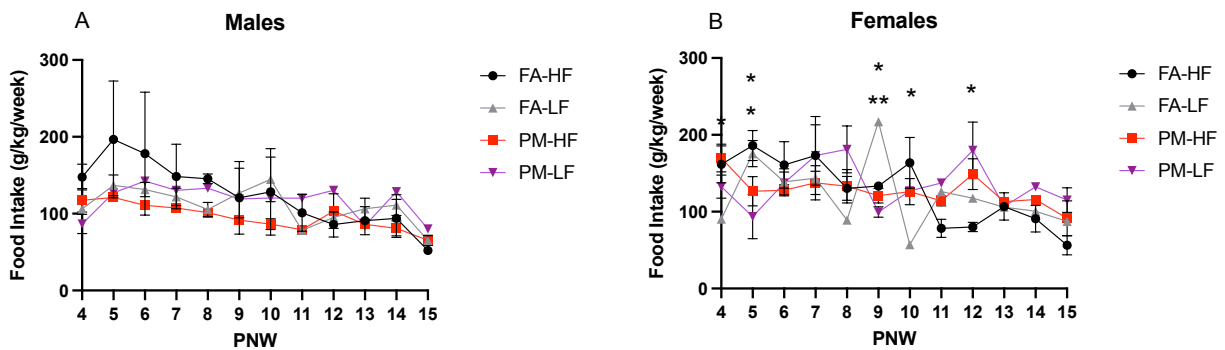


Fig 5. Offspring feed intake analysis measured post diet assignment. (A) Males, (B) Females. Values are presented as mean \pm SEM. Filtered air (FA), ultrafine particles (PM), low fat (LF), high fat (HF).

To evaluate for possible changes in glucose homeostasis between FA and PM exposed mice, glucose tolerance test (GTT) was employed to evaluate to measure glucose absorption over a time period of 120 minutes (Fig. 6). Blood glucose was measured at time points 0, 15, 30, 60, and 120 minutes following i.p. injection dose of 0.2 ml/20 g. C57Bl/6n mice were subjected to blood glucose assessment at PNW 3, 7, and 11. No significant differences or trends were observed in glucose processing in either sex, exposure groups, or diet treatment groups.

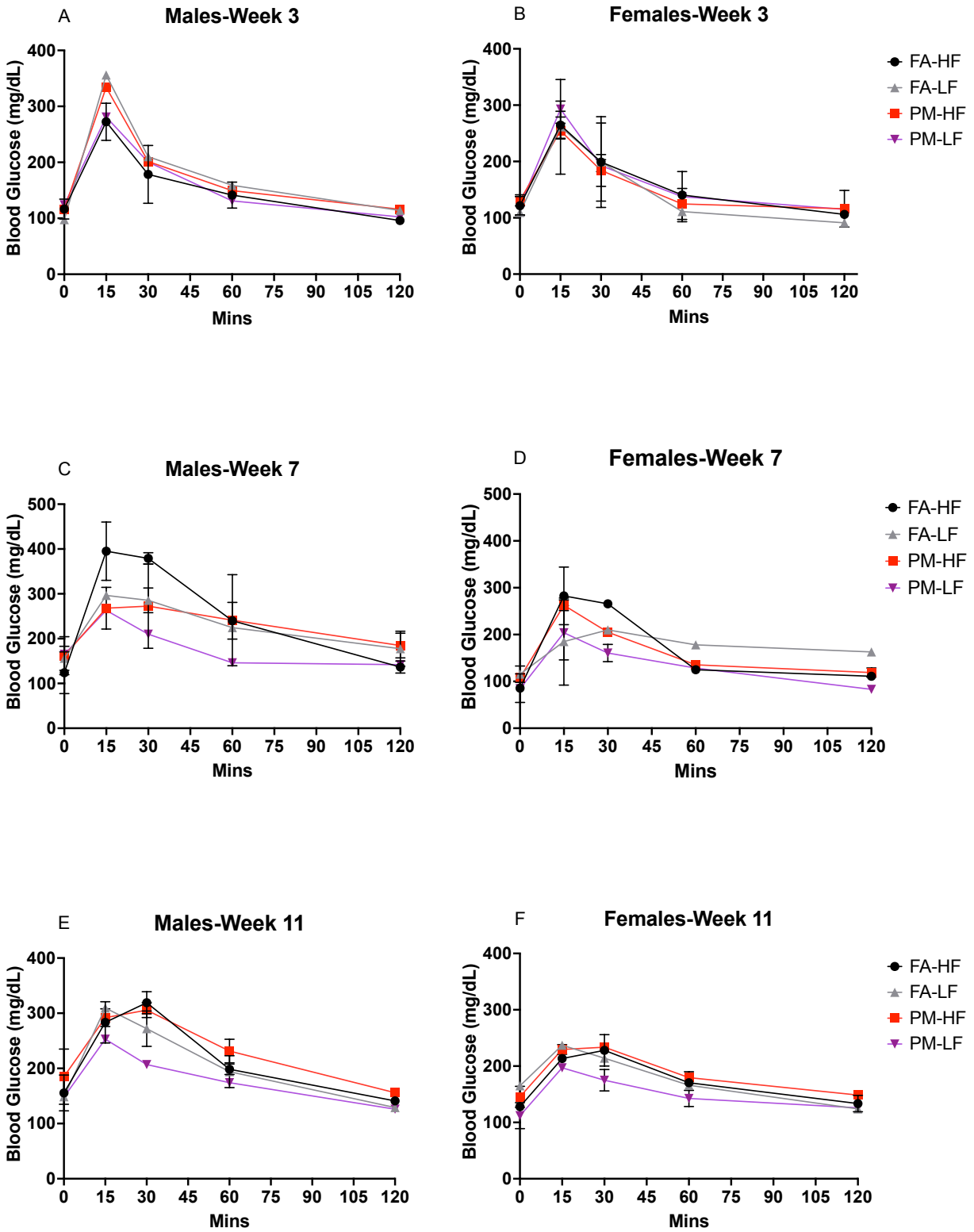


Fig. 6. Offspring glucose tolerance test trends. (A-B) Males and Females during postnatal week 3 glucose tolerance test following 6 hour fasting period. (C-D) Male and Female GTT trends

during PNW 7 (PND49). (E-F) Male and Female GTT trends in PNW 11. All data are presented in mg/dL mean \pm SEM at time points 0, 15, 30, 60, and 120 minutes.

On PND105, following an overnight fasting, offspring underwent full body scans via Echo MRI (Fig. 7). Male offspring showed no significant differences in either measure. Female offspring displayed significant differences in fat tissue mass, with the most significant reduction in the PM-LF group (0.0058). Moreover, female showed multiple significant differences in fat/lean ratios in comparison to FA-HF mice.

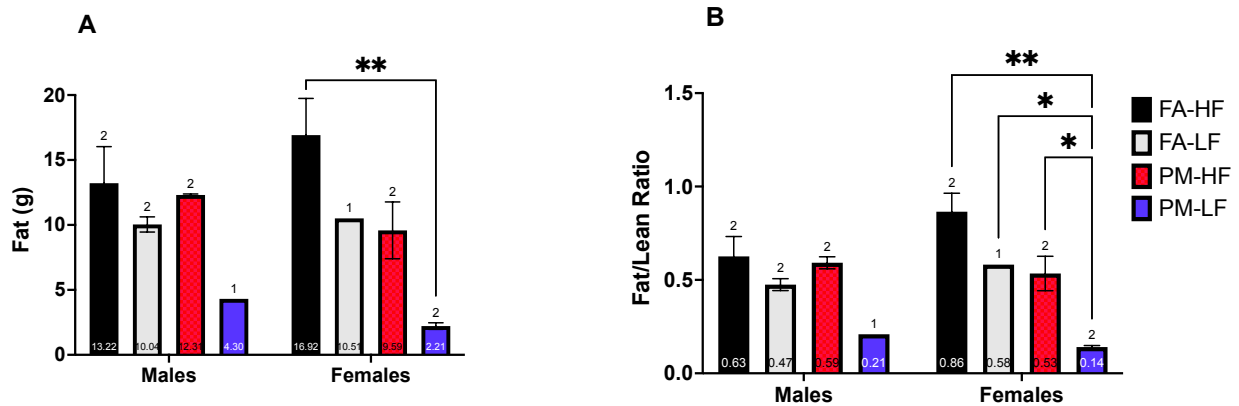


Fig 7. Offspring body composition analysis measured by Echo MRI on PND105. (A) Fat (g), (B) fat/lean ratio. Values are mean \pm SEM. * $p < 0.05$. FA (filtered air), PM (ultrafine particles), low fat (LF), high fat (HF). Significant differences detected by Two-Way ANOVA.

Upon reaching PND105/PNW15, all mice were sacrificed and tissues were collected and their weights recorded (Fig. 8.). Tissues from male mice displayed no significant differences between exposure groups or diet groups. Female mice, however, did exhibit significant differences for relative liver weights. Histological assessment was carried out to determine lipid content in hepatic tissue (Table 1). No significant differences were determined between groups.

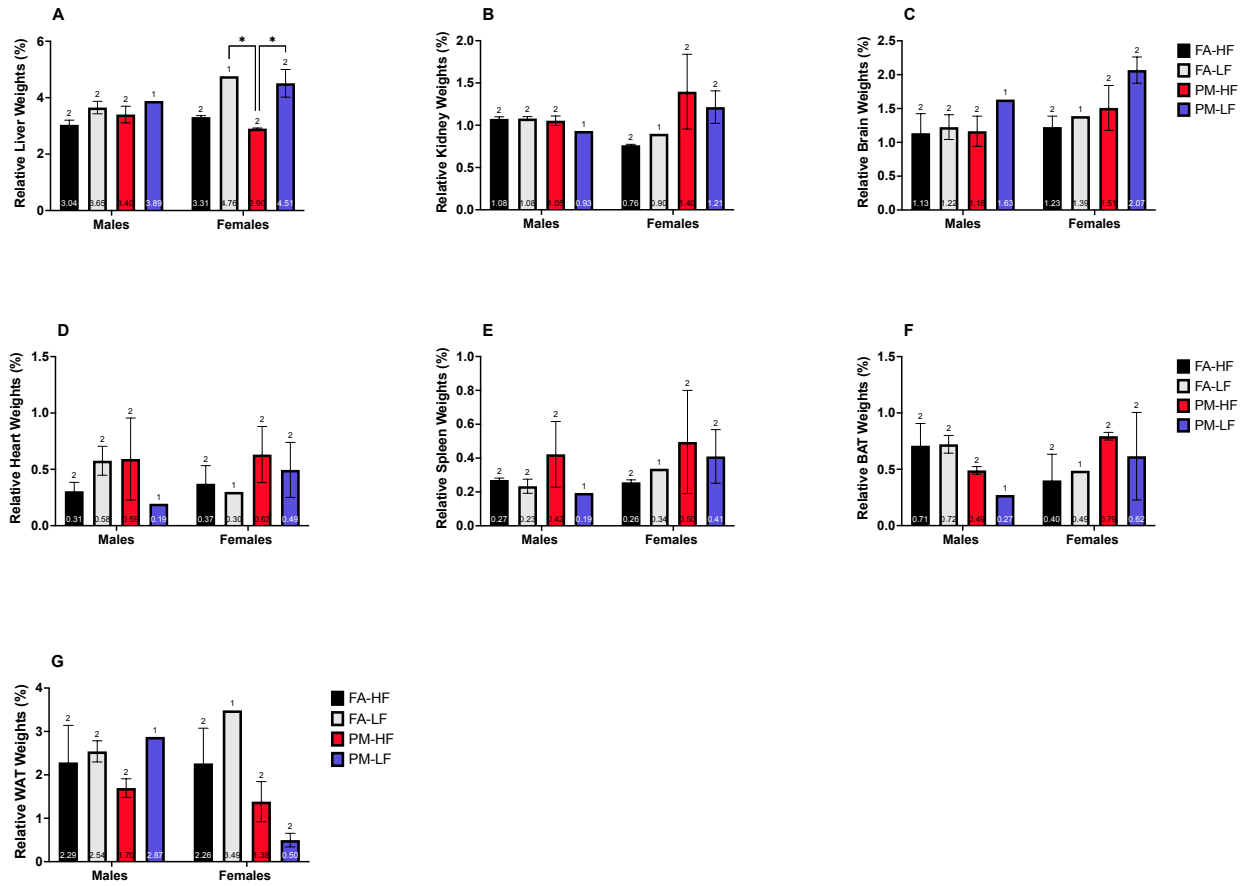


Fig 8. Offspring relative organ weight on PND105. Relative organ weights correspond to the percentages of the BW. (A) relative liver weight, (B) relative kidney weight, (C) relative brain weight, (D) relative heart weight, (E) relative spleen, (F) relative brown adipose tissue (BAT), (G) relative white adipose tissue. Values are mean \pm SEM. * $p < 0.05$. FA (filtered air), PM (ultrafine particles), low fat (LF), high fat (HF). Significant differences detected by Two-Way ANOVA.

Table 2.1.: Hepatic lipid accumulation

	Group	Score
Overall	FA LF	0 ± 0
	FA HF	1.3 ± 0.7
	PM LF	0.1 ± 0.3
	PM HF	1.1 ± 0.5
Males	FA LF	0.6 ± 0.5
	FA HF	0.8 ± 1.2
	PM LF	0 ± 0
	PM HF	1.1 ± 0.9
Females	FA LF	0.6 ± 0.5
	FA HF	0.8 ± 1.2
	PM LF	0 ± 0
	PM HF	1.1 ± 0.9

Table 2.1. Histological evaluation was performed on Oil Red O stained slides using a scoring system ranging from 0-3 (0-no lesions; 1-mild; 2-moderate; 3-marked). Scores were compared among groups in offspring and are displayed as mean ± standard error. n=3-4 mice/group.

Discussion & Conclusions:

In this study, we developed a novel model for evaluating adverse impacts of *in utero* UFP exposure on offspring growth, development, and metabolic disease risk. We developed an exposure model representative of relevant urban environments. To accomplish this, we designed our model to employ a whole-body exposure system connected to an atomizer and diluted PM solution. This solution contains typical components of urban air pollution, including ammonium sulfate, ammonium nitrate, potassium chloride, and diesel soot. This multicomponent aerosol mixture was introduced into the exposure system in a controlled manner to enable a stable maternal exposure. Currently there are no regulatory standard for UFPs. We employed a high dose exposure group, wherein dams received PM concentration levels of 500 µg/m³ daily (6 hours) throughout gestation. Daily six-hour exposure values correlated to a 24-h average dose of

125 $\mu\text{g}/\text{m}^3$. This reflects air pollution levels in heavily urbanized areas such as Beijing, China. Thus, these high levels may represent health effects observed in environments which experience high levels of air pollution.

Maternal exposure to $\text{PM}_{2.5}$ and UFPs has been documented to yield an array of adverse health effects in offspring (Johnson et al., 2021). In regards to growth effects of prenatal PM exposure, evidence from human epidemiological studies and experimental animal models have suggested an association between *in utero* PM exposure and the likelihood of developing obesity, diabetes, or insulin resistance (Hales et al., 2017, Gingras et al., 2018, Alderete et al., 2018). The primary objective of our study was to evaluate the adverse impacts of UFP exposure on offspring development and metabolic health. Following *in utero* UFP exposure, we observed significant differences in the body weights of female pups but not males at PND 5. Additionally, on PND 5 we recorded the mass and calculated the relative weights of various organs including liver, kidneys, brain, heart, spleen, BAT, and WAT for comparison between FA and HD exposure groups. No significant differences were observed for these tissue assessments, however there are trends in several tissue weights including liver (decreased in PM groups), spleen (increased in PM groups), and BAT/WAT (decreased in female PM group). This suggests sex specific differences between exposed offspring. This evidence is comparable to those observed by Wu et al. in the impacts of gestational UFP exposure and organogenesis in a rat model employing ammonium sulfate nanoparticles which certain tissues displayed reduced mass following maternal UFP exposure (Wu et al., 2019). Following litter culling on PND 5, growth trends of remaining pups during lactation (PND 5-PND 21) displayed repressed weight gain of PM-exposed litters in comparison to FA-exposed litters (Fig. 3.). Significant differences in body weight were detected at specific points in time of lactation, and differences between FA and PM

exposed pups were more pronounced in females in comparison to males. These data points are reflective of those presented by Tsukeu et al. in which decreased body weight was detected in both sexes following maternal exposure to PM pre-pregnancy (Tsukeu et al., 2002). This is also reflected by the conclusions of Uwak et al. in which a meta-analysis was conducted to analyze evidence of low birth weight following PM exposure throughout pregnancy (Uwak et al., 2021). Additionally, PM exposed pups of both sexes displayed repressed weight gain from PND 21-PND 105 following assignment to low fat or high fat diet chow. Between exposure and diet groups in this study, significant differences were only observed in female pups from post-natal week 9 onward. Male mice did not display any measurably significant differences in weight between diet and exposure groups. Echo MRI whole body measurements performed on PND 105 revealed further evidence of sex specific differences in diet and exposure groups. Measurements of both fat content and fat/lean tissue ratios exhibit suppression in female PM treated groups in comparison to FA groups. These trends further imply that prenatal PM exposure may induce sustained weight suppression into adulthood. Our results follow the findings of Xie et al., which demonstrated reduced body weights in offspring following *in utero* PM exposure, albeit for male offspring (Xie et al., 2019). Conversely, these trends are in opposition to several investigations such as Wei et al. and Woodward et al. which showed greater weight gain in mice following gestational PM exposure (Wei et al., 2016, Woodward et al., 2019). Ultimately, these results differ in demonstrating greater burden of metabolic disease in offspring, in regards to GTT results, as well as lipid staining in hepatic tissues. Upon reaching PND 105/PNW 15, all C57Bl/6n mice were sacrificed and their tissues collected. Recorded tissue weights demonstrated few observably significant differences, however relative liver weights were significantly different for female offspring. Other tissues including kidneys, brain, heart, spleen, BAT, and

WAT failed to show significant differences; however, certain trends are suggested including sex driven differences between FA and PM exposed mice for brain, heart, BAT, and WAT.

In summary, our work demonstrates that maternal UFP exposure represents a window of susceptibility to environmental exposures. Our results indicate that *in utero* UFP exposure leads to a sustained growth suppression, particularly in female offspring. Further work is necessary to effectively explore and clarify the molecular mechanisms that contribute to reduced growth.

CHAPTER III METABOLIC STUDY 2: GESTATIONAL EXPOSURE TO ULTRAFINE PARTICLES ALTERS BONE DENSITY AND HEPATIC LIPID CONTENT

Introduction:

Ambient air pollution remains represents one of the most wide-reaching public health concerns of the 21st century. Of the many components and chemical hazards that constitutes the heterogenous makeup of air pollution, PM is associated with a wide variety health effects including cardiovascular disease, asthma, neurological impairment, and more recently diabetes and metabolic disease (Yang et al. 2009, Kim et al., 2015). These concerns are increasingly prevalent with smaller PM size fractions, fine particulate matter (PM_{2.5}) and ultrafine particulate matter (PM_{0.1}, UFPs). These tiny particles have large surface areas, high oxidative capacity, based on variable chemical constituents, and can cross the alveolar barrier circumventing primary airway defense mechanisms (Kwon et al., 2020). One of the primary sources of UFPs is motor traffic in the form of diesel exhaust PM that contributes heavily urban air pollution (Kumar et al., 2014). One of the main mechanisms by which fine and ultrafine PM causes disease is the combined effects of oxidative stress and inflammation. Numerous studies show PM constituents such as metals and organic PAHs induce ROS production in cells and tissues following inhalation (Beatriz Gonzalez et al., 2004). Specifically, copper and zinc in addition to organic compounds induce ROS (Wang et al., 2013). The release of free radicals (ROS) results in cellular damage, apoptosis, and tissue remodeling (Losacco et al., 2018).

Despite the large body of evidence of direct exposure to PM, only in recent years have studies focused on PM exposure during pregnancy and examined health impacts on the developing fetus. Impacts from environmental exposures during this sensitive period of development yields consequences for fetal growth (Liu et al., 2007). Accumulating evidence thus far associates PM exposure during pregnancy with increased risk of adverse pregnancy-related

conditions like preeclampsia and preterm birth, and birth outcomes like low birth weight and small for gestational age (Backes et al., 2013). In addition to inducing systemic maternal oxidative stress, UFPs may directly affect the fetus through transfer across the placenta. Black carbon particles, largely produced from vehicle combustion, have been observed to accumulate on the fetal side of the placenta in humans (Bove et al., 2019). This accumulation of black carbon, and possibly other forms of PM, may present potential harm on the developing fetus. A recent investigation in our laboratory employing gestational UFP exposure in a mouse model demonstrated UFP exposure during gestation impacts fetal and placental weight, placental size and morphology, thus implicating placental dysfunction in adverse fetal effects (Behlen et al., 2021).

A topic of growing, yet currently under studied is the potential health impact of maternal UFP exposure on proper bone development and bone health. However, emerging evidence from human epidemiology studies suggest PM_{2.5} exposure may play a role in bone turnover. Liu et al. evaluated the association between air pollution, including PM_{2.5}, and markers of bone turnover and bone loss in children (Liu et al 2015). Investigators measured serum levels of osteocalcin and CTx (C-terminal telopeptide of type I collagen), two bone turnover markers, in 2,264 children aged 10 years. The coarse fraction, PM_{2.5-10}, PM was found to have a positive association with both markers. Additionally, living in close proximity to a major road (≤ 350 m) increased levels of bone turnover in children in both markers. Similarly, Chen et al. found that chronic exposure to traffic-derived PM was associated with lower total body bone mineral density (BMD) and pelvic BMD following adjustment for sex, weight, age, and height in adults living within 500 m of a freeway. Adjusted mean total body and pelvic BMD for adults living within 500 m of a freeway was 0.002 and 0.03 g/cm² lower than participants living further than

1,500 m from a major freeway (Chen et al., 2015). Additionally, studies have strongly suggested an association between chronic PM exposure and increased risk of bone fractures or osteoporosis. Prada et al. demonstrated an increased risk of osteoporosis through two independent studies, one of which examined high PM_{2.5} and found greater risk of bone fractures within low income communities (Prada et al., 2017). To better understand the mechanisms of how early life exposure to PM influences bone health and metabolic disease risk, in this aim we employed our established mouse model by exposing time-mated C57Bl/6n mice throughout gestation to filtered air or UFPs at varying doses. Offspring were tracked until 15 weeks of age, for growth (including bone density analysis) and hepatic lipid accumulation.

Methods:

Animals and Particulate Matter Exposure:

Male and female C57BL/6n mice were maintained and bred in-house at the Texas A&M Institute for Genomic Medicine (TIGM) (College Station, Texas). Each mouse and litter were housed under climate-controlled conditions in cages at 25°C on a 12-hour light/12-hour dark and maintained on a typical chow diet. All procedures were approved by the Institutional Animal Care and Use Committee (IACUC) of Texas A&M University, and all methods were applied in accordance with the relevant guidelines. Female mice were time mated, checked for vaginal plugs, defined at GD 0.5, and then randomly assigned for an exposure group. Exposure occurred in our custom-built whole-body exposure chambers from GD 0.5 to 17.5 (Fig. 3.9.) as previously described. However, in this aim, we employed two UFP doses, low dose (LD) 100 µg/m³ or high dose (HD) 500 µg/m³ to investigate dose effects. Following the end of exposure period on GD 17.5, dams were transferred to individual housing and allowed to deliver.

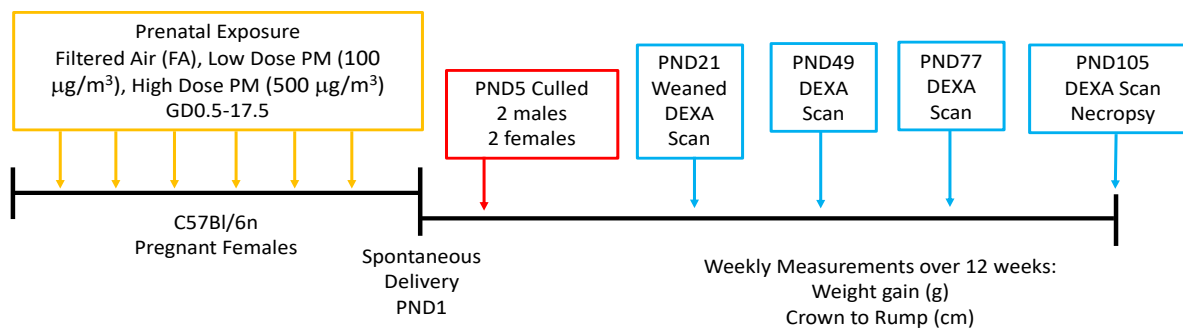


Fig 9. Study design for assessing effects of gestational exposure to ultrafine particles (UFPs) on offspring growth. C57Bl/6n mice were time-mated; confirmation of plug defined as GD 0.5. Accordingly, pregnant dams were exposed to filtered air (FA) or UFPs in concentrations of 100 $\mu\text{g}/\text{m}^3$ or 500 $\mu\text{g}/\text{m}^3$ for 6 hours per day from GD 0.5-17.5. Following delivery, litters were culled to 2 males and 2 females on postnatal day (PND) 5. Following culling and weight recording, remaining pups stayed with their dam until PND 21 and were then weaned onto standard rodent chow. Starting at PND 21, pups were subjected to DEXA scan for evaluating whole body bone development, which was repeated at PND 49, 77, and 105. Pups were frequently assessed for changes in weight and body length on a weekly basis until PND 105.

Offspring Assessments:

Following birth, pups were allowed to nurse with dam until post-natal day 5 (PND 5), wherein litters were culled to 2 males and 2 females. Major organs were collected from culled offspring, snap-frozen, and at -80°C . These remaining pups continued to nurse until PND 21, at which point they were weaned and maintained on a typical chow diet. Body weights of pups were measured at specific days following birth (PND 5, 10, 14, 21) and then on a weekly basis following weaning at PND 21 until PND 105 (15 weeks of age). Crown to rump measurements for each pup was measured on the same days as body weights were measured. Crown to rump measurements were conducted by using a standard, straight edged ruler beginning at the center of the top of the head “crown” and measuring the distance to the base of the tail, the “rump.” Quantified measurements of whole-body bone structure were obtained via dual-energy X-ray absorptiometry (DEXA) scanner according to manufacturer’s recommendations and guidelines following anesthetic application of isoflurane. Bone composition for each subject was evaluated

in terms of bone lengths and bone density on PND 21, 49, 77, and 105. After DEXA analysis on PND 105, mice were sacrificed using euthasol. Multiple tissues were collected including liver, spleen, kidneys, stomach, pancreas, intestines, genitalia, white adipose tissue (WAT), brown adipose tissue (BAT), brain, and lungs. All tissues were weighed by scale and saved via liquid nitrogen and stored at -80°C. Additionally, liver tissue was portioned into lobes for histological analysis. The left lateral and medial lobes were placed into a plastic mold containing a layer of OCT and then completely covered with compound. OCT-preserved lobes were kept cold on ice until storage in -80°C and subsequent Oil Red O staining for lipids.

Thiol Redox Analysis:

Sample Preparation:

Thiol redox analysis followed Jones and Liang with slight modifications (Jones & Liang et al., 2009). Liver samples collected on PND 5 from the culled offspring not assigned to longitudinal metabolic study were used for thiol redox analysis. Approximately 10-50 mg of liver tissue was quickly weighed before being homogenized in 1mL of buffer solution containing an internal standard, γ -glutamylglutamate (γ -Glu-Glu). Sample homogenate was kept cold during the homogenization process by storing the glass homogenizer and a beaker of sample buffer in a bucket of ice. Once tissue was fully homogenized and no large chunks were apparent, homogenate was transferred to a pre-labeled microcentrifuge tube. The same glass homogenizer and plunger were used and washed between samples with alconox soap and MilliQ water to prevent residue or contamination of following samples. Once all samples were homogenized and transferred to microcentrifuge tubes, they were centrifuged at 10,000 g for 10 minutes at 4°C to pellet proteins and lipids. Next, 300 μ L of supernatant was transferred to a newly labeled microcentrifuge tube and kept on ice. 60 μ L of 7.4 mg/mL iodoacetic acid (IAA) was added to

the supernatant and immediately vortexed. Following addition of IAA, sample solution pH's were adjusted to $\sim 9.0 \pm 0.2$ with $\sim 425 \mu\text{L}$ of KOH/tetraborate to precipitate proteins. KOH/tetraborate solution was added in aliquots of 25-200 μL , and then allowed to incubate at room temperature for 30 minutes. Once incubation time was completed, samples pH was assessed using pH strips to ensure correct pH range. During the incubation period, fresh dansyl chloride (DC) solution (20 mg/mL in acetone) was made. 300 μL was added to each sample and immediately vortexed. Once all samples received DC and were mixed, samples were incubated at room temperature in complete darkness for 16-28 hours. Following DC incubation period, 500 μL of HPLC-grade chloroform was added to samples, vortexed, and centrifuged. The upper aqueous layer was transferred to a final microcentrifuge storage tube and stored in -80°C until HPLC analysis.

HPLC Analysis:

Samples were thawed on ice and then centrifuged for 10 minutes in a microcentrifuge. Following centrifugation, an aliquot of each sample was transferred to an HPLC autosampler vial. 35 μL was injected on a Supelcosil LC-NH₂ column with internal dimensions of 5 μm , 4.6 mm X 25 cm (Supelco, Bellefonte, PA). Column oven operating temperature was held constant at 35°C . HPLC mobile phases included solvent A (80% v/v methanol/water) and solvent B (acetate-buffered methanol). Initial solvent conditions were 80% A, 20% B at 1 ml/minute for 10 minutes. A linear gradient to 20% A and 80% B was then run from 10-30 minutes. From 30 to 35 minutes, the flow gradient was maintained at 20% A and 80% B. Last, from 35 to 42 minutes, conditions were returned to 80% A and 20% B. Detection of desired thiols was obtained by fluorescence monitoring. Approximate elution time frames of compounds of interest were as followed: cystine (CySS) from 9 to 9.5 min; cysteine (Cys) from 10 to 10.5 min; γ -GluGlu from

12 to 13 min; glutathione (GSH) from 19 to 19.5; and glutathione disulfide (GSSG) from 23.5 to 24 min.

Statistical Analysis:

Data are expressed as mean values \pm SEM. All sample sizes are displayed within figures. Statistical analysis was performed using GraphPad Prism (V 9.0.2). Differences between groups were compared using two-way analysis of variance (ANOVA) with Tukey's multiple comparison test. $p < 0.05$ was considered statistically significant.

Results:

Initially, we assessed UFP impact on maternal weight gain via daily monitoring during pregnancy. There were no significant differences between exposure groups and control throughout gestation (Fig. 10A). Following parturition, dams were also weighed on PND 5, 10, 14, and 21. During this phase of observation, dams did not display measurably significant differences in weight by either one-way or two-way ANOVA. However, recorded weight data does suggest trends of differences in weight between exposure groups during the lactational period. These trends suggest both LD- and HD-exposed dams experience sustained reduction in weight (Fig. 10B).

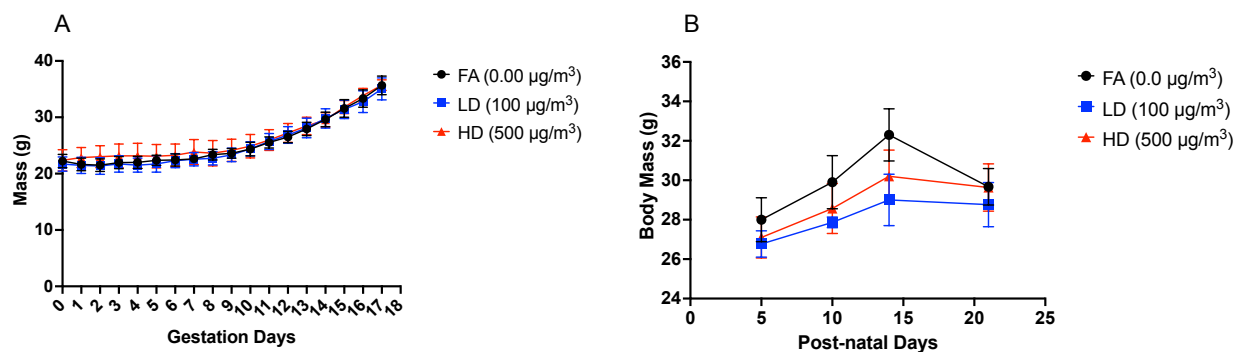


Fig 10. Dam weight gain data. (A) Dam gestational exposure data from GD 0.5-17.5. (B) Dam weight data during lactation PND 5-21.

Following delivery of pups, starting on PND5, offspring body weight was recorded on a weekly basis to monitor for changes in growth and development following gestational PM exposure (Fig. 11). Weight gain in male offspring revealed multiple significant differences throughout their long-term development, overall weight trends suggest the LD-exposed mice displayed somewhat lower body weights throughout the monitoring period (Fig. 11A). Measurements of female offspring body weights also were not significantly different among groups. However, a trend in decreased weight in the HD-exposed female mice is observed (Fig. 11B).

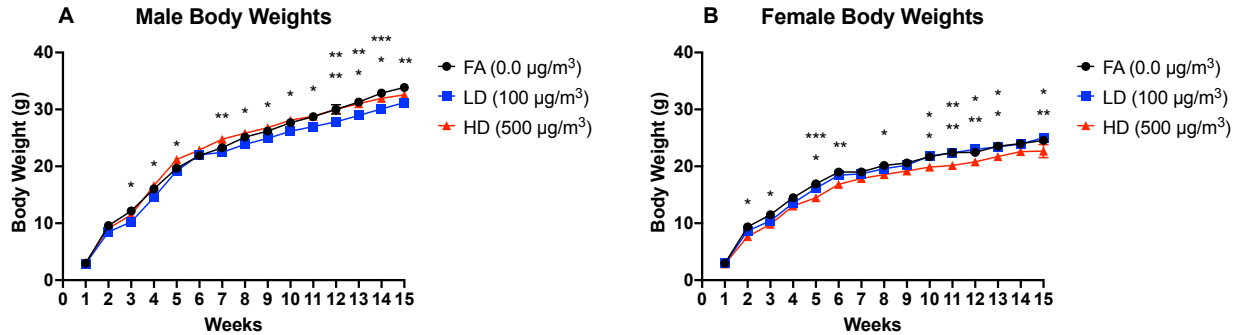


Fig 11. Offspring body weight (g) from postnatal week 1 to postnatal week 15. (A) Male offspring body weight measurements. (B) Female offspring body weight measurements. Values are reported in mean \pm SEM. Significant differences detected via two-way ANOVA.

In addition to frequent measurement of offspring body weights as they aged, crown to rump length (cm) was recorded for all offspring. Male and female offspring displayed few significant differences between exposure groups but did not correlate with any relevant trends via two-way ANOVA (Fig. 12).

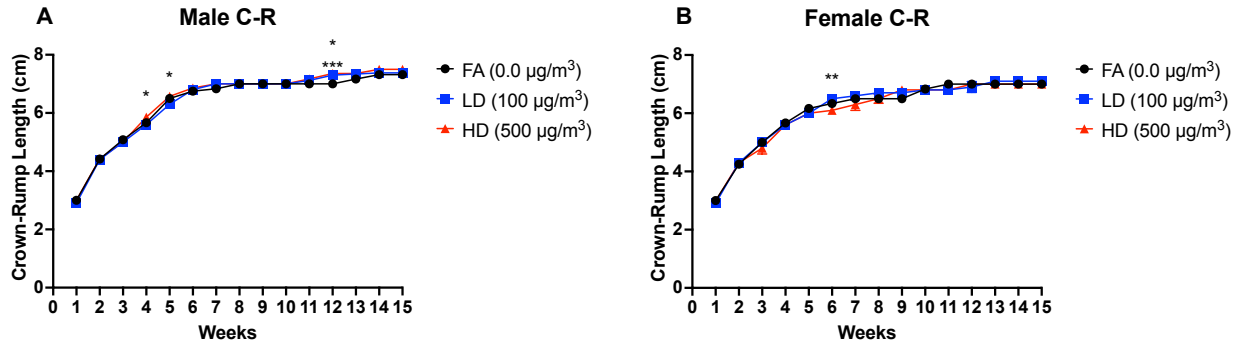


Fig 12. Pup Crown to Rump measurements (cm) from postnatal week 1 to 15. (A) Male C57Bl/6n pups crown to rump measurements in cm. (B) Female C57Bl/6n pups crown to rump measurements in cm.

Multiple measurements were recorded using a DEXA machine, including whole-body fat%, bone mineral density (BMD) and bone mineral content (BMC). For the %fat in male offspring (Fig. 13A), LD-exposed pups displayed a higher body fat% as compared to the FA control groups, but only on PND49. Female offspring (Fig. 13B) had significant differences later on in their development at PND 77 and 105. Specifically, on PND 77 LD-exposed females were significantly higher in fat% compared to FA. This significant difference continued into PND 105 with LD-exposed females displaying higher fat% in comparison to FA and HD groups.

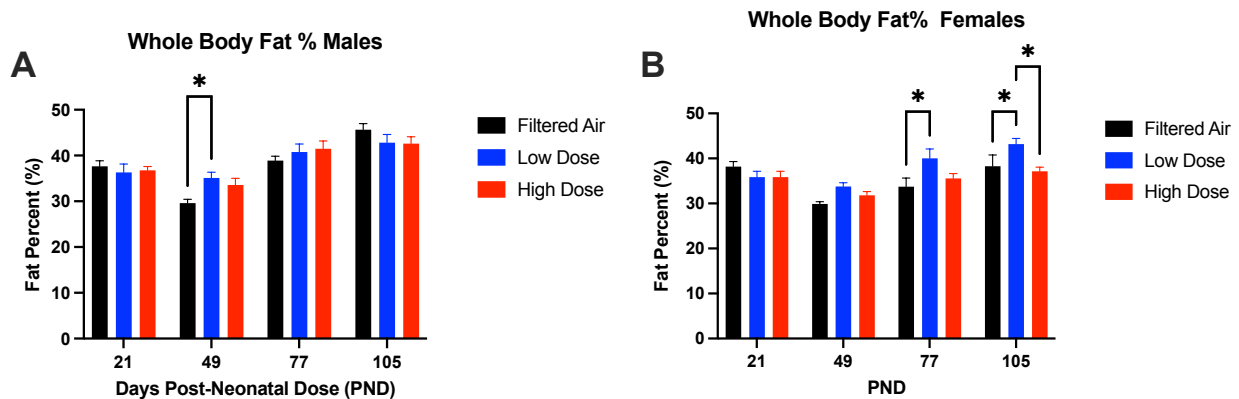


Fig 13. Whole body fat% determined via DEXA scanner. (A) Male offspring and (B) female offspring measured for whole body fat% on PND 21, 49, 77, and 105. *p<0.05.

To evaluate gestational UFP impact on hepatic lipid accumulation, liver tissues from exposed dams and prenatally-exposed offspring were harvested on PND 21 and PND 105, respectively. Liver samples were preserved via storage within OCT medium followed by oil red O staining for evaluation of lipid accumulation (Fig. 14). Dam livers harvested on PND 21 after delivery did not display significant differences in lipid accumulation score averages (Fig. 14A). Male offspring showed no significant differences in lipid accumulation scores among groups (Fig. 14B). Female offspring displayed significant differences in lipid accumulation scores, wherein LD-exposed mice had significantly higher lipid accumulation scores in comparison to both FA and HD groups (Fig. 14C).

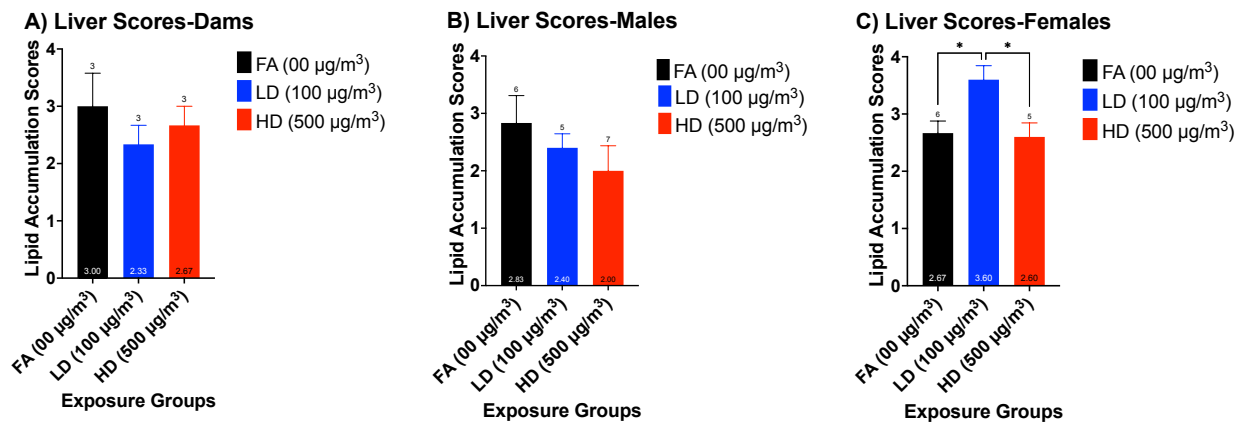


Fig 14. Liver histology via oil red O for evaluating lipid accumulation. (A) Liver histology scores for dams. (B) Liver histology scores for male pups. (C) Liver histology scores for female pups. *($p < 0.05$) Statistical significance detected via one-way ANOVA.

BMD is a measure of the amount of bone mineral in bone tissue. Overall, scans conducted on PND 21, 49, 77, and 105 revealed an expected general increase in BMD in both male and female offspring (Fig. 15). Male offspring evaluated throughout their development showed significant differences at multiple time points between exposure groups. At PND 77, the LD exposure group was significantly lower than the HD group. Additionally, significant differences were detected at PND 105 between all exposure groups, with the HD group

displaying the greatest BMD (Fig. 15A). Female offspring showed significant differences in BMD on PND 49. At this period of postnatal development, both LD and HD group averages were decreased in comparison to FA (Fig. 15B).

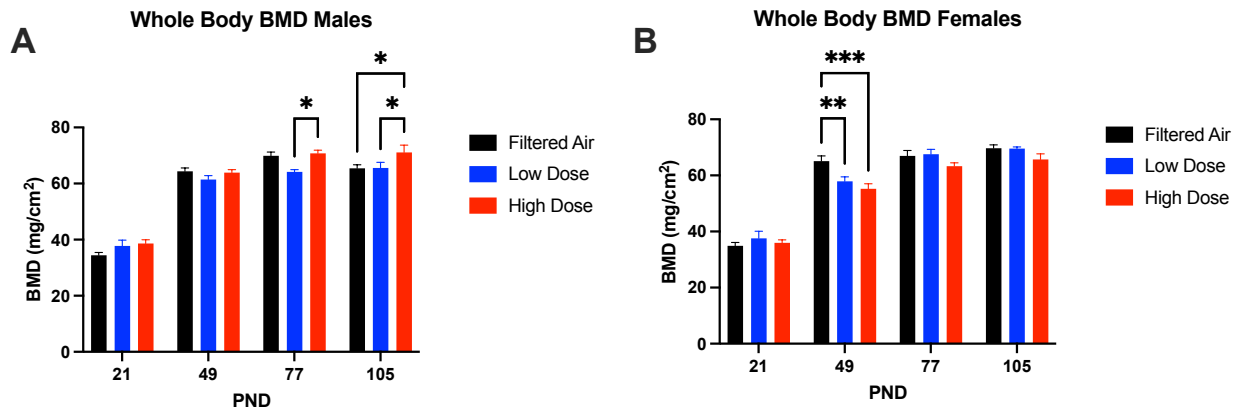


Fig 15. Whole body bone mineral density (BMD) determined via DEXA scanner. (A) Male offspring and (B) female offspring measured for whole body BMD on PND 21, 49, 77, and 105. *($p < 0.05$).

Additionally, whole body mineral content (BMC) is a measure of bone mineral in specific ROI (mg). Male offspring displayed significant differences at multiple points in time in their growth. From PND 49 onward, average BMC levels in LD-exposed males were significantly lower than HD-exposed males, and on PND 105 LD-exposed male values were significantly lower than both FA and HD groups (Fig. 16A). Female offspring only displayed significant differences on PND 49 mirroring BMD data wherein HD-exposed offspring values were significantly lower than FA control (Fig. 16B). Again, this difference was resolved by PND 77 and onward.

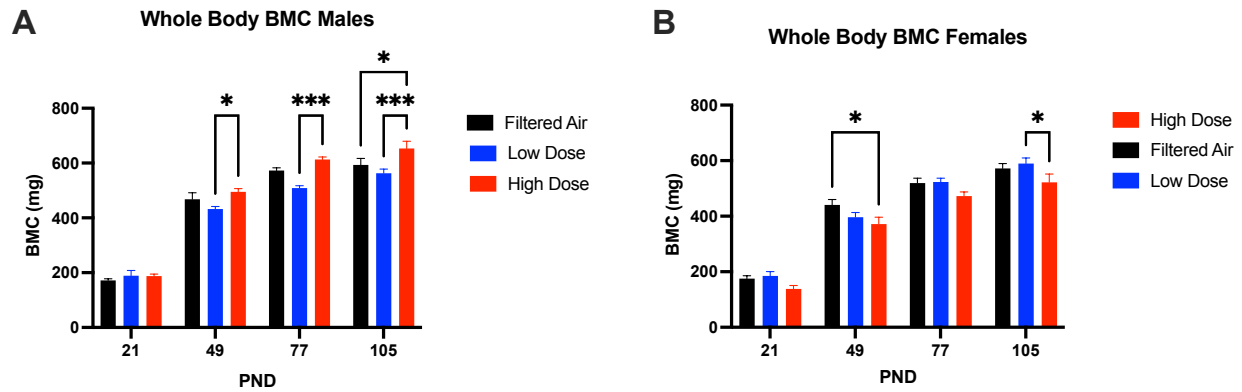


Fig 16. Whole body bone mineral content determined via DEXA scanner. (A) Male and (B) female offspring measured for whole body bone mineral content (BMC) on PND 21, 49, 77, 105. *($p < 0.05$).

Following whole body assessments, limbs and appendages BMD were also measured, beginning with the right femur of each mouse (Fig. 17). Male offspring displayed significant differences at multiple points in time. At PND 49, HD-exposed males had significantly greater BMD average levels than FA mice. This difference was sustained as time progressed to PND 77 and PND 105 where HD-exposed males showed BMD averages greater than both LD- and FA-exposed males (Fig. 17A). Conversely, female offspring displayed significant differences in bone mass density of their right femur only at PND 49, wherein HD-exposed females showed significantly lower BMD average levels versus the FA control group (Fig. 17B).

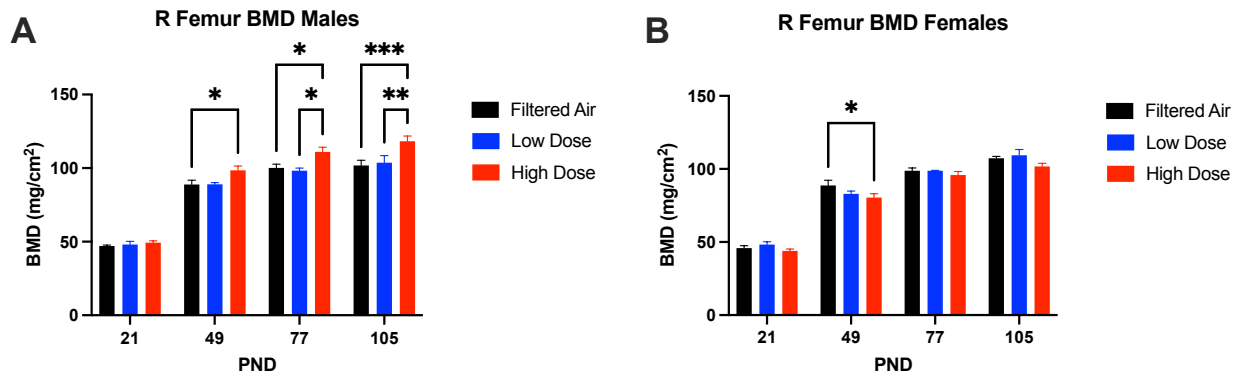


Fig 17. Right femur bone mineral density (BMD) determined via DEXA scanner. (A) Male and (B) female offspring measured for bone mineral density on PND 21, 49, 77, 105. *(p<0.05).

Following measurement of the right femur, the bone mineral density (BMD) of the left femur was evaluated (Fig. 18). Male offspring displayed significant differences on PND 77 wherein HD-exposed males displayed higher left femur BMD than LD mice. On PND 105 HD-exposed mice levels were significantly higher than FA mice (Fig. 18A). Conversely, female offspring showed significant differences at PND 49 wherein HD-exposed females had significantly lower left femur BMD average levels in comparison to HD-exposed females (Fig. 18B).

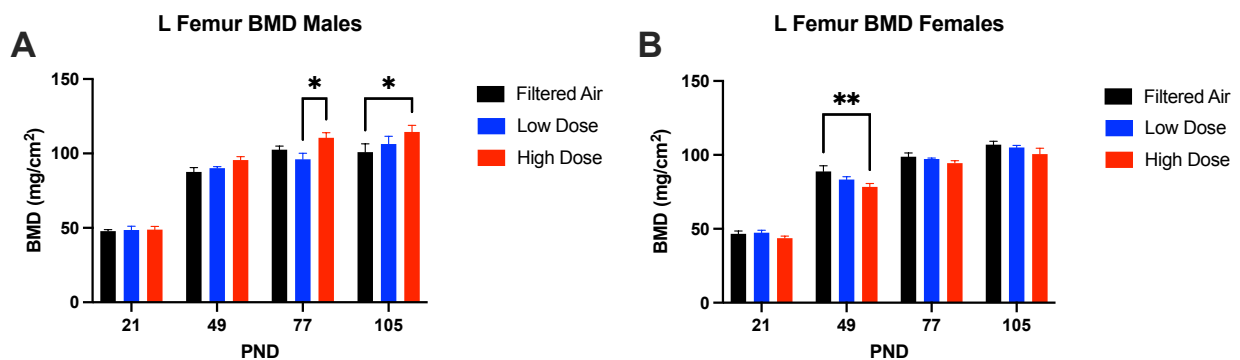


Fig 18. Left femur bone mineral density (BMD) determined via DEXA scanner. (A) Male and (B) female offspring measured on PND 21, 49, 77, and 105. *(p<0.05).

Right tibia BMD was measured in male and female offspring (Fig. 19). Male offspring displayed significant differences at multiple points in growth at PND 49, 77, and 105. At PND 49, HD-exposed males showed the greatest BMD in comparison to LD-exposed males, which continued at PND 77, and expanded at PND 105 where HD males had the highest right tibia BMD in comparison to both FA- and LD-exposed males (Fig. 19A). Female offspring only displayed significant differences on PND 49 where LD- and HD-exposed females had lower right tibia BMD average values compared to the FA control group (Fig. 19B).

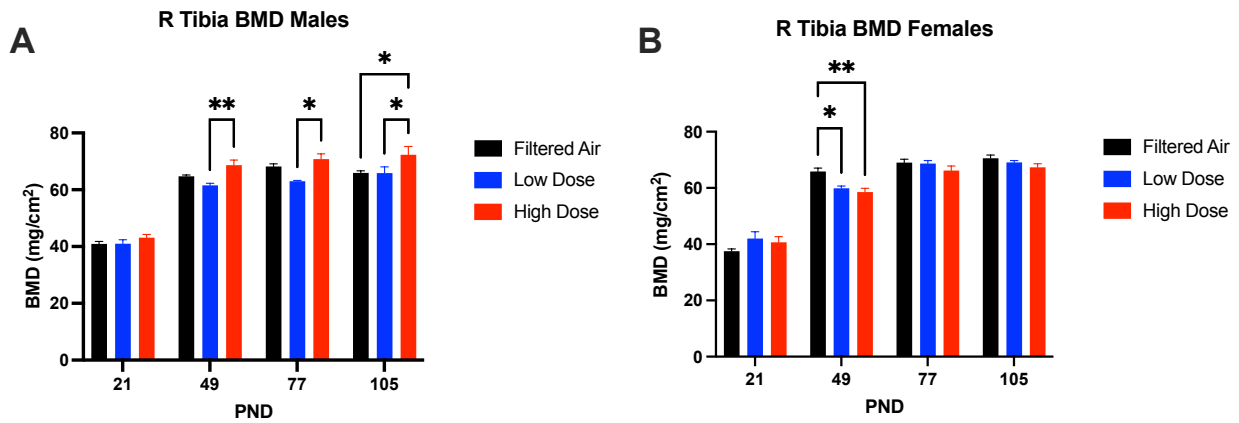


Fig 19. Right tibia bone mineral density (BMD) determined via DEXA scanner. (A) Male and (B) female offspring measured on PND 21, 49, 77, and 105. *($p < 0.05$).

Left tibia BMD measurements were recorded in 6 offspring (Fig. 20). Male offspring did not display any significant differences in left tibia BMD at any point in time (Fig. 20A). However, female offspring did demonstrate significant differences at PND49 where the HD-exposed females had significantly lower BMD average values than FA control (Fig. 20B).

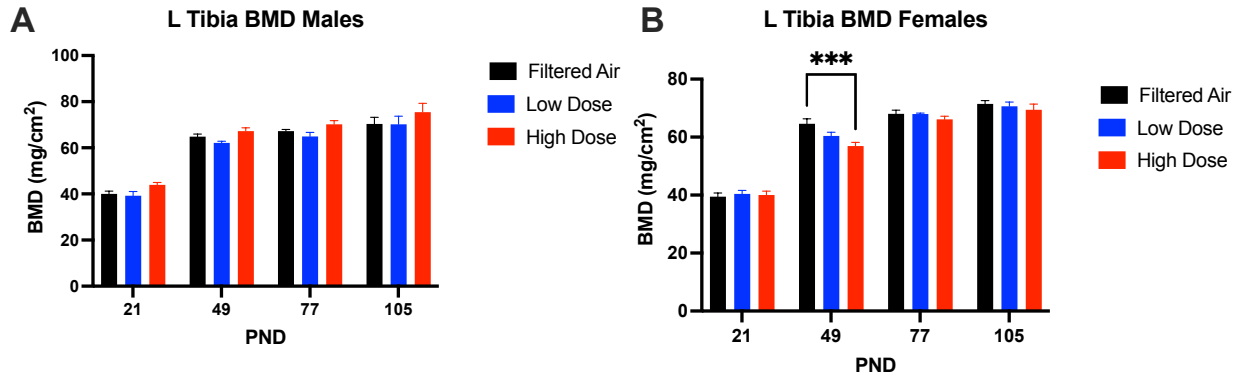


Fig 20. Left tibia bone mineral density (BMD) determined via DEXA scanner. (A) Male and (B) female offspring measured on PND 21, 49, 77, and 105. *(p<0.05).

The next measurements for bone health assessment were of the bone mineral density of segments of the femur. The first segment to be analyzed was the proximal portion of the femur (Fig. 21). Male offspring displayed significant differences at multiple points in time between several exposure groups. At PND 77, the HD-exposed males had the greatest proximal femur BMD in comparison to both FA- and LD-exposed males. This significant difference was observed at PND 105 as well (Fig. 21A). Female offspring did not display any significant differences at any point of observation.

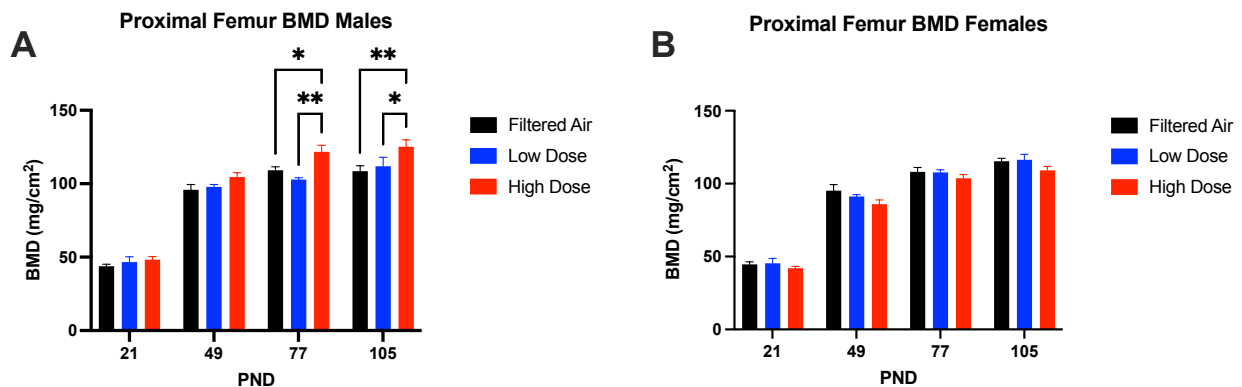


Fig 21. Proximal femur bone mineral density (BMD) determined via DEXA scanner. (A) Male and (B) female offspring measured on PND 21, 49, 77, and 105. *(p<0.05).

The next portion of the femur that was evaluated for BMD was the mid femur (Fig. 22). Significant differences between exposure groups were only observed on PND 105 in male offspring where the HD males displayed greatest mid femur BMD in comparison to both FA- and LD-exposed males (Fig. 22A). Female offspring did not display any significant differences at any point of observation (Fig. 22B).

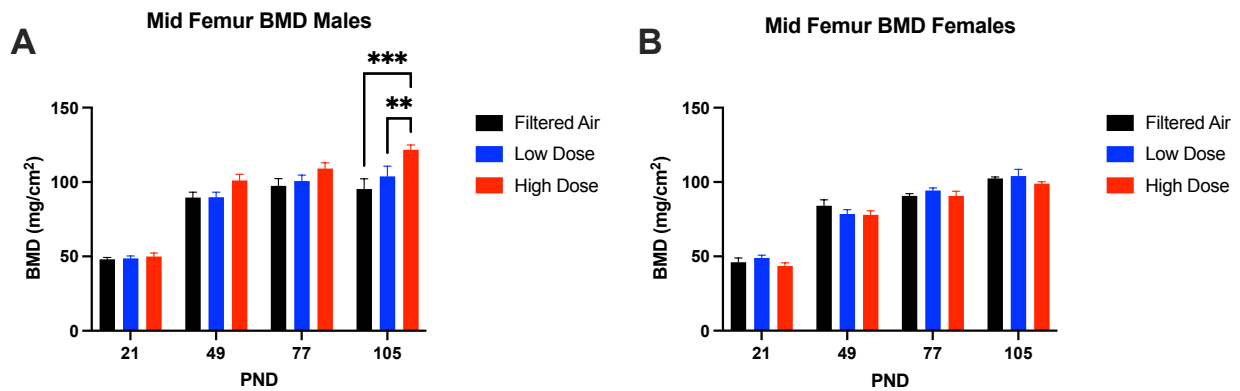


Fig 22. Mid femur bone mineral density (BMD) determined via DEXA scanner. (A) Male and (B) female offspring measured on PND 21, 49, 77, and 105. *($p < 0.05$).

The final portion of the femur that was assessed was the distal portion of the femur (Fig. 23). Significant differences were observed in most time points for males including PND 49, 77, and 105. On PND 49, HD-exposed males had the highest BMD in comparison to both FA- and LD-exposed mice, and this trend repeated on both PND 77 and 105 (Fig. 23A). Female offspring did not show any significant differences between exposure groups (Fig. 23B).

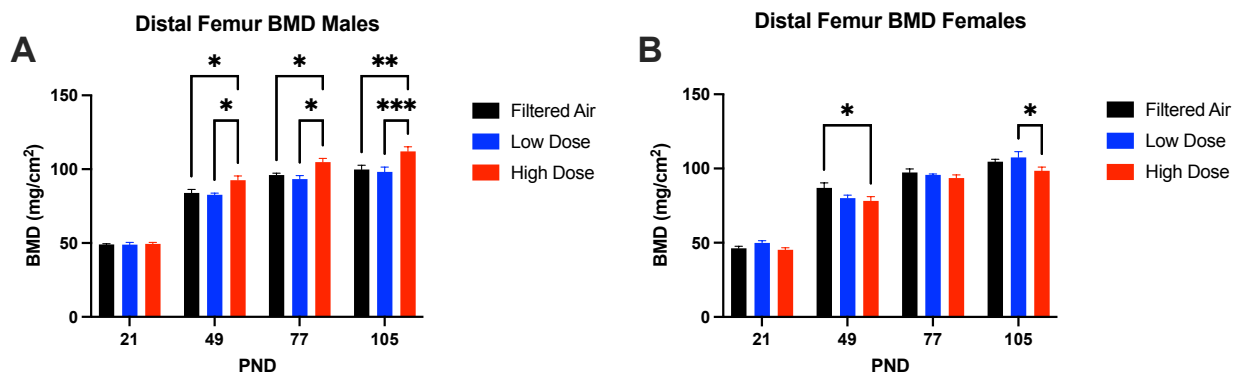


Fig 23. Distal femur bone mineral density (BMD) determined via DEXA scanner. (A) Male and (B) female offspring measured on PND 21, 49, 77, and 105. *($p < 0.05$).

Following evaluation of femur BMD, tibia BMD portions were measured. The first portion of the mouse tibia to be evaluated was the proximal portion (Fig. 24). Male offspring displayed significant differences at multiple points in their development, in particular PND 49, 77, and 105. Starting at PND 49, the HD-exposed male mice displayed the greatest BMD values of the proximal tibia in comparison to the LD-exposed males and was repeated on PND 77. On PND 105, the HD-exposed male BMD average value was significantly higher in comparison to the FA-exposed males (Fig. 24A). Female offspring showed a significant difference on PND49 in which the LD- and HD-exposed mice proximal tibia BMD average level was lower in comparison to the FA control (Fig. 24B).

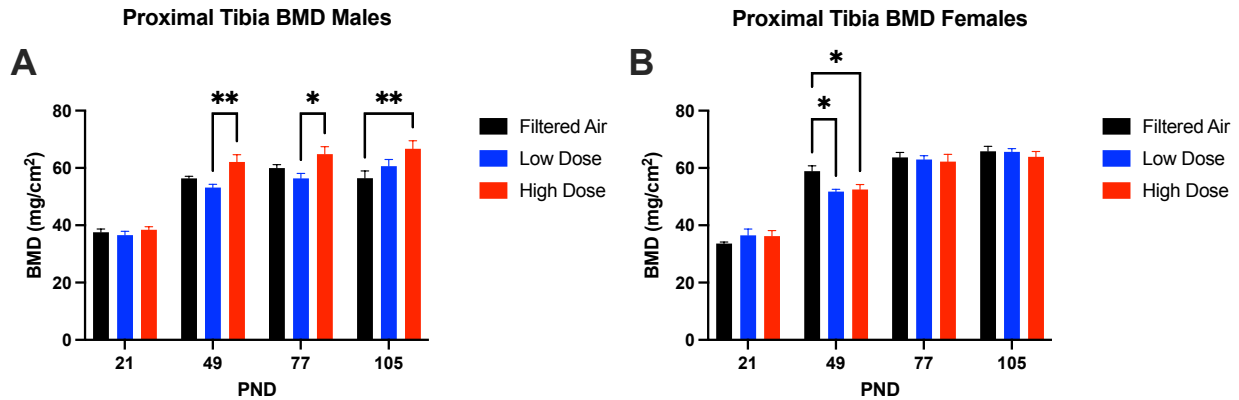


Fig 24. Proximal tibia bone mineral density (BMD) determined via DEXA scanner. (A) Male and (B) female offspring measured on PND 21, 49, 77, and 105. *(p<0.05).

Following proximal portion, the mid portion of the tibia was evaluated for significant differences in BMD between exposure groups (Fig. 25). Male offspring did not display any significant differences in BMD throughout the observation period (Fig. 25A). Female offspring displayed interesting significant differences at several intervals of observation. At PND 21, the LD- and HD-exposed female mice showed significantly greater mid tibia BMD levels compared to the FA group. However, this was reversed on PND 49 and PND 105, wherein the LD- and HD-exposed females showed lower average BMD values than the FA control group (Fig. 25B).

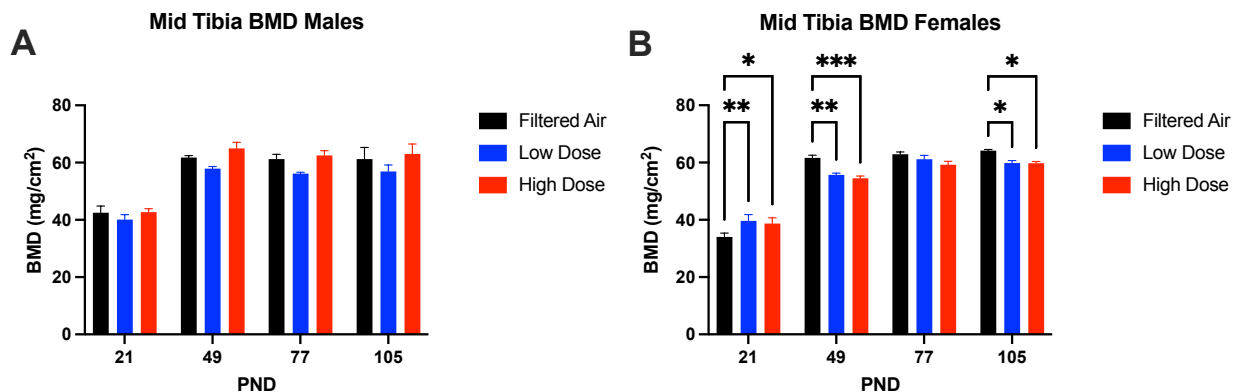


Fig 25. Mid tibia bone mineral density (BMD) determined via DEXA scanner. (A) Male and (B) female offspring measured on PND 21, 49, 77, and 105. *(p<0.05).

The final portion of measurement was for the BMD of the distal tibia (Fig. 26).

Significant differences in distal tibia BMD was observed in male offspring at PND 77 and PND 105. During these points in development, the HD-exposed male mice displayed higher distal tibia BMD in comparison to the LD-exposed males (Fig 26A). Female offspring also displayed significant differences in distal tibia BMD but in the earlier periods of development, namely PND 21 and 49. On PND 21, the LD-exposed females exhibited the highest BMD in comparison to FA exposed mice. However, on PND 49, the HD-exposed females displayed significantly lower average BMD values compared to FA control. Ultimately, these disparities seem to rebound in later periods (Fig. 26B).

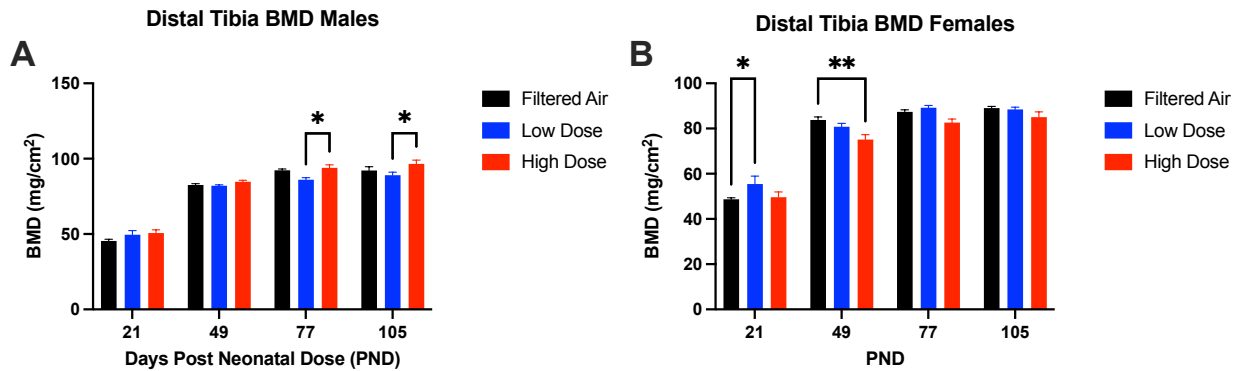


Fig 26. Distal tibia bone mineral density (BMD) determined via DEXA scanner. (A) Male and (B) female offspring measured on PND 21, 49, 77, and 105. *(p<0.05).

Table 3.1: DEXA Machine Data

Endpoint:	Males compared to FA:	Females compared to FA:
Whole body fat %	Increased LD (49)	Increased LD (77, 105)
Whole body BMD	Increased HD (105)	Decreased LD, HD (49)
Whole body BMC	Increased HD (105)	Decreased LD, HD (49)
Right femur BMD	Increased HD (49, 77, 105)	Decreased HD (49)
Left femur BMD	Increased HD (105)	Decreased HD (49)
Right tibia BMD	Increased HD (105)	Decreased LD, HD (49)
Left tibia BMD	NS	Decreased LD, HD (49)
Proximal femur BMD	Increased HD (77, 105)	NS
Mid femur BMD	Increased HD (105)	NS
Distal femur BMD	Increased HD (49, 77, 105)	NS
Proximal tibia BMD	Increased HD (105)	Decreased LD, HD (49)
Mid tibia BMD	NS	Increased LD, HD (21); Decreased LD, HD (49, 105)
Distal tibia BMD	NS	Increased LD (21); Decreased HD (49)

Gestational exposure to PM is known to cause systemic maternal and placental oxidative stress. Detection of oxidized thiols provides evidence for local or systemic oxidative stress, which may subsequently contribute to the develop of PM-induced inflammation and disease pathogenesis. In this model, we used an HPLC-based method for quantification of reduced glutathione (GSH) and cysteine (CyS), in addition to their oxidized counterparts glutathione disulfide (GSSG) and cystine (CySS) within samples liver tissues of offspring collected on PND5. Successful quantification of redox related thiols GSH, GSSG, CyS, and CySS yielded significant differences in thiol amounts between exposure groups in terms of raw concentrations and % change from reduced to oxidized thiols (Figs. 27-29). For GSH and GSSG, redox analysis showed significant differences between each exposure groups (Fig. 27). The HD-exposed group

had the highest amount of GSH compared to FA and LD groups (Fig. 27A). Alternatively, GSSG levels in the LD group were higher in comparison to both FA and HD groups (Fig. 27B).

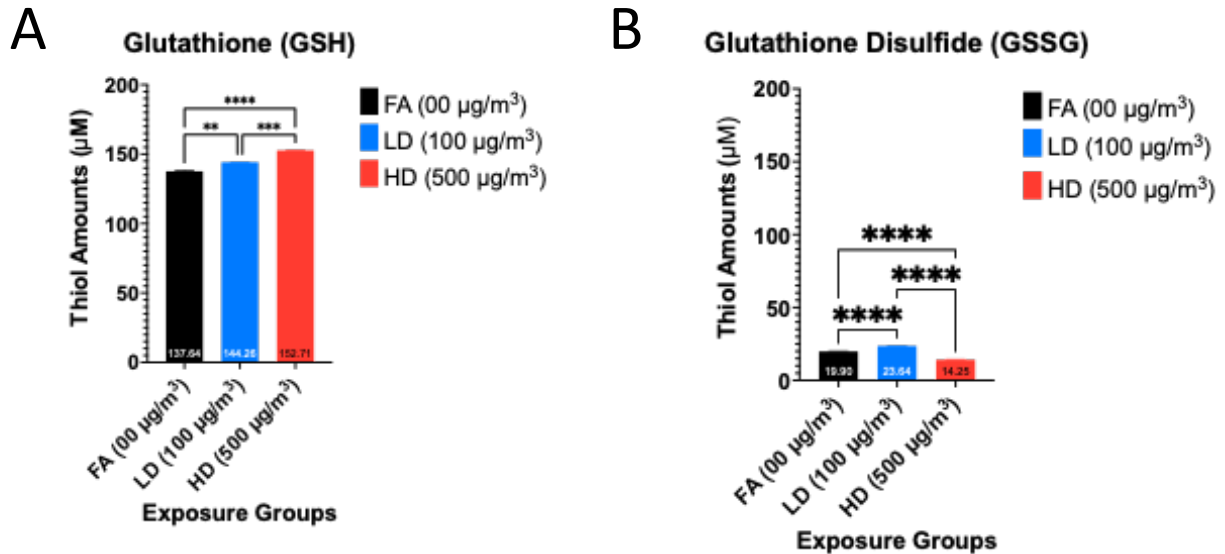


Fig 27. Thiol quantification for oxidative stress biomarkers. (A) Glutathione (GSH) and (B) glutathione disulfide (GSSG) measurements in PND5 offspring liver tissue. Values are presented as mean \pm SEM. * $p < 0.05$. Significant differences detected via one-way ANOVA with Tukey’s comparison test.

Likewise, measures of CyS and CySS revealed significant differences between exposure groups (Fig. 28). Analysis showed a significantly higher amount of CyS within HD-exposed pup liver tissue in comparison to both FA and LD exposure groups (Fig. 28A). CySS levels did not show significant differences, however there is a trend in which LD-exposed neonates had lower CySS than both FA- and HD-exposed pups (Fig. 28B).

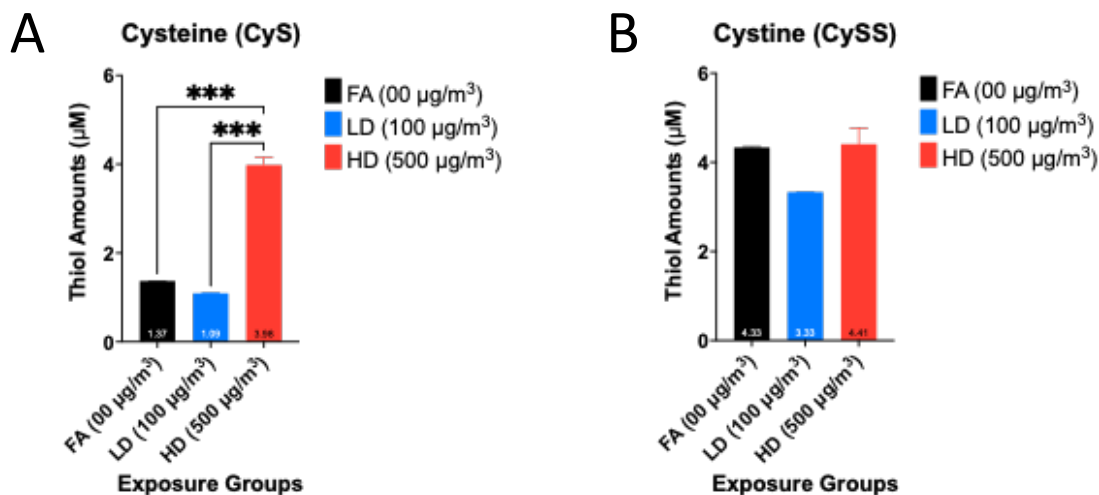


Fig 28. Thiol quantification for oxidative stress biomarkers. (A) Cystiene (CyS) and (B) cystine (CySS) measurements in PND5 offspring liver tissue. Values are presented as mean \pm SEM. * $p < 0.05$. Significant differences detected by one-way ANOVA with Tukey's comparison test.

Following quantification and detection of antioxidant thiols, % change from reduced to oxidized thiols within tissues were calculated by dividing oxidized thiols by the sum of reduced and oxidized thiols, all multiplied by 100 for final result: $(\text{Oxidized}/(\text{Reduced} + \text{Oxidized})) \times 100$ (Fig. 29). %CySS was reduced in the LD group in comparison to FA, with the greatest %change in the HD group vs. FA (Fig. 29A). %GSSG was significantly increased in the LD group, but decreased in the HD group (Fig. 29B).

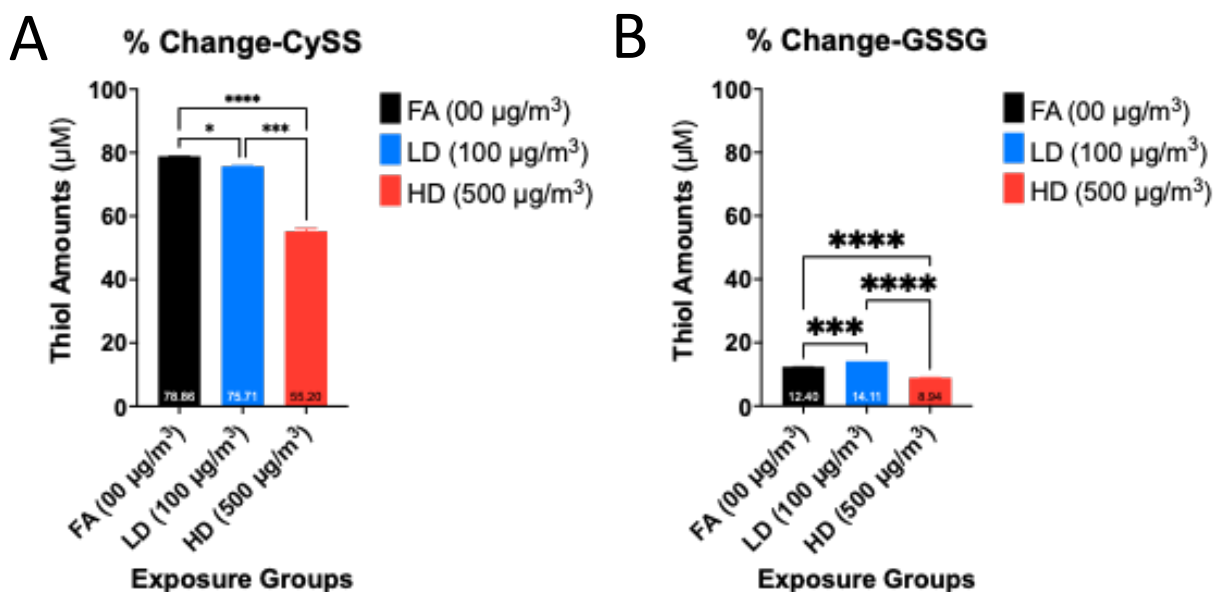


Fig 29. % change from reduced to oxidized thiols in offspring PND5 liver tissue following prenatal UFP. (A) % change CySS thiol and (B) % change GSSG thiol. Values are presented as mean ± SEM. *p<0.05. Significant differences detected by one-way ANOVA with Tukey’s comparison test.

Table 3.2: Met2 HPLC Thiol Data

Endpoint	ALL in comparison with FA
GSH	Increased LD, HD
GSSG	Increased LD; decreased HD
CYS	Increased HD
CYSS	NS
%GSSG	Increased LD; decreased HD
%CYSS	Decreased LD, HD

Summaries of HPLC redox assay thiol analysis and % change.

Discussion:

In this aim we employed a two exposure levels of UFPs, 100 and 500 μg/m³, low dose (LD) and high dose (HD), respectively, to better understand how gestational exposure to PM influences bone health and metabolic disease risk. These doses correspond to 24-hour average levels of 25 and 125 μg/m³. While UFPs are currently not regulated, the low dose level is under the US EPA limit for PM_{2.5} that is 35 μg/m³ for 24-hour average. Moreover, this level is at the

WHO guideline level considered “safe” for all populations. The high dose represents a highly polluted urban environment. The longitudinal study design allowed us to track offspring growth and bone development over time into adulthood (15 weeks of age).

Overall, offspring growth, assessed through body weight and length, was not significantly impaired from gestational UFP exposure. Slight decreases in the average male body weight in the LD group and decreases in the average female body weight in the HD group were observed. Conversely, whole body fat% was increased in LD-exposed male and female offspring, at 49 days (in males) and 77 and 105 days (in females). This is in agreement with outcomes from other animal models showing decreased body weight, yet increased fat mass in PM-exposed pups (Ding et al., 2019). Likewise, hepatic lipid content in LD-exposed females was significantly greater compared to FA-exposed females. This increase was not evident in the HD-exposed females. Other data from our laboratory models consistently show sensitivity in LD-exposed female mice (Behlen et al., 2020). Transcriptomic analysis of placenta exposed to LD or HD indicated several disturbed cellular functions related to lipid metabolism, which were most pronounced in the LD group and especially in female placental tissue. We cannot directly compare these findings to our aim 1 study since we only employed HD in that model.

The dose- and sex-specific differences were also consistent for data related to bone mineral density (BMD). In male offspring, we observed an interesting effect where HD-exposed offspring showed increased BMD and BMC for whole body measurements at PND 105, in comparison to the FA control. Likewise, at various timepoints in development, and sustained until PND 105, HD-exposed males showed increased BMD, particularly in the femur measurements. In contrast, female LD- and HD-exposed offspring showed decreased whole-body BMD and BMC measures, only evident at PND 49. Decreases were consistent for femur

BMD (HD group decreases) and tibia BMD (LD and HD group decreases). Portions within the tibia showed interesting effects with early increases (PND 21) followed by decreases later in life (PND 49 and even 105). These data signify the importance of assessing endpoints over time, and separating effects by sex. Recent studies, both human epidemiological observations and animal experiments, have begun to focus on the impacts of PM exposure on healthy bone development. However, there is little to no literature on prenatal UFP exposure in relation to bone development. In lieu of this gap in research, there is evidence related to PM exposure, oxidative stress, and bone loss as related to osteoporosis. Liu et al. published a meta-analysis in 2021 in which studies were collected and analyzed for the association between air pollution and osteoporosis. The search yielded 9 studies with a collection of 9,371,212 patients and found an increased risk of osteoporosis resulting from exposure to PM_{2.5}. Though few studies were found for this meta-analysis, the comprehensive evaluation of the evidence provided further proof with which to address the health concerns of air pollution. Even more so, such recent evidence and the many gaps in knowledge further draws attention to need for studies that include dose response assessment and exposure during critical periods of life, such as during pregnancy (Liu et al., 2021). It is widely confirmed that oxidative stress is involved in the development of osteoporosis. In a case control study conducted by Sanchez-Rodriguez et al., investigators evaluated antioxidant status, superoxide dismutase (SOD), and glutathione peroxidase (GPx), in relation to the BMD of 94 human subjects ≥ 60 years of age. Investigators observed significantly lower antioxidant activity in subjects with osteoporosis, as defined by BMD of 2.5 standard deviations or more below the mean value of young adults. The subjects that displayed osteoporosis exhibited lower GPx antioxidant activity and higher SOD/GPx ratio (Sanchez-Rodriguez et al., 2007). These findings complement a 2013 study by Calderon-Garciduenas et al.

in which the investigators studied the relationship between urban air pollution, inflammation, and BMD in children ~6 years of age in Mexico City (polluted city) vs. unpolluted (control). Children were given full pediatric examinations, with serum inflammatory marker analysis and DEXA scans. The children from Mexico City exhibited significant levels of IL-6, accompanied by marked reductions in total blood neutrophils and increased monocytes in comparison to control children from a city with little air pollution. However, these cohorts did not show a significant difference in DEXA scores (Calderon-Garciduenas et al., 2013).

With growing interest and exploration of the association between PM exposure and bone fragility, understanding the biology and metabolism of bone development is crucial. Bone tissue is complex and dynamic with a wide array of cellular signaling between a plethora of cell types ranging from osteoprogenitor cells, osteoblasts, osteoclasts, and osteocytes, all of which are integral to the proper growth and remodeling of bone tissue. There is a significant interplay with immune cells that is of growing interest in regards to regulating bone remodeling and cell signaling via key cytokines and signal pathways that determine mineralization and cell differentiation. This advanced degree of cell signaling and regulation is imperative to maintaining proper processes in bone tissue such as bone turnover and repairing fractures as detailed by Datta et al in a review of bone metabolism and immune cell interactions. In regards to bone development of offspring following maternal environmental exposures, there are a number of pathways that may be of great interest to investigate such as transcriptional factor Runx2, which is vital to osteoblast differentiation, skeletal development, and embryonic bone formation. Another potential target for study is referred to as “Wingless-ints” (Wnts), which are lipid-modified glycoproteins which are key in multiple intracellular signaling pathways. Additional targets that can be investigated include proinflammatory cytokines IL-1, IL-6, and

TNF-alpha which act synergistically on osteoclastogenesis while promoting osteoclast function. Although the specific mechanisms by which cytokines are still being investigated, it is suspected that they may regulate the expression of receptor activator of nuclear factor-kB (RANK) and receptor activator of nuclear factor-kB ligand (RANKL), both of which are expressed on osteoclasts and osteoblasts and modulate various cell signals. Another potential target for investigation, that connects bone health with energy metabolism would be the receptor-like protein tyrosine phosphatase called Esp which is expressed in osteoblasts has been observed to regulate insulin secretion (Datta et al., 2008). Returning to the subject of proinflammatory cytokines, IL-1 has been demonstrated to be crucial TNF-alpha mediated bone loss. According to a 2010 study by Polzer et al utilizing human TNF-alpha containing mice crossed with IL-1 knockout mice, lack of IL-1 revealed a near complete reversal of TNF mediated bone loss and altered bone structure. In this study, mice with human TNF-alpha displayed severe and systemic bone loss via increased resorption by elevated osteoclast numbers compared to wild type mice (Polzer et al., 2010). Furthermore with regard to IL-1, according to Lee et al. in 2010, this cytokine is also responsible for activating RANK signaling aside from inducing RANKL to promote osteoclastogenesis and holds a vital role in bone metabolism under disease conditions (Lee et al., 2010). Another important target of molecular significance that is being investigated in osteoporosis is NADPH oxidase 4 (NOX4). NOX4 is an enzyme that produces ROS as it transfers electrons to as part of aerobic reactions and maintaining homeostasis. However, the ROS produced by NOX4 is important to the development and maintenance of bone. NOX4 was found to negatively affect bone density by increasing osteoclast numbers in mouse models. Additionally, alterations to NOX4 such as single nucleotide polymorphisms can further alter the bone density as well as bone turnover (Goettsch et al., 2013). Another important molecular

receptor relevant to bone homeostasis is that of aryl hydrocarbon receptor (AhR). According to Yu et al., osteoclastic AhR conveys a significant function in maintaining bone homeostasis and regulating bone metabolism under pathologic conditions (Yu et al., 2014).

Oxidative Stress, Bone Health, Development:

There is a direct and negative association between oxidative stress and osteoporosis that can be measured with the use of 8-iso-PGF₂α as a measure of oxidative stress combined with 15-keto-dihydro-PGF₂α as a biomarker of inflammation. Utilizing these markers in a human 2001 study by Basu et al., the investigators established a quantitative association between oxidative stress and loss of bone density (Basu et al., 2001). Moreover in regards to inflammation and osteoporosis, the severity and risk of bone fragility is modified if not dependent on risk factors such as age, xenobiotics, BMI, and more. For effective therapy and intervention in chronic inflammatory diseases, it is necessary to account for these factors (Briot et al., 2017).

Additional evidence and studies have revealed significant aspects on the mechanisms that connect oxidative stress, inflammation, and ultimately osteoporosis following exposure to PM. As previously mentioned, ambient PM and UFPs are now understood and demonstrated to increase serum concentrations of NK cells, helper T cells, monocytes, and proinflammatory cytokines as observed in both in vivo and in vitro models. The subsequent inflammation induced by PM and UFPs is mediated by activated alveolar macrophages and airway epithelial cells, from which signals including toll-like receptors induce the expression of TNF-α, IL-1, IL-6, and IL-8. This inflammatory response is further modified by PM components such as metals and organics (PAHs) which exhibit oxidative damage inducing potential in living tissues. The resulting oxidative stress, failing to subside due to the continual release of ROS, progresses to systemic oxidative stress and systemic inflammation. These conditions further modify and alters the

structure and function of many signaling proteins which leads to dysregulation of key cell processes including cell proliferation, apoptosis, and gene expression. Key signal transduction pathways such as Nrf2, FOXO, NF-kB, and many more redox sensitive transcription factors are over expressed under oxidative stress conditions, leading to an over production of antioxidant defenses and an accumulation of inflammatory mediators. This adverse and oxidative environment contributes to the loss of homeostasis and the accumulation of molecular damage in key bone cells including mesenchymal stem cells. The damage to which leads to a significant reduction in cellular functionality with age and greatly increases the risk of osteoporosis (Prada et al., 2020).

Conclusions:

In summary, our data demonstrated possible trends and connections between UFP exposure, oxidative stress, and predisposition to bone loss in females following maternal UFP exposure. The differential effects in males warrant further investigation. This work is significant in regards to the lack and absence of studies and investigation connecting oxidative stress and bone health to prenatal air pollution exposure.

CHAPTER IV. GESTATIONAL EXPOSURE TO ULTRAFINE PARTICLES AND ANTIOXIDANT NRF2 PROTECTION FROM OXIDATIVE STRESS

Introduction:

UFPs & Oxidative Stress:

As we acknowledge and recognize the prevalence of air pollution and its PM constituents in addition to the growing health concerns driven and influenced by exposure to ambient particulate matter, the continuation of research and study of particulate matter becomes ever more imperative to public health. After decades of investigation and research, we are fully aware that exposure to airborne PM, especially in the fine and ultrafine size range is linked to a variety of debilitating health issues. Prolonged exposure to fine and ultrafine PM (UFP) has been confirmed to induce disease through several mechanisms including oxidative stress and systemic inflammation (Jantzen et al., 2016). This ubiquitous environmental pollutant is of especially high importance and concern in the context of children's health and prenatal exposure. With recent scientific evidence and investigations in the form of human epidemiological observations and animal studies, we now understand that maternal exposure to UFPs during gestation presents a critical window of vulnerability to the growth and health of the developing fetus'. Disturbances from environmental exposures during this period of early life can yield numerous adverse birth outcomes and impacts on the development of children later in life (Johnson et al., 2021).

Nrf2 & Oxidative Stress:

A major and prevalent form of PM that is of great concern to global public health is that of traffic related diesel exhaust originating from automobiles and fuel combustion. A significant aspect of DE, like many other forms of airborne PM, is its ability to induce the generation of ROS following initial inhalation into the respiratory system, and after it has translocated across

the lower portions of the lungs into systemic circulation. As cells and tissues continue to generate ROS as part of an inflammatory reaction to PM and its many toxic chemical constituents, oxidative stress conditions grow excessively worse. Under these conditions, redox sensitive molecular networks and signal transduction pathways are disturbed and undergo adverse changes that cause downstream effects. A key protective antioxidant pathway that has been frequently studied is that of Keap1-Nrf2, the function of which is to protect cells and important macromolecules against oxidative stress (Kobayashi et al., 2005). Under basal conditions, Keap1 acts as a stress sensor protein which keeps Nrf2 in a sequestered and inactive state until disturbed by an oxidizing agent, thus repressing Keap1 and activating Nrf2 (Nguyen et al., 2009). The activation of Nrf2 signaling pathway provides an adaptive response to stresses and renders protection to an organism to prevent, or reduce, chemical carcinogenesis and other forms of toxicity (Bryan et al., 2013, Suzuki et al., 2015). However, disruption of the Nrf2 signal pathway has been observed to cause enhanced harm and injury (Wakabayashi et al., 2010). As demonstrated in Li et al in a 2010 study, the removal of Nrf2 from C57Bl/6 mice followed by prolonged exposure to diesel exhaust particles for 7 hours, 5 days a week, over the course of 8 weeks. The Nrf2 ^{-/-} mice in this study exhibited significantly greater changes in IL-5 and inflammatory cell infiltration in the lungs whereas the wildtype mice displayed higher reduced glutathione (GSH)/oxidized glutathione (GSSG) ratio within whole blood (Li et al., 2010).

Placental/Birth Effects & Oxidative Stress:

As previously mentioned, exposure to stressors such as oxidizing agents or airborne PM can have significant impacts on the health and development of a fetus. Effects of PM exposure that have been identified following investigation and numerous studies have included intrauterine growth restriction, reduced gestational length, and smaller size for gestational age.

Molecular analysis and experimental methods have raised evidence that such adverse birth outcomes may result in the development of various disorders such as metabolic disease or diabetes later in life. This phenomenon has been referred to as “fetal programming” and is associated with increased oxidative stress in utero that may yield consequences for redox sensitive mechanisms and pathways present during pregnancy. As our body of evidence has continued to accumulate more evidence, Nrf2 has been revealed to play multiple important roles and functions in mitigating oxidative stress induced injury and preventing developmental abnormalities (Chapple et al., 2015).

Redox Basics & Quantification:

Recalling back to the definition of oxidative stress, the most frequently used definition is that oxidative stress is an imbalance between pro-oxidants and antioxidants within living systems. This imbalance can be quantified as the redox state of cellular and extracellular thiols, especially GSH and GSSG. However, a more apt alternative definition for oxidative stress may simply be defined as “a disruption of redox signaling and control” (Jones et al., 2006). It is now understood and documented that the central and cellular thiol couples GSH/GSSG and CyS/CySS do not exist in equilibrium with one another and differ drastically in relation to compartment, pH, nutrition, age, and physiological stimuli (Jones et al., 2009).

Materials & Methods:

Animal Care & Husbandry:

Nrf2-deficient mice (Nrf2 ^{-/-}) on C57Bl/6J background were obtained from Dr. Tom Kensler, which were generated and genotyped as previously described (Itoh et al., 1997). To effectively study the role of Nrf2 in response to gestational UFP exposure, 8- to 10- week-old female mice were acclimated to filtered air (FA) for one-week within our whole-body inhalation

exposure chambers. Following acclimation, time-mating, and identification of a vaginal plug, termed gestational day (GD 0.5), wildtype (WT) or Nrf2 ^{-/-} pregnant mice were randomly assigned to three groups: filtered air (FA) control, low dose (LD; 100 µg/m³), or high dose (500 µg/m³) UFPs. Particle generation and gestational exposures were conducted as previously described.

Preparation and Exposure of UFPs:

Female C57BL/6n mice were time mated and checked for vaginal plugs after being placed in a mating pair and then assigned for exposure to either filtered air (FA) or aerosolized ultrafine particulate matter (100 µg/m³ or 500 µg/m³) for 6 hours/day from gestation day zero (GD 0.5) through GD 17.5. PM was composed of diesel soot/black carbon, sulfates, nitrates, and chlorides to represent real-world components of traffic-related air pollution. After birth, pups were allowed to nurse with dam until post-natal day 5 (PND5) on which they were culled to 2 males and 2 females. These remaining pups were then allowed to continue nursing with their dam until PND21 at which point they were assigned to a diet consisting of standard rodent chow. Exposure chambers were measured to consist of 12" X 8" X 32" stainless steel boxes, with separated internal compartments and a ¼" clear acrylic lid. Air was continuously pumped through the chambers via aerosol distribution lines attached to the lid and out via return lines in the bottom of these chambers. UFPs were generated via a commercial atomizer (TSI 3076, TSI Inc., Shoreview, MN). Throughout exposure period, particulate matter was highly controlled by monitoring and adjusting multiple variables including particle number, size, concentration, water content, and charge. PM concentration and size were continuously monitored via a Scanning Mobility Particle Sizer (SMPS) system and adjusted by altering the ratio of PM and water within the PM solution. The SMPS was set and operated with a flow of 6.5 liters/minute and a sample

flow of 1 liter/minute. The mass concentration of accumulation mode PM was maintained near $100 \mu\text{g}/\text{m}^3$, corresponding to a total number concentration of about $105 \text{ particles}/\text{cm}^3$ for 50 nm geometric mean diameter particles. Particle mass concentration was calculated based on the measured size distribution and particle density, which was estimated from the weighted average density of 10 wt% diesel exhaust, 44 wt% NH_4NO_3 , 39 wt% $(\text{NH}_4)_2\text{SO}_4$, and 7 wt% KCl, with a corresponding value of 1.63 g cm^{-3} . Following the end of exposure period on GD18, dams were transferred to individual housing and allowed to deliver.

HPLC Redox Analysis:

Sample Preparation:

Liver samples were collected, snap-frozen, and stored upon post-natal day 5 (PND5) sacrifice of pups not assigned to longitudinal metabolic study. Upon reaching ready time for derivatization, 10-50mg of liver tissues were quickly weighed and recorded before being homogenized in 1mL of sample buffer using a cold, glass homogenizer and plunger. Sample homogenate was kept cold during homogenization process by storing the glass homogenizer and a beaker of sample buffer in a bucket of ice before tissue was placed within the homogenizer. Once tissue was fully homogenized and no large chunks were apparent, homogenate was transferred to a labeled microcentrifuge tube. The same glass homogenizer and plunger were used and washed between samples with alconox soap and MilliQ water to prevent residue or contamination of following samples. This process was repeated for each sample and all tubes were kept cold on ice to prevent oxidation until ready for centrifuge. Once all samples were homogenized and transferred to microcentrifuge tubes and centrifuged with parameters 10,000 g for 10 minutes at 4°C to pellet proteins and lipids. Once centrifugation was completed, 300 μL of supernatant was transferred to a new labeled microcentrifuge tube and kept on ice. These tubes

were then given 60 μ L of iodoacetic acid (IAA) (7.4 mg/mL of HPLC grade water) and immediately vortexed to ensure thorough mix and attachment of charges to desired thiols. Following addition of IAA, sample solution pH's were adjusted to $\sim 9.0 \pm 0.2$ with ~ 425 μ L of KOH/tetraborate to precipitate proteins. KOH/tetraborate solution was added in aliquots of 25-200 μ L and then allowed to incubate at room temperature for 30 minutes. Once incubation time was completed, samples pH were assessed using pH strips to ensure correct pH range. During incubation period to adjust pH, dansyl chloride (20 mg/mL acetone) solution was made and then 300 μ L added to each sample and immediately vortexed to ensure mixing. Once all samples received DC and mixed, samples were incubated at room temperature in complete darkness for 16-28 hours. Following DC incubation period completion in a dark space, 500 μ L of HPLC chloroform was added to samples, vortexed, centrifuged, and the upper aqueous layer transferred to a new and final microcentrifuge tube. Samples of derivatized liver thiols were stored in -80°C freezer.

HPLC Analysis:

Samples were thawed on ice until liquid (do not allow samples to reach room temperature before analysis) and then centrifuged for 10 minutes in a microcentrifuge. Following centrifugation, an aliquot of each sample was transferred to an autosampler vial. Injection volume for analysis was 35 μ L. Separation of thiols was achieved using a Supelcosil LC-NH₂ column with internal dimensions of 5 μ m, 4.6 mm X 25 cm and originating from Supelco, Bellefonte, PA, USA. Initial solvent conditions were 80% A, 20% B at 1 ml/minute for 10 minutes. A linear gradient to 20% A and 80% B is then run from 10-30 minutes into sequence. From 30 to 35 minutes, flow gradient was maintained at 20% A and 80% B. From 35 to 42 minutes, conditions were returned to 80% A and 20% B. Detection of desired thiols was obtained

by fluorescence monitoring with bandpass filters, 305-395 nm excitation and 510-650 nm emission. Quantification was obtained by standard dilution of thiols from 5 μ M. Quantification can also be obtained via integration relative to the internal standard.

Results:

HPLC Redox Assay Thiol Quantities & Ratios (Reduced/Oxidized):

High Performance Liquid Chromatography (HPLC) was used to evaluate and quantify antioxidant thiols relevant to oxidative stress. Hepatic tissue from the offspring of either FA or LD exposed dams were homogenized and treated for analysis and quantification to measure oxidative stress. Fig. 30 features the measures of reduced glutathione (GSH) and oxidized glutathione (GSSG) from pooled samples and sex separated samples, in addition to the calculated ratios of those samples. Fig. 31 depicts measures of reduced cysteine (CyS) and oxidized cysteine (CySS) from pooled samples and sample measures by sex and finally the redox ratios for these samples.

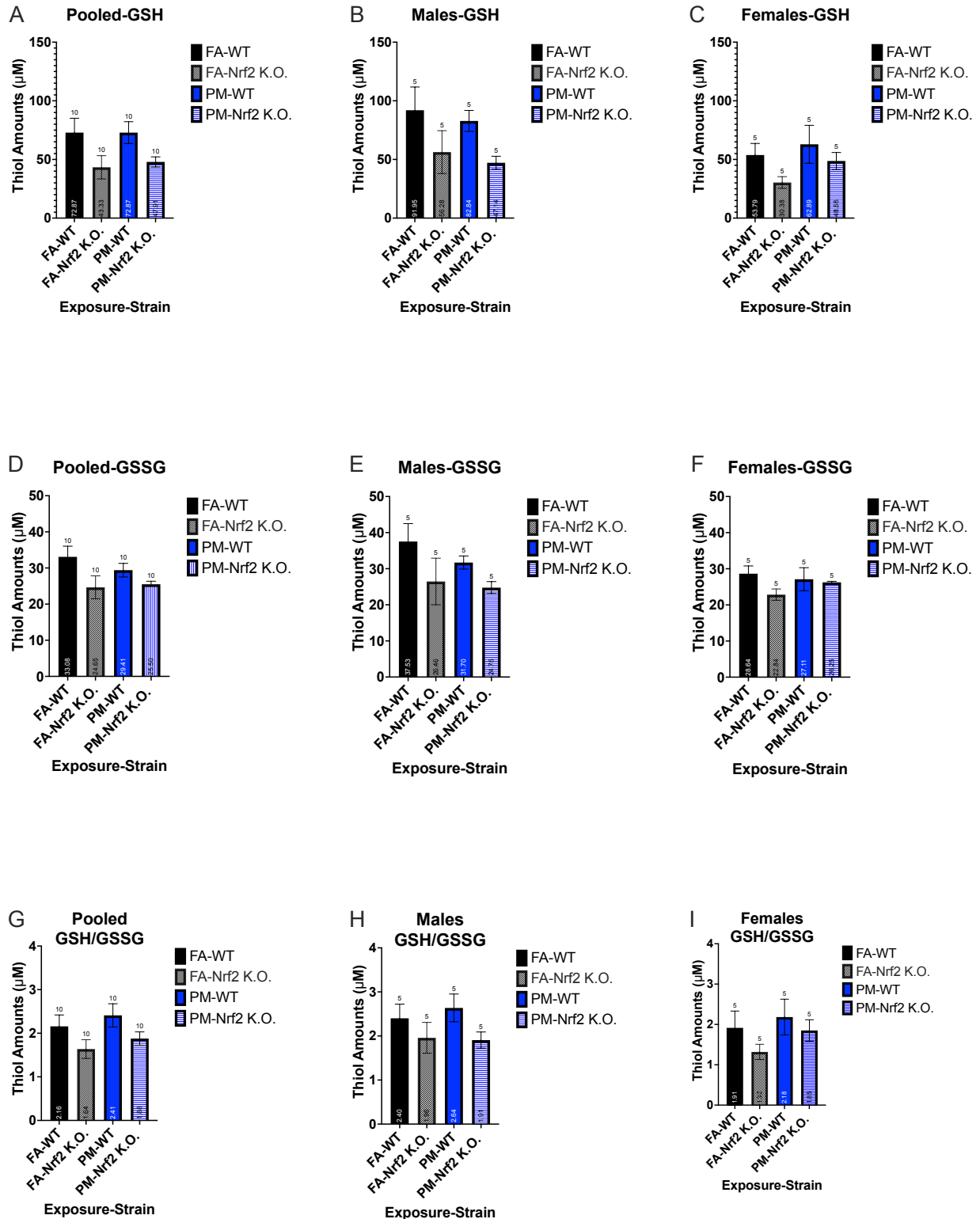


Fig. 30. Reduced glutathione (GSH) and oxidized glutathione (GSSG) measurements of PND5 liver samples via HPLC redox assay. One-way ANOVA performed for statistical analysis, * $p < 0.05$.

Glutathione content analysis within pup liver samples were recorded for comparison between all PND5 pup samples. Pups were exposed to either FA or LD (100 $\mu\text{g}/\text{m}^3$) dose of UFPs during gestation. Redox ratio was calculated by dividing reduced glutathione (GSH) by oxidized glutathione (GSSG), ratio values being >1 represented samples in which oxidative stress was detected following prenatal exposure.

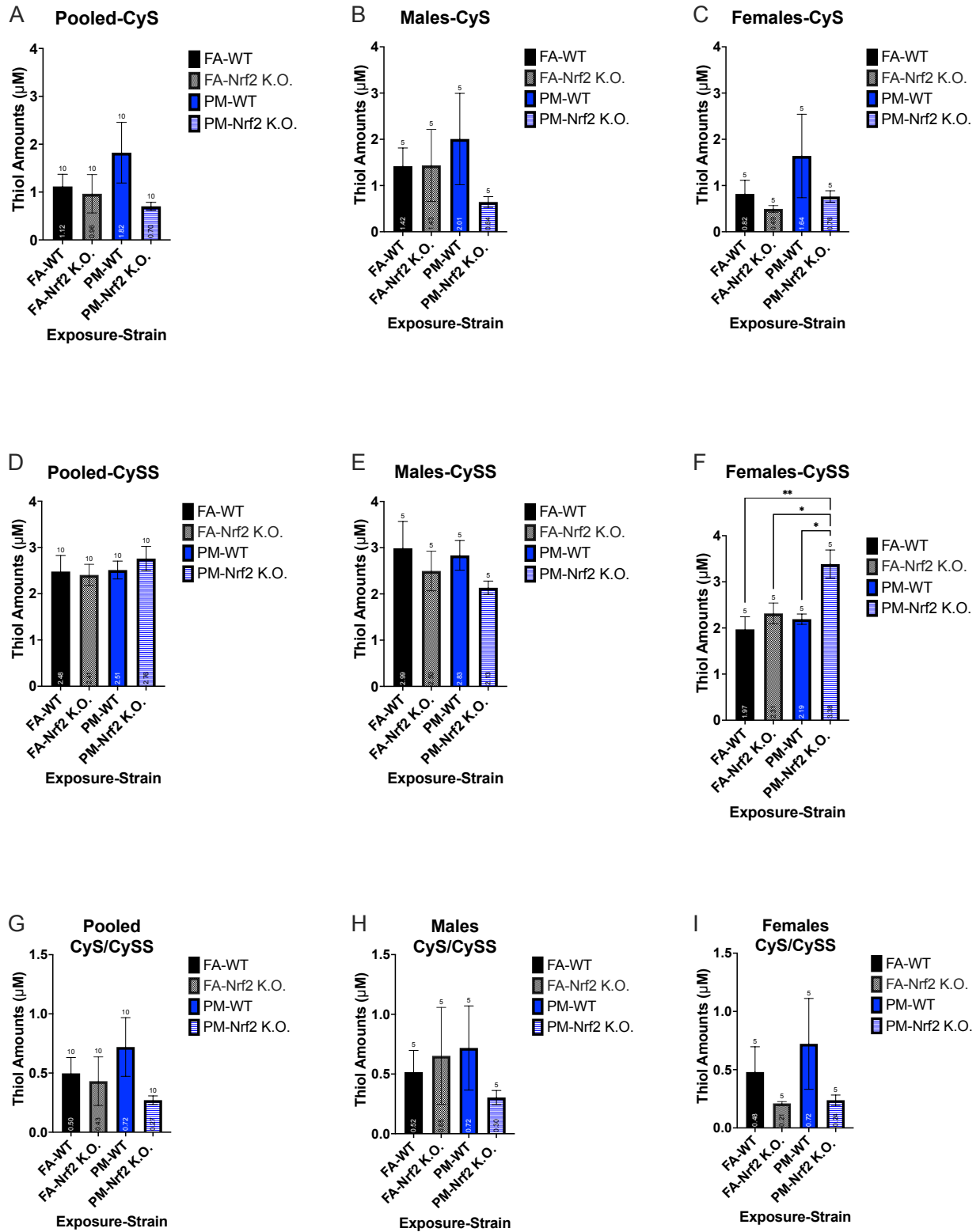


Fig. 31. Reduced cysteine (CyS) and oxidized cysteine (CySS) measurements of PND5 liver samples via HPLC redox assay. One-way ANOVA performed for statistical analysis, * $p < 0.05$.

Cysteine content analysis within pup liver samples were recorded for comparison between all PND5 pup samples. Pups were exposed to either FA or LD (100 $\mu\text{g}/\text{m}^3$) dose of UFPs during gestation. Redox ratio was calculated by dividing reduced cysteine (CyS) by oxidized cysteine (CySS), ratio values being $1 <$ represented samples in which oxidative stress was detected following prenatal exposure.

Discussion:

Model & innovation:

This model represents a significant departure from most experimental models in that not only does the ambient PM level reflect that of real-world urban traffic, but also that it incorporates a dose response for maternal exposure to air pollution.

UFPs-Oxidative Stress-Nrf2-Health:

As previously discussed, Nrf2 or nuclear E2-related factor 2 is a transcription factor which responds to oxidative stress, whether induced by exogenous agents or regular cellular processes necessary for development and signaling, by binding to the antioxidant response element (ARE) located in the promoter of genes coding for antioxidant enzymes such as NAD(P)H: quinone oxidoreductase 1 and proteins for glutathione synthesis. This pathway is vital for regulation of adipocyte differentiation, mitochondrial biogenesis, and liver energy metabolism (Vomhof-DeKrey et al., 2012, Kovac et al., 2015). This goes even further in regard to skeletal muscle and ageing. The removal or disruption of Nrf2 produces elevated levels of ROS and oxidative stress in the skeletal muscle of aged mice, as confirmed by Miller et al (Miller et al., 2012). With increasing concern over the health impacts of PM exposure and the continued risks of exposure to ambient PM and its many toxic constituents, the need to better our understanding of the molecular mechanisms involved in protection against oxidative stress grows

ever more undeniable (Gangwar et al., 2020). The complex interplay of PM, ROS, various mediators of inflammation, antioxidant thiols, and the Nrf2 signal pathway requires further investigation to elucidate. Additionally, a relevant factor to be considered in this study model and in future study models comes from Skoko and coworkers on Nrf2 loss and altered hepatic outcomes. This study revealed that the removal of Nrf2 from C57Bl/6J generates a congenital intrahepatic shunt present in two-thirds of mice Nrf2 knockout mice. This shunt altered hepatic oxygen and protein expression gradients in Nrf2 knockout mice in comparison to wild type mice, which was observed to alter several physiological and pathophysiological functions such as metabolism and drug detoxification through changes in hepatic oxygenation and protein expression. This poses a serious confounding variable not only for this study model but also future study models that feature hepatic tissue effects from environmental exposures (Skoko et al., 2014).

Restate Outcomes:

Our findings from this study essentially demonstrated findings from multiple studies and reviews regarding the functions and importance of Nrf2 in regards to oxidative stress. Relative to glutathione (GSH/GSSG), Nrf2 knockout mice consistently displayed lower quantities of both reduced and oxidized glutathione in comparison to wild type C57Bl/6 mice. Measurements of reduced and oxidized cysteine (CyS/CySS) revealed a significant increase in quantities of oxidized cysteine in PM exposed female Nrf2 knockout mice in comparison to FA exposed wildtypes and knockout mice. Our results demonstrate consistent decrease in relevant antioxidants following maternal exposure to UFPs, potentially indicating challenges to protection from oxidative stress induced disease states later in life.

Conclusions:

In conclusion, Nrf2 is not only key in mounting a protective, antioxidant response to PM induced oxidative stress, but differs by sex. Additionally, antioxidant thiols are shown to not be in equilibrium with one another in hepatic tissues. Finally, further research is necessary to assess redox states following in utero UFP exposure in multiple bodily compartments of these mice to obtain a wider scope of oxidative stress in organ systems.

CHAPTER V SUMMARY OF KEY FINDINGS AND RECOMMENDATIONS FOR FUTURE STUDIES

Our laboratory previously developed a gestational exposure murine model to mimic representative urban air pollution, specifically modeling the ultrafine particle (UFP) component. Studies had yet to determine long-term consequences on offspring health, so a major objective of this dissertation was to characterize later in life effects by evaluating prenatally-exposed offspring into adulthood.

Findings of Aim 1:

From our aim 1 study, we observed signs of growth suppression in terms of body weight and relative weights of certain tissues including liver, brain, and more. We also observed differences between sexes in weight gain following diet treatment, more specifically lower weight in PM-treated groups in both high fat and low-fat groups. In addition, significant reduction in body fat and fat/lean ratios were detected in female mice. These results suggest a possible mechanism or phenomenon of diet and exposure induced weight reduction in females as opposed to males in regards to *in utero* exposure to PM.

Findings of Aim 2:

In this aim 2 study, the addition of a dose-response and removal of diet as a variable yielded surprising results that were not observed in the first study model. Whole body fat% of low dose (LD)-exposed female mice were found to differ significantly from FA-exposed mice on PND77 and PND105 according to DEXA scans performed throughout the developing and adult periods of these mice. Additionally, this observation was substantiated by significantly increase lipid accumulation in LD-exposed female mice, as measured by liver histology. Interestingly enough, males of this same study exhibited a trend of decreasing lipid accumulation as PM

exposure gradient progressed from zero (FA) to 100 $\mu\text{g}/\text{m}^3$ (LD) and 500 $\mu\text{g}/\text{m}^3$. In regards to whole body mineral density (BMD), sex-specific effects were again detected. LD exposure appears to have a differential effect on males. Whereas in females, HD exposure appears to have produced a suppressive effect later in life possibly corresponding with osteoporosis. These findings are further reflected in bone mineral content in which LD-exposed males often displayed lower BMC than both FA- and HD-exposed males, while HD-exposed females were often lower in BMC in later ages. Overall, most bone data produced from this study displayed a sex driven divergence in bone health development, namely that males often exhibited an increase in BMD with PM exposure while females demonstrated a decrease in BMD as they progressed towards PND105. HPLC redox analysis of reduced and oxidized thiols following prenatal PM exposure demonstrated significantly increased amounts of GSH, GSSG, and CyS within LD- and HD-exposed pups in comparison to FA-exposed pups. These measurements provide evidence of oxidative stress in PND5 pups following *in utero* PM exposure that may predispose them to disease later in life.

Findings of Aim 3:

In this aim 3 study, the addition of a Nrf2-deficient mouse model allowed us to investigate the role of antioxidant responses to UFPs following *in utero* exposure. HPLC redox analysis of antioxidant thiols (GSH, GSSG, CyS, CySS) demonstrated trends of lower quantities of thiols within mouse subjects in which Nrf2 has been removed. The disruption of the Nrf2 signal pathway also impaired the antioxidant response to PM, clearly for CyS/CySS redox, again in female offspring. Our model emphasizes the need to study the effects of early life PM exposure as related to offspring sex.

Overall:

In summary, our models and the results produced from our studies provides preliminary evidence of the health effects induced by UFPs which includes long term and chronic disorders such as impacts to metabolic processes and alterations in bone health. These models in particular provided credible evidence of the long-term impacts of gestational PM exposure and highlighted the need for future studies to investigate PM induced disease phenotypes over time from youth and into adulthood.

Recommendations for Future Studies:

It is recommended from this study that future study models investigate endpoints that include close examination of adipose tissues and skeletal muscle for the purpose of evaluating PM induced metabolic disease phenotypes. Additionally, the exposure chamber system and PM generation system would enable us to alter the chemical composition of our PM. This ability provides a significant opportunity to change the PM and UFPs to reflect characteristics of acidity, metals, and organic chemicals associated with real world urban sites and potentially disaster areas. This flexibility offers potential research on PM exposures to varying sites and conditions that are relevant to public health. Additionally, there are endpoints of interest that could provide more detailed information in future studies such as mitochondrial examination for dysfunction as well as evaluation of redox status in a multitude of tissues and compartments that are relevant to human growth and development. Lastly, future studies involving Nrf2 knockout mice should account for potential physiological and anatomical differences such as the congenital intrahepatic shunt (Skoko et al., 2014).

REFERENCES:

1. Ahmed, S. M. U., Luo, L., Namani, A., Wang, X. J., & Tang, X. (2017). Nrf2 signaling pathway: Pivotal roles in inflammation. *Biochimica Et Biophysica Acta (BBA)-Molecular Basis of Disease*, 1863(2), 585-597.
2. Alderete, T. L., Chen, Z., Toledo-Corral, C. M., Contreras, Z. A., Kim, J. S., Habre, R., . . . Gilliland, F. D. (2018). Ambient and traffic-related air pollution exposures as novel risk factors for metabolic dysfunction and type 2 diabetes. *Current Epidemiology Reports*, 5(2), 79-91.
3. Ali, R. (2011). Effect of Diesel Emissions on Human Health: A. *International Journal of Applied Engineering Research*, 6(11), 1333-1342.
4. Anderson, J. O., Thundiyil, J. G., & Stolbach, A. (2012). Clearing the air: a review of the effects of particulate matter air pollution on human health. *Journal of Medical Toxicology*, 8(2), 166-175.
5. Backes, C. H., Nelin, T., Gorr, M. W., & Wold, L. E. (2013). Early life exposure to air pollution: how bad is it? *Toxicology Letters*, 216(1), 47-53.
6. Backes, C. H., Nelin, T., Gorr, M. W., & Wold, L. E. (2013). Early life exposure to air pollution: how bad is it? *Toxicology Letters*, 216(1), 47-53.
7. Basu, R., Harris, M., Sie, L., Malig, B., Broadwin, R., & Green, R. (2014). Effects of fine particulate matter and its constituents on low birth weight among full-term infants in California. *Environmental Research*, 128, 42-51.
8. Basu, S., Michaëlsson, K., Olofsson, H., Johansson, S., & Melhus, H. (2001). Association between oxidative stress and bone mineral density. *Biochemical and Biophysical Research Communications*, 288(1), 275-279.

9. Behlen, J., Carmen, L., Li, Y., Stanley, J., Zhang, R., & Johnson, N. (2020). Exposure to Ultrafine Particulate Matter During Gestation Potentially Disrupts Placental Function. Paper presented at the *Birth Defects Research*, , 112(11) 853-853.
10. Bełcik, M., Trusz-Zdybek, A., Zaczyńska, E., Czarny, A., & Piekarska, K. (2018). Genotoxic and cytotoxic properties of PM_{2.5} collected over the year in Wrocław (Poland). *Science of the Total Environment*, 637, 480-497.
11. Bell, M. L., Belanger, K., Ebisu, K., Gent, J. F., Lee, H. J., Koutrakis, P., & Leaderer, B. P. (2010). Prenatal exposure to fine particulate matter and birth weight: variations by particulate constituents and sources. *Epidemiology (Cambridge, Mass.)*, 21(6), 884-891. doi:10.1097/EDE.0b013e3181f2f405 [doi]
12. Bell, M. L., Dominici, F., Ebisu, K., Zeger, S. L., & Samet, J. M. (2007). Spatial and temporal variation in PM(2.5) chemical composition in the United States for health effects studies. *Environmental Health Perspectives*, 115(7), 989-995. doi:10.1289/ehp.9621 [doi]
13. Birben, E., Sahiner, U. M., Sackesen, C., Erzurum, S., & Kalayci, O. (2012). Oxidative stress and antioxidant defense. *World Allergy Organization Journal*, 5(1), 9-19.
14. Bolton, J. L., Auten, R. L., & Bilbo, S. D. (2014). Prenatal air pollution exposure induces sexually dimorphic fetal programming of metabolic and neuroinflammatory outcomes in adult offspring. *Brain, Behavior, and Immunity*, 37, 30-44.
15. Bolton, J. L., Smith, S. H., Huff, N. C., Gilmour, M. I., Foster, W. M., Auten, R. L., & Bilbo, S. D. (2012). Prenatal air pollution exposure induces neuroinflammation and predisposes offspring to weight gain in adulthood in a sex-specific manner. *The FASEB Journal*, 26(11), 4743-4754.

16. Borgie, M., Ledoux, F., Verdin, A., Cazier, F., Greige, H., Shirali, P., . . . Dagher, Z. (2015). Genotoxic and epigenotoxic effects of fine particulate matter from rural and urban sites in Lebanon on human bronchial epithelial cells. *Environmental Research*, *136*, 352-362.
17. Bové, H., Bongaerts, E., Slenders, E., Bijmens, E. M., Saenen, N. D., Gyselaers, W., . . . Ameloot, M. (2019). Ambient black carbon particles reach the fetal side of human placenta. *Nature Communications*, *10*(1), 1-7.
18. Briot, K., Geusens, P., Bultink, I. E., Lems, W., & Roux, C. (2017). Inflammatory diseases and bone fragility. *Osteoporosis International*, *28*(12), 3301-3314.
19. Bryan, H. K., Olayanju, A., Goldring, C. E., & Park, B. K. (2013). The Nrf2 cell defence pathway: Keap1-dependent and-independent mechanisms of regulation. *Biochemical Pharmacology*, *85*(6), 705-717.
20. Burhans, W. C., & Heintz, N. H. (2009). The cell cycle is a redox cycle: linking phase-specific targets to cell fate. *Free Radical Biology and Medicine*, *47*(9), 1282-1293.
21. Calderón-Garcidueñas, L., Mora-Tiscareño, A., Franco-Lira, M., Torres-Jardón, R., Peña-Cruz, B., Palacios-López, C., . . . Montesinos-Correa, H. (2013). Exposure to urban air pollution and bone health in clinically healthy six-year-old children. *Arhiv Za Higijenu Rada i Toksikologiju*, *64*(1), 23-23.
22. Chandra, J., Samali, A., & Orrenius, S. (2000). Triggering and modulation of apoptosis by oxidative stress. *Free Radical Biology and Medicine*, *29*(3-4), 323-333.
23. Chang, H. H., Reich, B. J., & Miranda, M. L. (2012). Time-to-event analysis of fine particle air pollution and preterm birth: results from North Carolina, 2001–2005. *American Journal of Epidemiology*, *175*(2), 91-98.

24. Chang, K. H., Chang, M. Y., Muo, C. H., Wu, T. N., Hwang, B. F., Chen, C. Y., . . . Kao, C. H. (2015). Exposure to air pollution increases the risk of osteoporosis: a nationwide longitudinal study. *Medicine*, *94*(17), e733. doi:10.1097/MD.0000000000000733 [doi]
25. Chapple, S. J., Puszyk, W. M., & Mann, G. E. (2015). Keap1–Nrf2 regulated redox signaling in utero: Priming of disease susceptibility in offspring. *Free Radical Biology and Medicine*, *88*, 212-220.
26. Chen, H., Chen, X., Hong, X., Liu, C., Huang, H., Wang, Q., . . . Sun, Q. (2017). Maternal exposure to ambient PM_{2.5} exaggerates fetal cardiovascular maldevelopment induced by homocysteine in rats. *Environmental Toxicology*, *32*(3), 877-889.
27. Chen, M., Liang, S., Qin, X., Zhang, L., Qiu, L., Chen, S., . . . Zhang, Y. (2018). Prenatal exposure to diesel exhaust PM_{2.5} causes offspring β cell dysfunction in adulthood. *American Journal of Physiology-Endocrinology and Metabolism*, *315*(1), E72-E80.
28. Chen, M., Liang, S., Zhou, H., Xu, Y., Qin, X., Hu, Z., . . . Zhang, Y. (2017). Prenatal and postnatal mothering by diesel exhaust PM_{2.5}-exposed dams differentially program mouse energy metabolism. *Particle and Fibre Toxicology*, *14*(1), 1-11.
29. Chen, Z., Salam, M. T., Karim, R., Toledo-Corral, C. M., Watanabe, R. M., Xiang, A. H., . . . Lurmann, F. (2015). Living near a freeway is associated with lower bone mineral density among Mexican Americans. *Osteoporosis International*, *26*(6), 1713-1721.
30. Chiu, J., & Dawes, I. W. (2012). Redox control of cell proliferation. *Trends in Cell Biology*, *22*(11), 592-601.
31. Circu, M. L., & Aw, T. Y. (2010). Reactive oxygen species, cellular redox systems, and apoptosis. *Free Radical Biology and Medicine*, *48*(6), 749-762.

32. Cohen, A. J., Ross Anderson, H., Ostro, B., Pandey, K. D., Krzyzanowski, M., Künzli, N., . . . Samet, J. M. (2005). The global burden of disease due to outdoor air pollution. *Journal of Toxicology and Environmental Health, Part A*, 68(13-14), 1301-1307.
33. Cole, T. B., Coburn, J., Dao, K., Roqué, P., Chang, Y., Kalia, V., . . . Costa, L. G. (2016). Sex and genetic differences in the effects of acute diesel exhaust exposure on inflammation and oxidative stress in mouse brain. *Toxicology*, 374, 1-9.
34. Comini, M. A. (2016). Measurement and meaning of cellular thiol: disulfide redox status. *Free Radical Research*, 50(2), 246-271.
35. Darrow, L. A., Klein, M., Strickland, M. J., Mulholland, J. A., & Tolbert, P. E. (2011). Ambient air pollution and birth weight in full-term infants in Atlanta, 1994-2004. *Environmental Health Perspectives*, 119(5), 731-737. doi:10.1289/ehp.1002785 [doi]
36. Datta, H. K., Ng, W. F., Walker, J. A., Tuck, S. P., & Varanasi, S. S. (2008). The cell biology of bone metabolism. *Journal of Clinical Pathology*, 61(5), 577-587. doi:10.1136/jcp.2007.048868 [doi]
37. Davidson, C. I., Phalen, R. F., & Solomon, P. A. (2005). Airborne particulate matter and human health: a review. *Aerosol Science and Technology*, 39(8), 737-749.
38. De Kok, T. M., Drieste, H. A., Hogervorst, J. G., & Briedé, J. J. (2006). Toxicological assessment of ambient and traffic-related particulate matter: a review of recent studies. *Mutation Research/Reviews in Mutation Research*, 613(2-3), 103-122.
39. Deyssenroth, M. A., Rosa, M. J., Eliot, M. N., Kelsey, K. T., Kloog, I., Schwartz, J. D., . . . Marsit, C. J. (2021). Placental gene networks at the interface between maternal PM_{2.5} exposure early in gestation and reduced infant birthweight. *Environmental Research*, 199, 111342.

40. Ema, M., Naya, M., Horimoto, M., & Kato, H. (2013). Developmental toxicity of diesel exhaust: a review of studies in experimental animals. *Reproductive Toxicology*, *42*, 1-17.
41. Erickson, A. C., & Arbour, L. (2014). The shared pathoetiological effects of particulate air pollution and the social environment on fetal-placental development. *Journal of Environmental and Public Health*, 2014
42. Espinosa-Diez, C., Miguel, V., Mennerich, D., Kietzmann, T., Sánchez-Pérez, P., Cadenas, S., & Lamas, S. (2015). Antioxidant responses and cellular adjustments to oxidative stress. *Redox Biology*, *6*, 183-197.
43. Fleisch, A. F., Rifas-Shiman, S. L., Koutrakis, P., Schwartz, J. D., Kloog, I., Melly, S., . . . Oken, E. (2015). Prenatal exposure to traffic pollution: associations with reduced fetal growth and rapid infant weight gain. *Epidemiology (Cambridge, Mass.)*, *26*(1), 43-50.
doi:10.1097/EDE.0000000000000203 [doi]
44. Forman, H. J., & Torres, M. (2001). Redox signaling in macrophages. *Molecular Aspects of Medicine*, *22*(4-5), 189-216.
45. Gangwar, R. S., Bevan, G. H., Palanivel, R., Das, L., & Rajagopalan, S. (2020). Oxidative stress pathways of air pollution mediated toxicity: Recent insights. *Redox Biology*, *34*, 101545.
46. Ghezzi, P., Bonetto, V., & Fratelli, M. (2005). Thiol–disulfide balance: from the concept of oxidative stress to that of redox regulation. *Antioxidants & Redox Signaling*, *7*(7-8), 964-972.
47. Gingras, V., Hivert, M., & Oken, E. (2018). Early-life exposures and risk of diabetes mellitus and obesity. *Current Diabetes Reports*, *18*(10), 1-10.

48. Go, Y. M., & Jones, D. P. (2013). The redox proteome. *The Journal of Biological Chemistry*, 288(37), 26512-26520. doi:10.1074/jbc.R113.464131 [doi]
49. Goettsch, C., Babelova, A., Trummer, O., Erben, R. G., Rauner, M., Rammelt, S., . . . Kampschulte, M. (2013). NADPH oxidase 4 limits bone mass by promoting osteoclastogenesis. *The Journal of Clinical Investigation*, 123(11), 4731-4738.
50. González-Flecha, B. (2004). Oxidant mechanisms in response to ambient air particles. *Molecular Aspects of Medicine*, 25(1-2), 169-182.
51. Gorr, M. W., Velten, M., Nelin, T. D., Youtz, D. J., Sun, Q., & Wold, L. E. (2014). Early life exposure to air pollution induces adult cardiac dysfunction. *American Journal of Physiology-Heart and Circulatory Physiology*, 307(9), H1353-H1360.
52. Gray, S. C., Edwards, S. E., & Miranda, M. L. (2010). Assessing exposure metrics for PM and birth weight models. *Journal of Exposure Science & Environmental Epidemiology*, 20(5), 469-477.
53. Grevendonk, L., Janssen, B. G., Vanpoucke, C., Lefebvre, W., Hoxha, M., Bollati, V., & Nawrot, T. S. (2016). Mitochondrial oxidative DNA damage and exposure to particulate air pollution in mother-newborn pairs. *Environmental Health*, 15(1), 1-8.
54. Hales, C. M., Carroll, M. D., Fryar, C. D., & Ogden, C. L. (2017). Prevalence of obesity among adults and youth: United States, 2015–2016.
55. Hanzalova, K., Rossner Jr, P., & Sram, R. J. (2010). Oxidative damage induced by carcinogenic polycyclic aromatic hydrocarbons and organic extracts from urban air particulate matter. *Mutation Research/Genetic Toxicology and Environmental Mutagenesis*, 696(2), 114-121.

56. Heal, M. R., Kumar, P., & Harrison, R. M. (2012). Particles, air quality, policy and health. *Chemical Society Reviews*, *41*(19), 6606-6630.
57. Heo, J., Schauer, J. J., Yi, O., Paek, D., Kim, H., & Yi, S. (2014). Fine particle air pollution and mortality: importance of specific sources and chemical species. *Epidemiology*, *25*, 379-388.
58. Hu, C., Sheng, X., Li, Y., Xia, W., Zhang, B., Chen, X., . . . Sun, X. (2020). Effects of prenatal exposure to particulate air pollution on newborn mitochondrial DNA copy number. *Chemosphere*, *253*, 126592.
59. Huynh, M., Woodruff, T. J., Parker, J. D., & Schoendorf, K. C. (2006). Relationships between air pollution and preterm birth in California. *Paediatric and Perinatal Epidemiology*, *20*(6), 454-461.
60. Hyder, A., Lee, H. J., Ebisu, K., Koutrakis, P., Belanger, K., & Bell, M. L. (2014). PM2.5 exposure and birth outcomes: use of satellite- and monitor-based data. *Epidemiology (Cambridge, Mass.)*, *25*(1), 58-67. doi:10.1097/EDE.0000000000000027 [doi]
61. Itoh, K., Mimura, J., & Yamamoto, M. (2010). Discovery of the negative regulator of Nrf2, Keap1: a historical overview. *Antioxidants & Redox Signaling*, *13*(11), 1665-1678.
62. Jalaludin, B., Mannes, T., Morgan, G., Lincoln, D., Sheppard, V., & Corbett, S. (2007). Impact of ambient air pollution on gestational age is modified by season in Sydney, Australia. *Environmental Health*, *6*(1), 1-9.
63. Jantzen, K., Møller, P., Karottki, D. G., Olsen, Y., Bekö, G., Clausen, G., . . . Loft, S. (2016). Exposure to ultrafine particles, intracellular production of reactive oxygen species in leukocytes and altered levels of endothelial progenitor cells. *Toxicology*, *359*, 11-18.

64. Jaramillo, M. C., & Zhang, D. D. (2013). The emerging role of the Nrf2-Keap1 signaling pathway in cancer. *Genes & Development*, *27*(20), 2179-2191. doi:10.1101/gad.225680.113 [doi]
65. Johnson, N. M., Hoffmann, A. R., Behlen, J. C., Lau, C., Pendleton, D., Harvey, N., . . . Tian, Y. (2021). Air pollution and children's health—a review of adverse effects associated with prenatal exposure from fine to ultrafine particulate matter. *Environmental Health and Preventive Medicine*, *26*(1), 1-29.
66. Jones, D. P. (2006). Redefining oxidative stress. *Antioxidants & Redox Signaling*, *8*(9-10), 1865-1879.
67. Jones, D. P. (2008). Radical-free biology of oxidative stress. *American Journal of Physiology-Cell Physiology*, *295*(4), C849-C868.
68. Jones, D. P., & Liang, Y. (2009). Measuring the poise of thiol/disulfide couples in vivo. *Free Radical Biology and Medicine*, *47*(10), 1329-1338.
69. Kannan, S., Misra, D. P., Dvornch, J. T., & Krishnakumar, A. (2006). Exposures to airborne particulate matter and adverse perinatal outcomes: a biologically plausible mechanistic framework for exploring potential effect modification by nutrition. *Environmental Health Perspectives*, *114*(11), 1636-1642. doi:10.1289/ehp.9081 [doi]
70. Kelly, F. J., & Fussell, J. C. (2012). Size, source and chemical composition as determinants of toxicity attributable to ambient particulate matter. *Atmospheric Environment*, *60*, 504-526.

71. Kelly, F. J., & Fussell, J. C. (2012). Size, source and chemical composition as determinants of toxicity attributable to ambient particulate matter. *Atmospheric Environment*, *60*, 504-526.
72. Kim, K., Kabir, E., & Kabir, S. (2015). A review on the human health impact of airborne particulate matter. *Environment International*, *74*, 136-143.
73. Kingsley, S. L., Deyssenroth, M. A., Kelsey, K. T., Awad, Y. A., Kloog, I., Schwartz, J. D., . . . Wellenius, G. A. (2017). Maternal residential air pollution and placental imprinted gene expression. *Environment International*, *108*, 204-211.
74. Kobayashi, A., Kang, M., Watai, Y., Tong, K. I., Shibata, T., Uchida, K., & Yamamoto, M. (2006). Oxidative and electrophilic stresses activate Nrf2 through inhibition of ubiquitination activity of Keap1. *Molecular and Cellular Biology*, *26*(1), 221-229.
75. Kovac, S., Angelova, P. R., Holmström, K. M., Zhang, Y., Dinkova-Kostova, A. T., & Abramov, A. Y. (2015). Nrf2 regulates ROS production by mitochondria and NADPH oxidase. *Biochimica Et Biophysica Acta (BBA)-General Subjects*, *1850*(4), 794-801.
76. Kumar, P., Morawska, L., Birmili, W., Paasonen, P., Hu, M., Kulmala, M., . . . Britter, R. (2014). Ultrafine particles in cities. *Environment International*, *66*, 1-10.
77. Kwon, H. (2020). Ultrafine particles: unique physicochemical properties relevant to health and disease. *Experimental and Molecular Medicine*, *52*, 1-11.
78. Kwon, H., Ryu, M. H., & Carlsten, C. (2020). Ultrafine particles: unique physicochemical properties relevant to health and disease. *Experimental & Molecular Medicine*, *52*(3), 318-328.
79. Lai, C., Lee, C., Bai, K., Yang, Y., Chuang, K., Wu, S., & Chuang, H. (2016). Protein oxidation and degradation caused by particulate matter. *Scientific Reports*, *6*(1), 1-9.

80. Lamichhane, D. K., Leem, J. H., Lee, J. Y., & Kim, H. C. (2015). A meta-analysis of exposure to particulate matter and adverse birth outcomes. *Environmental Health and Toxicology*, *30*, e2015011. doi:10.5620/eht.e2015011 [doi]
81. Landkocz, Y., Ledoux, F., André, V., Cazier, F., Genevray, P., Dewaele, D., . . . Courcot, L. (2017). Fine and ultrafine atmospheric particulate matter at a multi-influenced urban site: physicochemical characterization, mutagenicity and cytotoxicity. *Environmental Pollution*, *221*, 130-140.
82. Laurent, O., Hu, J., Li, L., Cockburn, M., Escobedo, L., Kleeman, M. J., & Wu, J. (2014). Sources and contents of air pollution affecting term low birth weight in Los Angeles County, California, 2001–2008. *Environmental Research*, *134*, 488-495.
83. Lavigne, E., Ashley-Martin, J., Dodds, L., Arbuckle, T. E., Hystad, P., Johnson, M., . . . Fisher, M. (2016). Air pollution exposure during pregnancy and fetal markers of metabolic function: the MIREC study. *American Journal of Epidemiology*, *183*(9), 842-851.
84. Lee, Y., Fujikado, N., Manaka, H., Yasuda, H., & Iwakura, Y. (2010). IL-1 plays an important role in the bone metabolism under physiological conditions. *International Immunology*, *22*(10), 805-816.
85. Li, Y. J., Takizawa, H., Azuma, A., Kohyama, T., Yamauchi, Y., Takahashi, S., . . . Sugawara, I. (2010). Nrf2 is closely related to allergic airway inflammatory responses induced by low-dose diesel exhaust particles in mice. *Clinical Immunology*, *137*(2), 234-241.
86. Liu, A., Qian, N., Yu, H., Chen, R., & Kan, H. (2017). Estimation of disease burdens on preterm births and low birth weights attributable to maternal fine particulate matter exposure in Shanghai, China. *Science of the Total Environment*, *609*, 815-821.

87. Liu, C., Fuertes, E., Flexeder, C., Hofbauer, L. C., Berdel, D., Hoffmann, B., . . . Heinrich, J. (2015). Associations between ambient air pollution and bone turnover markers in 10-year old children: results from the GINIplus and LISAplus studies. *International Journal of Hygiene and Environmental Health*, 218(1), 58-65.
88. Liu, J., Fu, S., Jiang, J., & Tang, X. (2021). Association between outdoor particulate air pollution and the risk of osteoporosis: a systematic review and meta-analysis. *Osteoporosis International*, , 1-9.
89. Liu, S., Krewski, D., Shi, Y., Chen, Y., & Burnett, R. T. (2007). Association between maternal exposure to ambient air pollutants during pregnancy and fetal growth restriction. *Journal of Exposure Science & Environmental Epidemiology*, 17(5), 426-432.
90. Losacco, C., & Perillo, A. (2018). Particulate matter air pollution and respiratory impact on humans and animals. *Environmental Science and Pollution Research*, 25(34), 33901-33910.
91. Lu, F., Xu, D., Cheng, Y., Dong, S., Guo, C., Jiang, X., & Zheng, X. (2015). Systematic review and meta-analysis of the adverse health effects of ambient PM_{2.5} and PM₁₀ pollution in the Chinese population. *Environmental Research*, 136, 196-204.
92. Mao, G., Nachman, R. M., Sun, Q., Zhang, X., Koehler, K., Chen, Z., . . . Zong, G. (2017). Individual and joint effects of early-life ambient PM_{2.5} exposure and maternal prepregnancy obesity on childhood overweight or obesity. *Environmental Health Perspectives*, 125(6), 067005.
93. Mazzoli-Rocha, F., Fernandes, S., Einicker-Lamas, M., & Zin, W. A. (2010). Roles of oxidative stress in signaling and inflammation induced by particulate matter. *Cell Biology and Toxicology*, 26(5), 481-498.

94. Miller, C. J., Gounder, S. S., Kannan, S., Goutam, K., Muthusamy, V. R., Firpo, M. A., . . . Rajasekaran, N. S. (2012). Disruption of Nrf2/ARE signaling impairs antioxidant mechanisms and promotes cell degradation pathways in aged skeletal muscle. *Biochimica Et Biophysica Acta (BBA)-Molecular Basis of Disease*, 1822(6), 1038-1050.
95. Miranda, M. L., Maxson, P., & Edwards, S. (2009). Environmental contributions to disparities in pregnancy outcomes. *Epidemiologic Reviews*, 31(1), 67-83.
96. Møller, P., Danielsen, P. H., Karottki, D. G., Jantzen, K., Roursgaard, M., Klingberg, H., . . . Cao, Y. (2014). Oxidative stress and inflammation generated DNA damage by exposure to air pollution particles. *Mutation research/Reviews in Mutation Research*, 762, 133-166.
97. Mostofsky, E., Schwartz, J., Coull, B. A., Koutrakis, P., Wellenius, G. A., Suh, H. H., . . . Mittleman, M. A. (2012). Modeling the association between particle constituents of air pollution and health outcomes. *American Journal of Epidemiology*, 176(4), 317-326.
98. Neven, K. Y., Saenen, N. D., Tarantini, L., Janssen, B. G., Lefebvre, W., Vanpoucke, C., . . . Nawrot, T. S. (2018). Placental promoter methylation of DNA repair genes and prenatal exposure to particulate air pollution: an ENVIRONAGE cohort study. *The Lancet Planetary Health*, 2(4), e174-e183.
99. Nguyen, T., Nioi, P., & Pickett, C. B. (2009). The Nrf2-antioxidant response element signaling pathway and its activation by oxidative stress. *Journal of Biological Chemistry*, 284(20), 13291-13295.
100. Pardo, M., Xu, F., Shemesh, M., Qiu, X., Barak, Y., Zhu, T., & Rudich, Y. (2019). Nrf2 protects against diverse PM2.5 components-induced mitochondrial oxidative damage in lung cells. *Science of the Total Environment*, 669, 303-313.

101. Parker, J. D., Woodruff, T. J., Basu, R., & Schoendorf, K. C. (2005). Air pollution and birth weight among term infants in California. *Pediatrics*, *115*(1), 121-128. doi:115/1/121 [pii]
102. Parvez, S., Long, M. J., Poganik, J. R., & Aye, Y. (2018). Redox signaling by reactive electrophiles and oxidants. *Chemical Reviews*, *118*(18), 8798-8888.
103. Pearson, J. F., Bachireddy, C., Shyamprasad, S., Goldfine, A. B., & Brownstein, J. S. (2010). Association between fine particulate matter and diabetes prevalence in the U.S. *Diabetes Care*, *33*(10), 2196-2201. doi:10.2337/dc10-0698 [doi]
104. Peixoto, M. S., de Oliveira Galvão, Marcos Felipe, & de Medeiros, Silvia Regina Batistuzzo. (2017). Cell death pathways of particulate matter toxicity. *Chemosphere*, *188*, 32-48.
105. Perrone, M., Gualtieri, M., Consonni, V., Ferrero, L., Sangiorgi, G., Longhin, E., . . . Camatini, M. (2013). Particle size, chemical composition, seasons of the year and urban, rural or remote site origins as determinants of biological effects of particulate matter on pulmonary cells. *Environmental Pollution*, *176*, 215-227.
106. Polzer, K., Joosten, L., Gasser, J., Distler, J. H., Ruiz, G., Baum, W., . . . Zwerina, J. (2010). Interleukin-1 is essential for systemic inflammatory bone loss. *Annals of the Rheumatic Diseases*, *69*(1), 284-290. doi:10.1136/ard.2008.104786 [doi]
107. Pope III, C. A., & Dockery, D. W. (2006). Health effects of fine particulate air pollution: lines that connect. *Journal of the Air & Waste Management Association*, *56*(6), 709-742.
108. Prada, D., López, G., Solleiro-Villavicencio, H., Garcia-Cuellar, C., & Baccarelli, A. A. (2020). Molecular and cellular mechanisms linking air pollution and bone damage. *Environmental Research*, *185*, 109465.

109. Prada, D., Zhong, J., Colicino, E., Zanobetti, A., Schwartz, J., Daghincourt, N., . . . Holick, M. (2017). Association of air particulate pollution with bone loss over time and bone fracture risk: analysis of data from two independent studies. *The Lancet Planetary Health, 1*(8), e337-e347.
110. Puett, R. C., Hart, J. E., Schwartz, J., Hu, F. B., Liese, A. D., & Laden, F. (2011). Are particulate matter exposures associated with risk of type 2 diabetes? *Environmental Health Perspectives, 119*(3), 384-389. doi:10.1289/ehp.1002344 [doi]
111. Pui, D. Y., Chen, S., & Zuo, Z. (2014). PM_{2.5} in China: Measurements, sources, visibility and health effects, and mitigation. *Particuology, 13*, 1-26.
112. Raaschou-Nielsen, O., Beelen, R., Wang, M., Hoek, G., Andersen, Z. J., Hoffmann, B., . . . Dimakopoulou, K. (2016). Particulate matter air pollution components and risk for lung cancer. *Environment International, 87*, 66-73.
113. Ris, C. (2007). US EPA health assessment for diesel engine exhaust: a review. *Inhalation Toxicology, 19*(sup1), 229-239.
114. Rosa, M. J., Just, A. C., Guerra, M. S., Kloog, I., Hsu, H. L., Brennan, K. J., . . . Rojo, M. M. T. (2017). Identifying sensitive windows for prenatal particulate air pollution exposure and mitochondrial DNA content in cord blood. *Environment International, 98*, 198-203.
115. Rudyk, O., & Eaton, P. (2014). Biochemical methods for monitoring protein thiol redox states in biological systems. *Redox Biology, 2*, 803-813.
116. Rychlik, K. A., Secret, J. R., Lau, C., Pulczynski, J., Zamora, M. L., Leal, J., . . . Johnson, N. M. (2019). In utero ultrafine particulate matter exposure causes offspring pulmonary immunosuppression. *Proceedings of the National Academy of Sciences of the United States of America, 116*(9), 3443-3448. doi:10.1073/pnas.1816103116 [doi]

117. Sant, K. E., Hansen, J. M., Williams, L. M., Tran, N. L., Goldstone, J. V., Stegeman, J. J., . . . Timme-Laragy, A. (2017). The role of Nrf1 and Nrf2 in the regulation of glutathione and redox dynamics in the developing zebrafish embryo. *Redox Biology, 13*, 207-218.
118. Santibáñez-Andrade, M., Quezada-Maldonado, E. M., Osornio-Vargas, Á., Sánchez-Pérez, Y., & García-Cuellar, C. M. (2017). Air pollution and genomic instability: The role of particulate matter in lung carcinogenesis. *Environmental Pollution, 229*, 412-422.
119. Schlesinger, R., Kunzli, N., Hidy, G., Gotschi, T., & Jerrett, M. (2006). The health relevance of ambient particulate matter characteristics: coherence of toxicological and epidemiological inferences. *Inhalation Toxicology, 18*(2), 95-125.
120. Selevan, S. G., Kimmel, C. A., & Mendola, P. (2000). Identifying critical windows of exposure for children's health. *Environmental Health Perspectives, 108 Suppl 3*, 451-455. doi:sc271_5_1835 [pii]
121. Shah, P. S., Balkhair, T., & Knowledge Synthesis Group on Determinants of Preterm/LBW births. (2011). Air pollution and birth outcomes: a systematic review. *Environment International, 37*(2), 498-516.
122. Skoko, J. J., Wakabayashi, N., Noda, K., Kimura, S., Tobita, K., Shigemura, N., . . . Kensler, T. W. (2014). Loss of Nrf2 in mice evokes a congenital intrahepatic shunt that alters hepatic oxygen and protein expression gradients and toxicity. *Toxicological Sciences, 141*(1), 112-119.
123. Sun, Q., Yue, P., Deiluiis, J. A., Lumeng, C. N., Kampfrath, T., Mikolaj, M. B., . . . Parthasarathy, S. (2009). Ambient air pollution exaggerates adipose inflammation and insulin resistance in a mouse model of diet-induced obesity. *Circulation, 119*(4), 538-546.

124. Sun, X., Luo, X., Zhao, C., Ng, R. W. C., Lim, C. E. D., Zhang, B., & Liu, T. (2015). The association between fine particulate matter exposure during pregnancy and preterm birth: a meta-analysis. *BMC Pregnancy and Childbirth*, *15*(1), 1-12.
125. Suzuki, T., & Yamamoto, M. (2015). Molecular basis of the Keap1–Nrf2 system. *Free Radical Biology and Medicine*, *88*, 93-100.
126. Symanski, E., Davila, M., McHugh, M. K., Waller, D. K., Zhang, X., & Lai, D. (2014). Maternal exposure to fine particulate pollution during narrow gestational periods and newborn health in Harris County, Texas. *Maternal and Child Health Journal*, *18*(8), 2003-2012.
127. Tipple, T. E., & Rogers, L. K. (2012). Methods for the determination of plasma or tissue glutathione levels. *Developmental Toxicology* (pp. 315-324) Springer.
128. Tsamou, M., Vrijens, K., Madhloum, N., Lefebvre, W., Vanpoucke, C., & Nawrot, T. S. (2018). Air pollution-induced placental epigenetic alterations in early life: a candidate miRNA approach. *Epigenetics*, *13*(2), 135-146.
129. Tsukue, N., Tsubone, H., & Suzuki, A. K. (2002). Diesel exhaust affects the abnormal delivery in pregnant mice and the growth of their young. *Inhalation Toxicology*, *14*(6), 635-651.
130. Uwak, I., Olson, N., Fuentes, A., Moriarty, M., Pulczynski, J., Lam, J., . . . Koehler, K. (2021). Application of the navigation guide systematic review methodology to evaluate prenatal exposure to particulate matter air pollution and infant birth weight. *Environment International*, *148*, 106378.
131. Valavanidis, A., Fiotakis, K., & Vlachogianni, T. (2008). Airborne particulate matter and human health: toxicological assessment and importance of size and composition of particles

- for oxidative damage and carcinogenic mechanisms. *Journal of Environmental Science and Health, Part C*, 26(4), 339-362.
132. Vattanasit, U., Navasumrit, P., Khadka, M. B., Kanitwithayanun, J., Promvijit, J., Autrup, H., & Ruchirawat, M. (2014). Oxidative DNA damage and inflammatory responses in cultured human cells and in humans exposed to traffic-related particles. *International Journal of Hygiene and Environmental Health*, 217(1), 23-33.
133. Vomhof-DeKrey, E. E., & Picklo Sr, M. J. (2012). The Nrf2-antioxidant response element pathway: a target for regulating energy metabolism. *The Journal of Nutritional Biochemistry*, 23(10), 1201-1206.
134. Wakabayashi, N., Slocum, S. L., Skoko, J. J., Shin, S., & Kensler, T. W. (2010). When NRF2 talks, who's listening? *Antioxidants & Redox Signaling*, 13(11), 1649-1663.
135. Wang, D., Pakbin, P., Shafer, M. M., Antkiewicz, D., Schauer, J. J., & Sioutas, C. (2013). Macrophage reactive oxygen species activity of water-soluble and water-insoluble fractions of ambient coarse, PM_{2.5} and ultrafine particulate matter (PM) in Los Angeles. *Atmospheric Environment*, 77, 301-310.
136. Wei, Y., Zhang, J., Li, Z., Gow, A., Chung, K. F., Hu, M., . . . Jia, G. (2016). Chronic exposure to air pollution particles increases the risk of obesity and metabolic syndrome: findings from a natural experiment in Beijing. *The FASEB Journal*, 30(6), 2115-2122.
137. Weldy, C. S., Liu, Y., Chang, Y., Medvedev, I. O., Fox, J. R., Larson, T. V., . . . Chin, M. T. (2013). In utero and early life exposure to diesel exhaust air pollution increases adult susceptibility to heart failure in mice. *Particle and Fibre Toxicology*, 10(1), 1-12.
138. Wichmann, H. (2007). Diesel exhaust particles. *Inhalation Toxicology*, 19(sup1), 241-244.

139. Wilhelm, M., Ghosh, J. K., Su, J., Cockburn, M., Jerrett, M., & Ritz, B. (2011). Traffic-related air toxics and preterm birth: a population-based case-control study in Los Angeles County, California. *Environmental Health*, *10*(1), 1-12.
140. Woodward, N. C., Crow, A. L., Zhang, Y., Epstein, S., Hartiala, J., Johnson, R., . . . Akbari, O. (2019). Exposure to nanoscale particulate matter from gestation to adulthood impairs metabolic homeostasis in mice. *Scientific Reports*, *9*(1), 1-11.
141. Woodward, N. C., Crow, A. L., Zhang, Y., Epstein, S., Hartiala, J., Johnson, R., . . . Akbari, O. (2019). Exposure to nanoscale particulate matter from gestation to adulthood impairs metabolic homeostasis in mice. *Scientific Reports*, *9*(1), 1-11.
142. Wu, G., Brown, J., Zamora, M. L., Miller, A., Satterfield, M. C., Meininger, C. J., . . . Zhang, R. (2019). Adverse organogenesis and predisposed long-term metabolic syndrome from prenatal exposure to fine particulate matter. *Proceedings of the National Academy of Sciences of the United States of America*, *116*(24), 11590-11595.
doi:10.1073/pnas.1902925116 [doi]
143. Wu, J., Ren, C., Delfino, R. J., Chung, J., Wilhelm, M., & Ritz, B. (2009). Association between local traffic-generated air pollution and preeclampsia and preterm delivery in the south coast air basin of California. *Environmental Health Perspectives*, *117*(11), 1773-1779.
doi:10.1289/ehp.0800334 [doi]
144. Xie, P., Zhao, C., Huang, W., Yong, T., Chung, A. C., He, K., . . . Cai, Z. (2019). Prenatal exposure to ambient fine particulate matter induces dysregulations of lipid metabolism in adipose tissue in male offspring. *Science of the Total Environment*, *657*, 1389-1397.

145. Xu, D., Xu, M., Jeong, S., Qian, Y., Wu, H., Xia, Q., & Kong, X. (2019). The role of Nrf2 in liver disease: novel molecular mechanisms and therapeutic approaches. *Frontiers in Pharmacology*, *9*, 1428.
146. Xu, M., Ge, C., Qin, Y., Gu, T., Lou, D., Li, Q., . . . Tan, J. (2019). Prolonged PM2.5 exposure elevates risk of oxidative stress-driven nonalcoholic fatty liver disease by triggering increase of dyslipidemia. *Free Radical Biology and Medicine*, *130*, 542-556.
147. Xu, X., Liu, C., Xu, Z., Tzan, K., Zhong, M., Wang, A., . . . Sun, Q. (2011). Long-term exposure to ambient fine particulate pollution induces insulin resistance and mitochondrial alteration in adipose tissue. *Toxicological Sciences*, *124*(1), 88-98.
148. Xu, Z., Xu, X., Zhong, M., Hotchkiss, I. P., Lewandowski, R. P., Wagner, J. G., . . . Harkema, J. R. (2011). Ambient particulate air pollution induces oxidative stress and alterations of mitochondria and gene expression in brown and white adipose tissues. *Particle and Fibre Toxicology*, *8*(1), 1-14.
149. Yang, W., & Omaye, S. T. (2009). Air pollutants, oxidative stress and human health. *Mutation Research/Genetic Toxicology and Environmental Mutagenesis*, *674*(1-2), 45-54.
150. Yorifuji, T., Naruse, H., Kashima, S., Murakoshi, T., Tsuda, T., Doi, H., & Kawachi, I. (2012). Residential proximity to major roads and placenta/birth weight ratio. *Science of the Total Environment*, *414*, 98-102.
151. Yu, T., Kondo, T., Matsumoto, T., Fujii-Kuriyama, Y., & Imai, Y. (2014). Aryl hydrocarbon receptor catabolic activity in bone metabolism is osteoclast dependent in vivo. *Biochemical and Biophysical Research Communications*, *450*(1), 416-422.